OKLAHOMA DEPARTMENT OF TRANSPORTATION

ODOT 83-07-2 (Item 2128)

ORA 155-487

CONSTRUCTION AND PERFORMANCE OF THE STABILIZED BASE COURSE ON U.S. 77 PONCA CITY, KAY COUNTY

Joakim G. Laguros

M. Saleh Keshawarz

THE UNIVERSITY OF OKLAHOMA

July 1987

TECHNICAL REPORT STANDARD TITLE PAGE

1. REPORT NO.	2. GOVERNMENT ACCESSION NO.	3. RECIPIENT'S CATALOG NO.
FHWA/OK 87(7)		

4. TITLE AND SUBTITLE	5. REPORT DATE
Construction and Performance of the Stabilized Base Course on U.S. 77 Ponca City, Kay County	5 July 1987
	6. PERFORMING ORGANIZATION CODE

7. AUTHOR(S)	8. PERFORMING ORGANIZATION REPORT
Joakim G. Laguros and M. Saleh Keshawarz	ORA 155-487

9. PERFORMING ORGANIZATION NAME AND ADDRESS	10. WORK UNIT NO.
The University of Oklahoma Norman, OK 73019	Proj. Agreement No. 32
	11. CONTRACT OR GRANT NO.
	ODOT 83-07-2, Item 2128

12. SPONSORING AGENCY NAME AND ADDRESS	13. TYPE OF REPORT AND PERIOD COVERED
Oklahoma Department of Transportation Research and Development Division 200 N.E. 21st Oklahoma City, Oklahoma 73105	14. SPONSORING AGENCY CODE

15. SUPPLEMENTARY NOTES

Done in cooperation with FHWA

16. ABSTRACT

This study investigates the field implementation of shale stabilization on an experimental project. A number of test sections were set on the south bound lane of U.S. Highway 77, north of Ponca City, Kay County, Oklahoma. To compare the effectiveness of various stabilizing agents, the base courses of these test sections were stabilized with cement (14%), quicklime (4.5%), fly ash (25%), and an optimum mixture of 8% cement + 3% quicklime + 18% fly ash used conjunctively. Also a control (non-stabilized) section was set as a reference section.

Analyses of the samples prepared during construction and those cored from under the pavement after construction showed significant amelioration of the engineering properties of stabilized shale as manifested by their plasticity, compressive and beam strength compared to raw (non-stabilized) shale. Benkelman beam measurements ascertained the improvement in deformation resistance.

The microstructure of stabilized shale was studied using X-ray diffraction (XRD). The non basal (hkl) reflections in stabilized oriented specimens suggest that the clay particles in the stabilized shale acquired high resistance to dispersive forces. This, together with the reduction in the integrated intensities of clay minerals help explain the improved stability as a result of stabilization. SEM observations in conjunction with EDS, depicted the presence of some newly formed hydration products and a rather dense degree of packing. The various data converge to the conclusion that field stabilization is a viable solution to the use of expansive shales.

17. KEY WORDS	18. DISTRIBUTION STATEMENT
shale stabilization, cement, lime, fly ash, pavement performance, XRD, SEM, strength	

19. SECURITY CLASSIF. (OF THIS REPORT)	20. SECURITY CLASSIF. (OF THIS PAGE)	21. NO. OF PAGES	22. PRICE
none	none	244	

FINAL REPORT

ODOT Study No. 83-07-2

ORA 155-487

CONSTRUCTION AND PERFORMANCE OF THE STABILIZED BASE COURSE ON U.S. 77 PONCA CITY, KAY COUNTY

Prepared by

Joakim G. Laguros, David Ross Boyd Professor
School of Civil Engineering and Environmental Science
University of Oklahoma

M. Saleh Keshawarz, Assistant Professor
Texas A & I University, Kingsville, Texas;
formerly Research Assistant, University of Oklahoma

Submitted to

Research Division
OKLAHOMA DEPARTMENT OF TRANSPORTATION

From the

OFFICE OF RESEARCH ADMINISTRATION
UNIVERSITY OF OKLAHOMA
Norman, Oklahoma
July 1987

DISCLAIMER

The contents of this report reflect the views of the author who is responsible for the facts and the accuracy of the data presented herein. The contents do not necessarily reflect the official views of the Oklahoma Department of Transportation or the Federal Highway Administration. This report does not constitute a standard, specification, or regulation. While equipment and contractor names are used in this report, it is not intended as an endorsement of any machine, contractor, or process.

SUMMARY

The use of expansive shales as roadbeds in Oklahoma has led to pavement failures. Attempts at stabilizing these shales in the laboratory have met with some success. However, no scientific information was available on the performance of stabilized shales under actual climatic and loading conditions in the field. This study is an attempt to investigate the field implementation of shale stabilization on an experimental project.

A number of test sections were set on the south bound lane of U.S. Highway 77, north of Ponca City, Kay County, Oklahoma. To compare the effectiveness of various stabilizing agents, the base courses of these test sections were stabilized with cement (14 percent), quicklime (4.5 percent), fly ash (25 percent), and an optimum mixture of 8 percent cement + 3 percent quicklime + 18 percent fly ash used conjunctively. Also a control (non-stabilized) section was set as a reference section.

Analyses of the samples prepared during construction and those cored from under the pavement after construction showed significant amelioration of the engineering properties of stabilized shale as manifested in their

plasticity and strength compared to raw (non-stabilized) shale. The improvement in strength was measured in terms of unconfined compressive strength, cohesion, angle of internal friction, and beam action. In addition, Benkelman beam measurements obtained from the test sections reflected higher deformation resistance (improved stability) of the stabilized section.

The microstructure of stabilized shale was studied using X-ray diffraction (XRD) and scanning electron microscopy (SEM) in conjunction with energy dispersive spectroscopy (EDS). The non basal (hkl) reflections in stabilized oriented specimens suggest that the clay particles in the stabilized shale acquired high resistance to dispersive forces. This, together with the reduction in the integrated intensities of clay minerals helps explain the improved stability as a result of stabilization. SEM observations in conjunction with EDS, depicted the presence of some newly formed hydration products and a rather dense degree of packing. Both of these characteristics are significant in improving strength and deformation properties of stabilized shale. While the laboratory samples yielded higher strength values than their field counterparts, the latter are at an acceptable level strongly indicating that field stabilization is a viable solution to the use of expansive shales.

TABLE OF CONTENTS

TABLE OF CONTENTS (continued)

TABLE OF CONTENTS (continued)

LIST OF TABLES

LIST OF TABLES (continued)

LIST OF ILLUSTRATIONS (continued)

LIST OF ILLUSTRATIONS (continued)

LIST OF TABLES (continued)

LIST OF ILLUSTRATIONS

PREFACE

In cooperation with the Oklahoma Department of Transportation a research project was undertaken in 1982 by the University of Oklahoma Office of Research Administration encompassing the construction and field performance of a stabilized base course on U.S. 77 in Ponca City.

During the course of this effort, which was conducted by the School of Civil Engineering and Environmental Science, reports were submitted quarterly, and the present constitutes the final report.

The opinions, findings and conclusions expressed in this publication are those of the authors and not necessarily those of the Oklahoma Department of Transportation.

ACKNOWLEDGEMENTS

This investigative study was supported by the Research Division of the Oklahoma Department of Transportation and the Federal Highway Administration under ODOT study 83-07-2 (ORA 155-487).

During the conduct of this study numerous meetings were held with representatives of the sponsoring agency and the authors are grateful for all the helpful suggestions and cooperation they received.

Special thanks are also extended to Mr. Curtis J. Hayes, Research Division, ODOT, for supplying the materials used in this study and for his support in general. The authors are also grateful for certain X-ray diffraction analyses and interpretations provided by Dr. T. Demirel, Professor of Civil Engineering and Mr. Scott S. Schlorholtz, Research Associate, at Iowa State University, Ames, Iowa.

The assistance of Mr. Douglas Powell of the University of Oklahoma X-ray Diffraction Laboratory and Mr. William Chessoe of the University of Oklahoma Electron Microscopy Laboratory is well acknowledged.

We would be remiss, however, if we did not acknowledge Ms. Barbara Jones, Ms. Betty Craig and Ms. Debi Sofer who demonstrated care and patience in the typing of the manuscript.

FIELD STABILIZATION OF PONCA CITY SHALE

CHAPTER I

INTRODUCTION

Shales are commonly occurring sedimentary rocks. Depending on the degree of weathering, they are classified as either rocks or soils ranging from a hard durable rock to a stiff plastic clay. The engineering properties of shales are affected by a number of intrinsic characteristics such as grain size, clay content, degree of cementation, and presence of moisture. By virtue of their abundance, shales have been used in the construction of many engineering projects and primarily as foundation materials for highways.

In Oklahoma, shales are extensively used as subgrade material in highway construction. Unfortunately their performance has been unpredictable; sometimes it is satisfactory but at other times shales deform excessively resulting in pavement failure. To approach the problem in a scientific manner, the Oklahoma Department of Transportation, in cooperation with the University of Oklahoma, initiated a series of research projects to

identify the "problem" and "no problem" shales, and to upgrade the former. The first study in 1968 centered on classifying shales (Laguros, 1972). The second study focused on the response of shales to stabilization by Portland cement, lime, and fly ash (Laguros and Jha, 1977) and based on the recommendations thereof, a section (3000 ft) of the south-bound lane of U.S. Highway 77, north of Ponca City, Kay County, Oklahoma was chosen as the site for a field test project. The project consists of four sections with stabilized base courses and one control (non-stabilized) section. The first phase encompassed the laboratory investigation (Laguros and Medhani, 1984), in which the optimum amounts of stabilizing agents were determined. Thus, 14 percent of Portland cement, 4.5 percent of quicklime, 25 percent of fly ash, and for the conjunctive use, 8 percent cement + 3 percent quicklime + 18 percent fly ash were used.

The present study covers the performance of stabilized base test sections under field conditions with the following objectives:

1. Identifying the differences between laboratory and field stabilization by comparing the results of the laboratory prepared samples(Laguros and Medhani, 1984), hereinafter referred to as laboratory samples, to those: i) obtained from samples prepared during constrution in the field, but cured

in the laboratory, hereinafter referred to as construction samples, and ii) results obtained from samples retrieved after the pavement layer(s) were placed, cured under field conditions and had experienced traffic induced stresses; these are hereinafter referred to as field samples.

The purpose of studying construction samples was to investigate the influence of the variations in compaction and curing conditions (laboratory vs. field) as manifested by the plasticity, strength, and microstructure of the stabilized shale.

2. Analyzing the microstructure of raw and stabilized shale using scanning electron microscopy (SEM) and X-ray diffraction (XRD) techniques, so as to relate the changes in engineering behavior of stabilized shale to its microfabric and clay mineral structure, and the formation of reaction products.

CHAPTER II

LITERATURE REVIEW

The literature on shales is quite abundant. In so far as shale classification, stabilization and mechanisms of soil stabilization are concerned, they are extensively covered in previous studies conducted at the University of Oklahoma (Anessi, 1968; Kumar, 1974; Laguros and Jha, 1977; Laguros and Medhani, 1984). The present study is focused on the field application and performance of stabilized shale under actual field conditions. Therefore, the literature review presented herein is limited to this latter topic.

2.1 Cement Stabilization

In the literature the terms "cement stabilization" and "soil-cement" are used interchangeably. According to the Highway Research Board Committee on Soil-Portland Cement Stabilization (1959), soil cement is defined as "a hardened material formed by curing a mechanically compacted intimate mixture of pulverized soil-Portland cement and water."

The use of cement as a stabilizing agent in the

construction of roadways dates back to the early 20th century. According to Davidson (1961), Bert Reno, an enterprising contractor, used soil-cement for the first time in Sarasota, Florida in 1915. Although during the 1920's, Texas, California, Iowa, and South Dakota experimented with soil-cement, lack of knowledge of the application of soil science to road building apparently caused unsatisfactory service performance, and therefore the method was given up.

Soil-cement in road construction was brought to the attention of highway engineers after the South Carolina State Highway Department (1932) began investigation of a mixture of soil and cement. Several test sections were built in 1933 and 1934, and based on the performance of these test sections it was concluded that soil and cement were compatible materials, and that they could be mixed together to form a low-cost base material for roads (Mills, 1935 and 1936). This led to another study wherein the South Carolina State Highway Department in cooperation with the Portland Cement Association and the Bureau of Public Roads, constructed a 1½ mile section of pavement near Johnsonville, S.C., in 1935. This project is known as the first "engineered" soil-cement road (Davidson, 1961). The success of this soil-cement project made other states follow the South Carolina example quickly and build their own soil-cement projects.

Willis (1947), reported on another experimental soil-cement base course in South Carolina, where twenty-two sections of a 6-mile road base course were stabilized with cement. The thickness of soil-cement base course varied from 4 to 8 inches, and the cement content varied from 3 to 11 percent. The performance of this experimental road was monitored over a period of eight years during which it was found that the addition of cement to soil reduced the plasticity, increased the durability of base course, and increased the quality of performance. It was also found that 3 percent cement content was not sufficient to produce the required base course stability, even though the base thickness was increased to 8 inches. On the other hand, soil-cement bases 4 inches thick were inadequate even with cement content as high as 9 percent.

Hoover et al., (1962) reported the results of three years of field and laboratory observations of 600 feet of stabilized soil base and subbase course of primary Highway 117, Jasper County, Iowa. Lime-fly ash, lime-fly ash-accelerating agent, and cement were used in stabilizing the 7-inch base course test sections. The base course material consisted of sand-loess mix plus 8 percent type I Portland cement. The unconfined compressive strength of the cores obtained three years after construction ranged from 1,100 to 2,600 psi. On the other hand, the average unconfined compressive strength of

cement stabilized field mixed laboratory molded specimens were 550, 834, and 720 psi after 26, 183 and 365 days of curing, respectively. The performance of the experimental base and subbase was reported as excellent after three years of service.

In an attempt to develop a freeze-thaw test for the design of soil-cement, George and Davidson (1963), studied the performance of an experimental section in Iowa. The cement content of the 7 inch stabilized base varied from 7 to 13 percent. The AASHTO classification of natural soil varied from A-4(8) to A-6(10), and the plasticity index of the natural soil varied from 9 to 15 percent. The immersed strength of cores obtained after 360 days of curing ranged from 700 psi for 7 percent cement, to 1500 psi for 13 percent cement.

The effectiveness of various types of stabilizing agents in the laboratory and in the field was evaluated by Stewart et al., (1971). Portland cement was one of the three stabilizing agents that was studied in this investigation. The AASHTO classification of the natural soil ranged from A-2 to A-7, and the plasticity index ranged from non-plastic to 21. The laboratory prepared samples were tested in immersed condition. Their unconfined compressive strength ranged from 183 psi to 526 psi, while the compressive strength of one-month cured field samples ranged from 97 to 217 psi.

Extensive performance surveys of the soil-cement have been carried out by several investigators. A detailed literature review on this subject is available in the Highway Research Board Bulletin 292 (1961).

Mills (1940), surveyed 64 projects of soil-cement roads in 23 states. He reported that 44 projects were in excellent condition, 17 projects in good condition and 3 projects in fair condition. He also reviewed the construction history of early soil-cement projects (Mills, 1941) and reported that scaling of wearing surface was the most frequently occurring defect in soil-cement roads. The actual structural damage to the pavement was light. He listed low cement content, poor drainage, unsatisfactory compaction, and excessive mixing time after application of cement and water to soil as causes of failure for soil-cement roads.

Reid (1948), summarized two surveys that were conducted during 1945 to 1946 and 1946 to 1947. The first survey included 18 projects ranging in age from 5½ to 9 years. The condition survey showed that 12 of these projects were performing in excellent, four in good and one in average manner. In the second survey, 59 projects from 19 states with a total of 273 miles of roads were surveyed. The thickness of the soil-cement layer in these projects ranged from 5 to 10½ inches. The cement content ranged from 6 to 14 percent by volume. The

natural soil had a plasticity index up to 35 percent. The condition survey showed that base failure occurred in 32 projects. Twenty-seven projects experienced some failure and only six projects experienced failures that warranted analysis. The reason for excessive failures were given as insufficient moisture and thickness, and frost heave on silty soils.

Loughborough (1948), reported the performance of ten individual projects of soil-cement constructed in Virginia since 1938. The natural soils ranged from silty sand to silty clays. The report concludes that in spite of severe climatic conditions in the region, no distress in the soil-cement was apparent.

Redus (1958), studied the service behavior of seven airfields where soil-cement had been used in construction. Field and laboratory tests were run on only four of the airfields. The major findings of this study were: (a) cracking was caused by shrinkage of soil-cement and was not connected with induced load; (b) plastic binders at the time of construction were rendered non-plastic one to 10 years after construction; and (c) the reduction in plasticity index appeared to be permanent.

Mitchell and Freitag (1959), carried out an intensive performance study of field test sections and airfields in the United States and overseas. The performance of field test sections and airfields was compared

with the performance of conventional flexible pavements. Among their findings were: (i) out of a total of 85 the performance of 42 test panels was equal to that expected of flexible pavements having the same or greater thickness, (ii) the performance of 19 highway test panels and airfields was poorer than expected from a flexible pavement of equal thickness, and the rest could not be compared for a variety of reasons. Also, they found that cracking in soil-cement is to be expected and should not be treated as a sign of failure.

Several researchers have carried out studies to correlate the strength of laboratory prepared soil-cement specimens to that of specimens cored from the field. As the degree of control becomes less strict from laboratory to the field, the level of strength attainment with stabilization becomes lower. Mixing, degree of pulverization, curing conditions, and disturbance of specimens during coring are some of the factors responsible for lower strength of field samples.

The Waterways Experiment Station in Vicksburg, Mississippi, performed unconfined compressive strength tests on the laboratory mixed and compacted, and undisturbed samples obtained from their field tests at the same water content, dry density and curing time. It was found that the ratio of the strength of field samples to laboratory samples was 0.63. Also, it was found that the

ratio of the strength of field to laboratory samples decreased as the cement content increased. For example, with cement contents of 3, 6 and 10 percent the corresponding ratios were 0.75, 0.60 and 0.56. The strength of field-mixed but laboratory compacted samples were also found to be less than the laboratory mixed and compacted specimens. In general, it was discovered that the strength of the former was about 86 percent of the latter. Again the ratio of the strength of the field-mixed laboratory compacted specimens to laboratory mixed and compacted specimens decreased as the cement content increased. For 3, 6, and 10 percent cement content the ratios were 0.97, 0.83, and 0.78, respectively. It is obvious that mixing operations, curing conditions, and compaction are important elements of strength gain of soil-cement (Chu, 1977).

Maclean (1956), noticed that the strength of "mixed-in-place" stabilized soil was about 67 percent of that made in the laboratory. Wang (1968), reported that the ratio of the unconfined compressive strength of the undisturbed to that of laboratory compacted specimens was about 0.50.

Robert and Schoeneman (1965), found that the average difference in compressive strength between laboratory prepared samples (after seven days of curing) and cores obtained from the field (after eight days of curing) was

about 400 psi.

Stewart et al., (1971) reported that the ratio of the strength of field to laboratory samples ranged from 0.3 to 0.7.

2.2 Lime Stabilization

Lime, the oxides or hydroxides of calcium and magnesium, has long been used in the stabilization of cohesive soils. The physical and chemical changes which are imparted to the soil as a result of lime stabilization, have made lime an ideal stabilizing agent in the construction of bases and subbases of highways. Numerous laboratory and field studies have been conducted on soil-lime stabilization.

An excellent annotated bibliography of soil-lime literature was presented by Herrin and Mitchell (1961). The review indicated the beneficial effects of lime stabilization on the plasticity, shrinkage, workability, and strength properties of soils. In general, the plasticity index was reduced, the shrinkage limit increased, workability improved, and strength increased. There have been limited attempts to correlate laboratory strength test results and the actual field performance of lime-soil stabilized roads. The reason is probably related to the problems encountered in obtaining cores of lime soil mixtures from field that can be used in the laboratory for

evaluating strength (Herrin and Mitchell, 1961).

The field performance of a few lime stabilized roads was documented by Herrin and Mitchell (1961) which are reproduced in Table 2.1.

McDowell (1966), obtained cores from old lime stabilized roads and tested them in the laboratory. Some of his findings were:

i) the strength of the cores for properly constructed roads ranged from two and one-half to three times that obtained from samples cured under normal room temperature.

ii) there was no relation between the PI of the soil-lime mixture and its strength.

iii) higher percentages (8 percent) of lime had less tendency for PI to increase with age than lower percentages of lime (4.5 percent). Also, higher lime content produced less soil binder than lower lime content. He also found that the optimum lime content cannot be identified by short term strength, but it is essential in determining the reactivity of the soil to lime treatment. The purer and finer the lime, the easier it is to mix it with cohesive soils.

McDonald (1970), reported the effects of lime stabilization on Pierre shale. The natural soil was an AASHTO A-7-6(20) with a plasticity index close to 50.

Table 2.1. Field Performance of a Few Lime-Stabilized Roads*

Location	Soil Types	Reported Field Performance
Nebraska	High plastic glacial clay	Satisfactory performance was observed after 2 yr. service.
Perry Co., Missouri	Gravelly clays and silty clay loams	After 4.5 yr. service, all sections had an appearance of good to excellent. The PI's increased during this time.
Mascoutah, Illinois	Highly plastic clay	Performance of this section was very good after 4 yr. service.
Englemann Township, Illinois	Highly plastic Clay	This section was in excellent condition after 5 yr. service.
Mitchell Co., Kansas	Limestone gravel	The sections developed a few cracks after 1 yr. of service
Taylor, Texas	Taylor marl gravel	This section was holding up well after 5 yr. use.
Williamson Co., Texas	Grandular soil	After 8 yr. service this section was in excellent condition.
East of Taylor, Texas	Clay gravel	This road was used to serve light traffic for 5 yr. It was patched and resealed as many dry weather cracks had developed.
Texas	Old clay gravel	After 2 yr. service, the condition of the road was perfect.

* (after Herrin and Mitchell, 1961)

The soil was stabilized with 6 percent hydrated lime. Results of the plasticity index test over a period of four years showed that the PI was reduced from approximately 50 percent to slightly under 20 percent. He could not obtain any field specimens for strength testing.

Stewart et al., (1971) reported on the field application of lime stabilization of Piedmont soils where the results of laboratory investigation were applied to an experimental road. The raw soil in the project area had an AASHTO classification ranging from A-7-5(4) to A-2-4, and the plasticity index of the soil ranged from non-plastic to 14. The amount of lime used for stabilization varied from 4.3 to 6.3 percent. The ratio of compressive strength of field to laboratory specimens after one month ranged from 0.6 to 1.1.

Alexander (1976) made a detailed survey of the performance of lime-treated bases in California. He noted that:

> "Of the thirty-five roads constructed with lime treated native soils as a base, 22 (63%) were judged to be in fair to good condition by the end of the ten year service period. Two other roads, although unsurfaced prior to the end of the ten year service life, were considered to have performed satisfactorily with the additional thickness of asphalt concrete being added as preventive maintenance on slightly distressed pavement."

The roads that were judged to be poor indicated that structural deficiencies in lime treated bases resulted in an almost immediate distress of the road. It was found

that there was a correlation between performance and deficiency in the asphalt concrete thickness. Other factors contributing to the observed distress were treatment of non-responsive soil material, poor lime distribution uniformity, and deficiencies in the constructed thickness of the lime treated base or asphaltic concrete.

Dallaire (1973), reported on the largest project ever to stabilize swelling soils with lime. This project was the construction of the Dallas-Ft. Worth airport, where the native soil, a poor gumbo clay, was stabilized with 5 percent hydrated lime or 20 gallons of lime slurry per cubic yard to a depth of 18 inches. The reason for the great depth was to provide adequate pavement thickness in order to accommodate all types of heavy loads induced by planes including the giant 750,000 pounds 747s, and even heavier aircraft. The ultimate pavement design load was 2 million pounds. No data are available on the performance of this project.

2.3 Fly Ash Stabilization

Fly ash or pulverized fuel ash is the fine inorganic residue of combusted pulverized coal consumed in power generating plants (Diamond, 1981). The coal from which fly ash is derived is first ground and then injected into the boiler in a stream of hot air at a temperature of 1500° to 1700°C. The non-combustible mineral matter

which is deposited on the relatively cool boiler tubes from where it periodically falls to the lower section of the furnace is bottom ash (Stamp and Smith, 1984). The smaller particles (fly ash) remain in suspension in the hot gas stream and as they undergo melting the suspended liquid droplets assume a spherical shape, where upon cooling preserve the external spherical outline. Occasionally irregular shaped particles are also observed which are the result of incomplete melting, either because of their composition, insufficient high temperature or too short a time to heat exposure (Diamond, 1981). Fly ash is collected by electrical precipitators or mechanical means or a combination of the two.

Depending on the type of coal, fly ashes are classified into two classes. Low calcium ashes are derived from bituminous and anthracite coal and are referred to as Class F fly ash; high calcium fly ashes are derived from lignitic and subbituminous coals and are referred to as Class C fly ash.

The ever increasing coal consumption and restriction on the release of particulate material into the atmosphere resulted in the collection of large quantities of fly ash in recent years. In the United States, about 600 million tons of pulverized coal are burned annually and it is projected to reach one billion tons by 1990 (Burnet et al., 1984). Figure 2.1 depicts coal consumption and

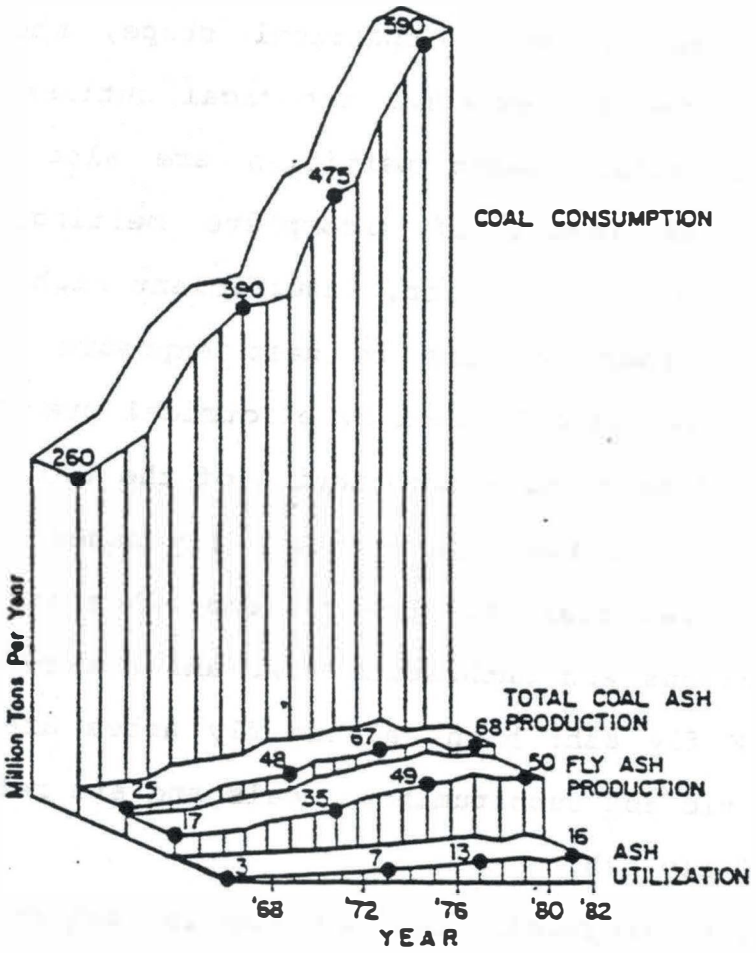

Figure 2.1: Coal consumption and ash generation by United States electric power stations (after Burnet et al., 1984)

ash generation in the United States. From the total ash produced currently only 20 percent is utilized for various purposes such as concrete, brickmaking, water pollution control, filler for plastics, oil drilling mud and soil stabilization (Burnet et al., 1984).

Fly ash in soil stabilization has been mainly used as a supplement or replacement for lime and cement in soils showing poor pozzolanic properties in order to enhance the lime-silica reaction. A pozzolan is defined as

> "A siliceous or siliceous aluminous material, which in itself possesses little or no cementitious value but which will, in finely divided form and in the presence of moisture, chemically react with calcium hydroxide at ordinary temperatures to form compounds containing cementitious properties" (ASTM, 1973).

Class F fly ash is mainly used as a synthetic pozzolan, while Class C fly ash, because of high calcium oxide content, exhibits both pozzolanic and self hardening properties. Laguros and Jha (1977) and later Laguros and Medhani (1984), in their study of Oklahoma shales have used Class C fly ash as a main stabilizing agent, and it proved effective when used in significant amounts (25 percent by weight). They reported that fly ash stabilization reduced the plasticity index, ameliorated durability and increased the strength of the shale.

Despite the favorable results obtained from laboratory studies of soils stabilized with fly ash alone, its field application in the construction of bases and sub-

bases of highways has not been tested, as yet adequately.

Joshi et al. (1975), reported on the effectiveness of two fly ashes in reducing the plasticity index of a Kansas City, Missouri, plastic clay. Both fly ashes were found to be effective in reducing the plasticity index of a clayey soil. As an extension of laboratory findings, 15 percent fly ash was added to a highly plastic subgrade with a plasticity index of 22 percent. The thickness of the modified subgrade was 9 inches, covered by 9 inches of asphaltic concrete. The performance of the pavement after two years of service under light traffic was reported excellent. In contrast to the stabilization of soils with fly ash alone, soil stabilization with lime-fly ash is accepted widely.

Minnick and Williams (1956), evaluated the performance of a number of field projects in which lime-fly ash-soil composition has been used in their construction. The materials in the projects included stone screenings, slags, cinders, and soils ranging from the sandy or gravelly forms to the fine grained and plastic variety. Unconfined compressive strength test was run on undisturbed cubic specimens. They found that the pozzolanic strength values varied from 100 to 4315 psi, and the ratio of field strength to laboratory strength varied approximately from 0.21 to 3.2.

2.4 Flexural Strength of Stabilized Soils

Although most pavements with stabilized bases and subbases are classified and designed as flexible pavements, they develop high moduli of elasticity which may impart in the pavement enough rigidity to make them perform as a slab or a beam. The required thickness is, however, in many cases less than that required for a conventional flexible pavement.

Several investigators have studied the flexural strength and correlated it to the unconfined compressive strength of stabilized soils.

Felt and Abrams (1957), found that the modulus of rupture (flexural strength) of soil-cement mixtures was approximately 20 percent of the compressive strength at all ages. According to Chu (1977), the flexural strength of Vicksburg silty clay stabilized with 3, 6 and 10 percent cement was about 25 to 30 percent of the compressive strength. Laguros and Medhani (1984), reported that the ratio of flexural strength to compressive strength of cement stabilized Oklahoma shale ranged from 0.17 to 0.23. Wang (1968), noted that the flexural strength of undisturbed cement stabilized soil was about 60 percent of the laboratory compacted specimens. He also reported that a nearly linear relationship between flexural strength and compressive strength exists, and the modulus of rupture is approximately 20 to 35 percent of the un-

confined compressive strength.

Thompson (1968), reported that the flexural strength of lime treated soils was about 25 percent of the unconfined compressive strength. Laguros and Medhani (1984), found that the ratio of flexural to compressive strength of Oklahoma shale stabilized with 6 percent lime ranged from 0.18 to 0.25.

In a study of lime-fly ash stabilized bases and subbases reported by NCHRP (1976), the ratio of flexural strength to compressive strength for most lime-fly ash-aggregate mixtures ranged from 0.18 to 0.25. Laguros and Medhani (1984), in their study of fly ash stabilized shales, reported these values to be in the range of 0.17 to 0.25.

2.5 Electron Microscopy

Over the years the need for higher resolution made it necessary to consider an electron source, rather than light, as the illumination source. Depending on whether the electrons are detected after being reflected by or transmitted through the specimen, electron microscopes are classified as transmission electron microscopes (TEM) or scanning electron microscopes (SEM). Figure 2.2 presents a schematic diagram of light microscope (LM), TEM and SEM.

Extensive use has been made of SEM in the study of

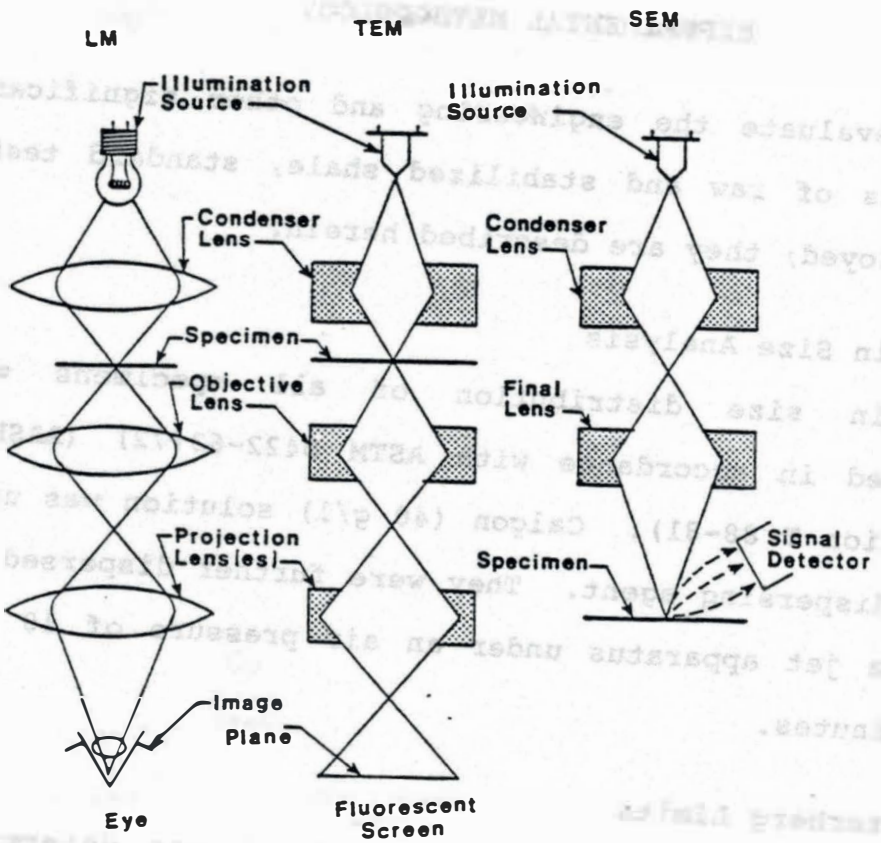

Figure 2.2: Comparison ray diagrams of light microscope, and transmission and scanning electron microscopes (after Postek et al., 1980)

CHAPTER IV

EXPERIMENTAL METHODOLOGY

To evaluate the engineering and other significant properties of raw and stabilized shale, standard tests were employed; they are described herein.

4.1 Grain Size Analysis

Grain size distribution of all specimens was determined in accordance with ASTM D422-63(72) (AASHTO Designation T 88-81). Calgon (40 g/l) solution was used as the dispersing agent. They were further dispersed by the Iowa jet apparatus under an air pressure of 10 psi for 5 minutes.

4.2 Atterberg Limits

The liquid limit of the specimens was determined according to ASTM D423-66(72) (AASHTO Designation T 89-81), and the plastic limits were determined in accordance with ASTM D424-59(71) (AASHTO Designation T-90-81).

Sloane (1964), utilized an electron microscope to study the early reaction between calcium hydroxide - kaolinite system. He observed the progressive dissolution of the kaolinite particles along the edges from the first 24 hours of treatment to the conclusion of the study i.e. after 15 days of treatment.

Mitchell and ElJack (1965), observed the fabric changes accompanying the hardening of soil-cement by electron microscope. They noticed that;

> "The fabric changes developing during the curing of soil-cement lead from a mixture of discrete soil particles and cement grains to a more homogeneous fabric of indistinguishable components".

Another study, Ormsby and Kinter (1973), utilized SEM for the identification of lime-clay reaction products. Unfortunately they could not identify any. However, based on their X-ray analysis of lime-montmorllonite-water system they concluded that CSH (gel) are the reaction products responsible for strength improvement in cured montmorillonite-lime mixtures.

Laguros and Medhani (1984), in their study of Oklahoma shales, utilized SEM to study the pore distribution and reaction products of stabilized shale. They reported that, as a result of stabilization, the shale revealed a dense packing of particles thereby reducing the open spaces or voids which led to increased unconfined compressive strength.

2.6 X-Ray Diffraction

Since its discovery in 1895 by the German physicist Roentgen, X-rays have provided the physicists and engineers a viable means of studying the internal structure of opaque objects.

X-ray diffraction has long been used to study the hydration products of soil-cement and soil-lime systems. Table 2.2 presents a summary of d-spacings for clays, lime-clay and cement-clay reaction products. Detailed literature review of the application of X-ray diffraction in soil-stabilization is given by Laguros and Medhani (1984). In many cases, X-ray diffraction analyses are performed on pure clay minerals stabilized with lime or cement under strict laboratory conditions. X-ray diffraction of field specimens is rare. One such study was done by Eades et al. (1962), in which they analyzed lime-stabilized field specimens using X-rays. They concluded that the increase in strength of soil-lime is partially due to formation of new materials, such as calcium silicate hydrates. They also reasoned that if the permanence of strength in Portland cement concrete is due to hydrated calcium silicates, then it must follow that lime-stabilization of soils by virtue of having the same hydration products would show permanence in strength.

Laguros and Medhani (1984), in their study of stabilization of Oklahoma shales, reported that hydrated lime

Table 2.2. Summary of Clays, Lime-Clay and Cement-Clay Reaction Products

Crystal	d-spacing, Å				Reference
Chlorite	14.00 4.70	7.18 3.60	7.02 3.50	4.80	ASTM (1966)
Kaolinite	7.18	3.58	2.50		ASTM (1966)
Illite	9.99-10.40	3.34			Carroll (1970) Grim (1968
Montmorillonite	15.40 (variable) 2.56	3.09	4.48	3.34	Carroll (1970), Ruff & Ho (1966)
Quartz	4.26	3.34	2.46		ASTM (1966)
Lime, Portlandite ($Ca(OH)_2$)		4.90	2.63	1.93	ASTM (1966)
Calcite ($CaCO_3$)	3.04	2.29	2.10		ASTM (1966)
Lime-Kaolinite	5.09	3.04	2.80	1.80	Eades and Grim (1962)
Lime-Montmorillonite	8.11	7.94	7.59		Hilt and Davidson (1961) Glenn and Handy (1963)
CAH	8.10	7.60	3.90		Noble (1967)
C_3AH	8.30	8.07	7.70		Noble (1967)
C_4AH_n	7.50	4.10	3.99	2.88	Ruff and Ho (1966)

(continued)

Table 2.2. Summary of Clays, Lime-Clay and Cement-Clay Reaction Products (continued)

Crystal	d-spacing, Å				Reference
CSH	17.30	12.60	10.00	3.08	Leonard and Davidson Glenn and Handy (1963)
C_3SH, Tobermorite	14.00 3.05 1.82	9.00 3.00	6.16 2.83	3.18 2.73	Glenn and Handy (1963) Ruff and Ho (1966) Taylor (1966)
C_2S	2.88				Taylor (1966)
C_3S	3.07	2.98	2.77		Herzog and Mitchell (1963)

(after Laguros and Medhani, 1984)

(6 percent) stabilization produced calcium aluminum silicate hydrate; fly ash (25 percent) stabilization produced tetracalcium aluminum silicate hydrate, calcium aluminum silicate and tricalcium silicate; and cement (14 percent) stabilization gave hydrated forms of calcium aluminum and calcium silicate.

CHAPTER III

FIELD TEST SECTIONS, MATERIALS AND SAMPLING

The main purpose of this investigation was to identify the differences between the laboratory and field behavior of stabilized shale.

The Oklahoma Department of Transportation in cooperation with the University of Oklahoma chose a portion of the southbound lanes of 4-lane divided U.S. 77, north of Ponca City, Kay County, Oklahoma, Project No. F-20(36), as the site for a field test section (Figure 3.1). The experiment was carried out in two phases. Phase I was a laboratory study of the stabilization of the shale found in the project area (Laguros and Medhani, 1984), and it was concluded that Portland cement (14 percent), hydrated lime (6 percent), fly ash (25 percent), and the conjunctive use of 8 percent cement + 4 percent hydrated lime + 18 percent fly ash can successfully stabilize this shale.

Phase II of the project, which covers the field implementation, is the subject of this study.

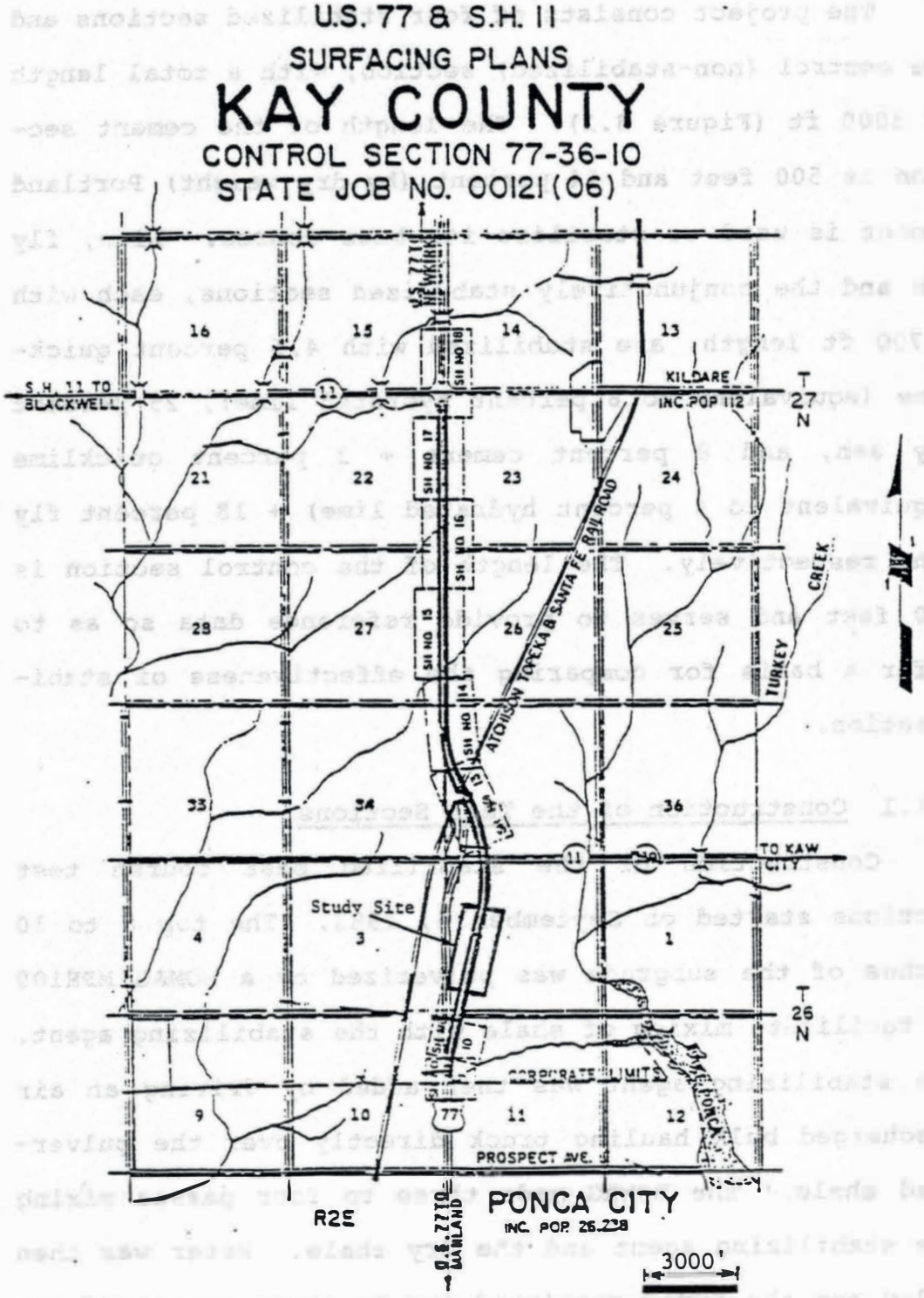

Figure 3.1: Location of study site

3.1 Field Test Sections

The project consists of four stabilized sections and one control (non-stabilized) section, with a total length of 3000 ft (Figure 3.2). The length of the cement section is 500 feet and 14 percent (by dry weight) Portland cement is used to stabilize its base course. Lime, fly ash and the conjunctively stabilized sections, each with a 700 ft length, are stabilized with 4.5 percent quicklime (equivalent to 6 percent hydrated lime), 25 percent fly ash, and 8 percent cement + 3 percent quicklime (equivalent to 4 percent hydrated lime) + 18 percent fly ash, respectively. The length of the control section is 400 feet and serves to provide reference data so as to offer a basis for comparing the effectiveness of stabilization.

3.1.1 Construction of the Test Sections

Construction of the stabilized base course test sections started on September 6, 1983. The top 8 to 10 inches of the subgrade was pulverized by a BOMAG MPH100 to facilitate mixing of shale with the stabilizing agent. The stabilizing agent was then added by driving an air discharged bulk hauling truck directly over the pulverized shale. The BOMAG made three to four passes mixing the stabilizing agent and the dry shale. Water was then added and the BOMAG continued two to three passes of wet mixing. The shale-stabilizing agent was further blade

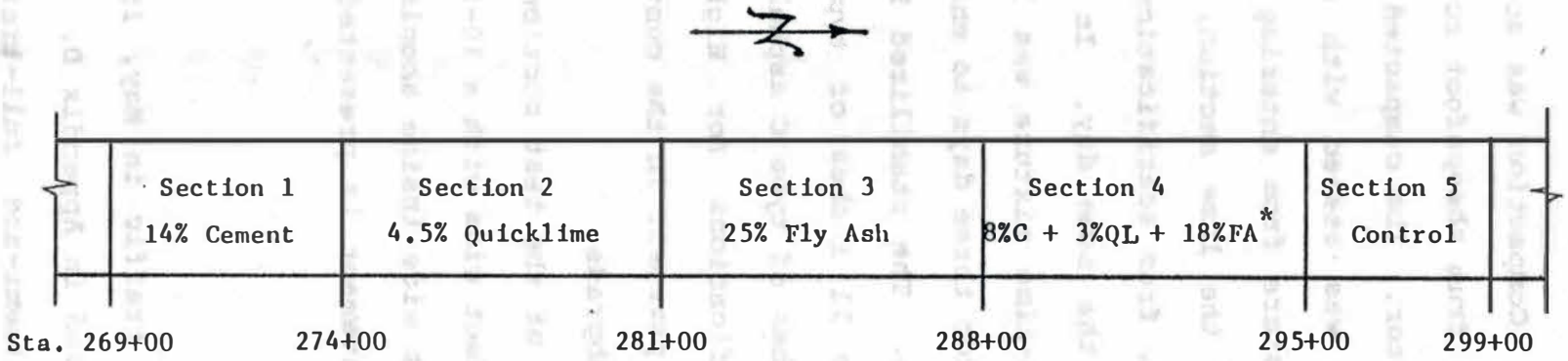

* C = Cement
QL = Quicklime
FA = Fly Ash

Figure 3.2: Location of test sections

mixed between each BOMAG mixing. Compaction was accomplished by a tractor towed double drum sheepsfoot roller followed by a rubber tired compactor. The compacted material was kept moist until it was sealed with SS-1 emulsion material to prevent moisture from entering the pavement. With the exception of the lime section, the entire construction activity, i.e. from scarification to compaction, was accomplished on the same day. In the lime section, however, the shale-lime mixture was left uncompacted but maintained moist for three days to ensure "rottening" of lime in the shale. The stabilized base course was then covered by 8 to 11 inches of type A asphaltic concrete and 2 to 3 inches of type C asphaltic concrete (ODOT, Standard Specifications for Highway Construction, 1976, p. 365). The pavement in the control section rests directly over the subgrade.

The top finished grade width of the test section is 38 feet. The driving lane is 24 feet wide with a 10-foot wide outside shoulder and a 4-foot wide inside shoulder. A typical cross-section of the pavement is presented in Figure 3.3.

3.1.2 Traffic Statistics

The test sections opened to traffic in May, 1984. The traffic statistics are presented in Appendix D. The data show that heavy trucks (semi-and full-trailer combinations) comprise about three percent of the total

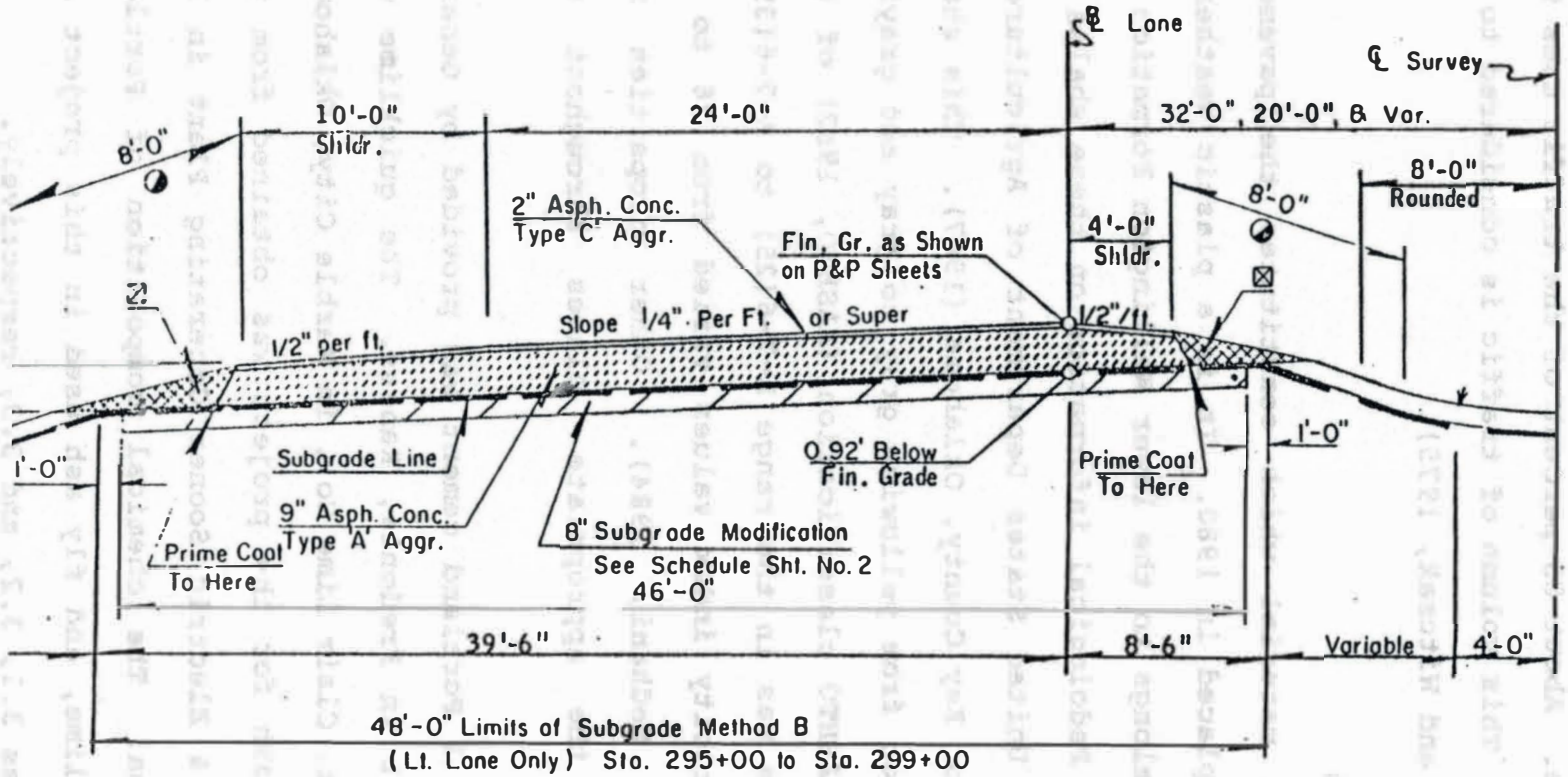

Figure 3.3: Typical cross-section of stabilized test section

traffic volume. About 85 percent of the traffic uses the outside lane. This volume of traffic is considered to be medium (Yoder and Witczak, 1975).

3.2 Materials

The fill material which constitutes the pavement subgrade was placed in 1980. It is a plastic weathered shale which belongs to the lower Wellington Formation of Permian age. Pedological information on these shales is found in the United States Department of Agriculture's Soil Survey for Kay County, Oklahoma (1967). This shale varied in color from yellowish gray to gray and grayish brown. The AASHTO classification (AASHTO, 1982) of the subgrade shale was in the range A-7-6(25) to A-7-6(39), and the plasticity index values varied from 26 to 37 (Laguros and Medhani, 1984). Other properties are reported in the appropriate places throughout the report.

The type I Portland cement was provided by General Portland Plant in Fredonia, Kansas. The quicklime was supplied by St. Clair Lime Co., in Marble City, Oklahoma, and the fly ash for the project was obtained from the Oklahoma Gas & Electric Sooner Generating Plant in Red Rock, Oklahoma. The chemical composition of Portland cement, quicklime, and fly ash used in this project are shown in Tables 3.1, 3.2, and 3.3, respectively.

Table 3.1. Chemical Composition of Type I Portland Cement, from General Portland Plant, Fredonia, Kansas *

SiO_2	20.86%
Al_2O_3	5.66%
Fe_2O_3	2.89%
CaO	63.49%
MgO	2.17%
SO_3	2.70%
Na_2O	0.16%
K_2O	0.62%
Loss on Ignition	0.12%

* Based on telephone conversation with Mr. Larry Parker, Control Manager

Table 3.2. Chemical Composition of Quicklime, From St. Claire Lime Co., Marble City, Oklahoma *

CaO	96.4%
MgO	1.1%
SiO_2	0.7%
Fe_2O_3	0.1%
Al_2O_3	0.13%
SO_3	0.04%
Loss on Ignition	1.5%

* Based on telephone conversation with Mr. Don Stuart, Sales Representative

Table 3.3. Chemical Composition of Fly Ash*, from Oklahoma Gas & Electric Sooner Generating Plant, Red Rock, Oklahoma

SiO_2	33.31%
Al_2O_3	23.09%
Fe_2O_3	7.91%
SO_3	2.67%
CaO	27.53%
MgO	5.14%
Na_2O	0.37%
Loss on Ignition	0.16%

* Composite figures for December, 1983

Table 3.4. Sampling Location of Stabilized Material

Test Section	Station		Offset Distance from Centerline ft
	Construction	Field	
Control	298+05	298+05	6 L
Cement Stab.	269+22	-	5 L
	272+37	272+37	10.3 R
Lime Stab.	275+46	275+46	1.8 R
	279+64	-	4.5 L
Fly Ash Stab.	284+60	-	11.8 R
	285+36	285+36	5.5 L
Conjunctively Stab.	289+22	289+22	3.4 R
	292+89	-	10.2 L

3.3 Sampling

Sampling locations were determined based on statistical randomness, and are depicted in Table 3.4. Sampling was carried out in two phases.

3.3.1 Construction Samples

Immediately after final mixing and before compaction, samples were retrieved from two locations in each stabilized section (Table 3.4), and transferred to the field laboratory for molding. These samples later were transported to the laboratory for testing after curing periods of one, six, twelve, and twenty two months. Figure 3.4 depicts a flow chart of sampling and testing sequence of stabilized construction samples.

3.3.2 Field Samples

These samples were obtained from under the pavement. They were taken one, six, eighteen, and twenty two months after the construction of the test sections. With the exception of the twenty two month cured samples which were obtained by hand auger, all others were obtained by coring. It should be noted that the curing period for field samples of the last observation is different from that of construction samples (twelve months). The reason being, that after twelve months of curing, a decision was made to postpone field sampling so as to allow more curing time for strength development of field samples.

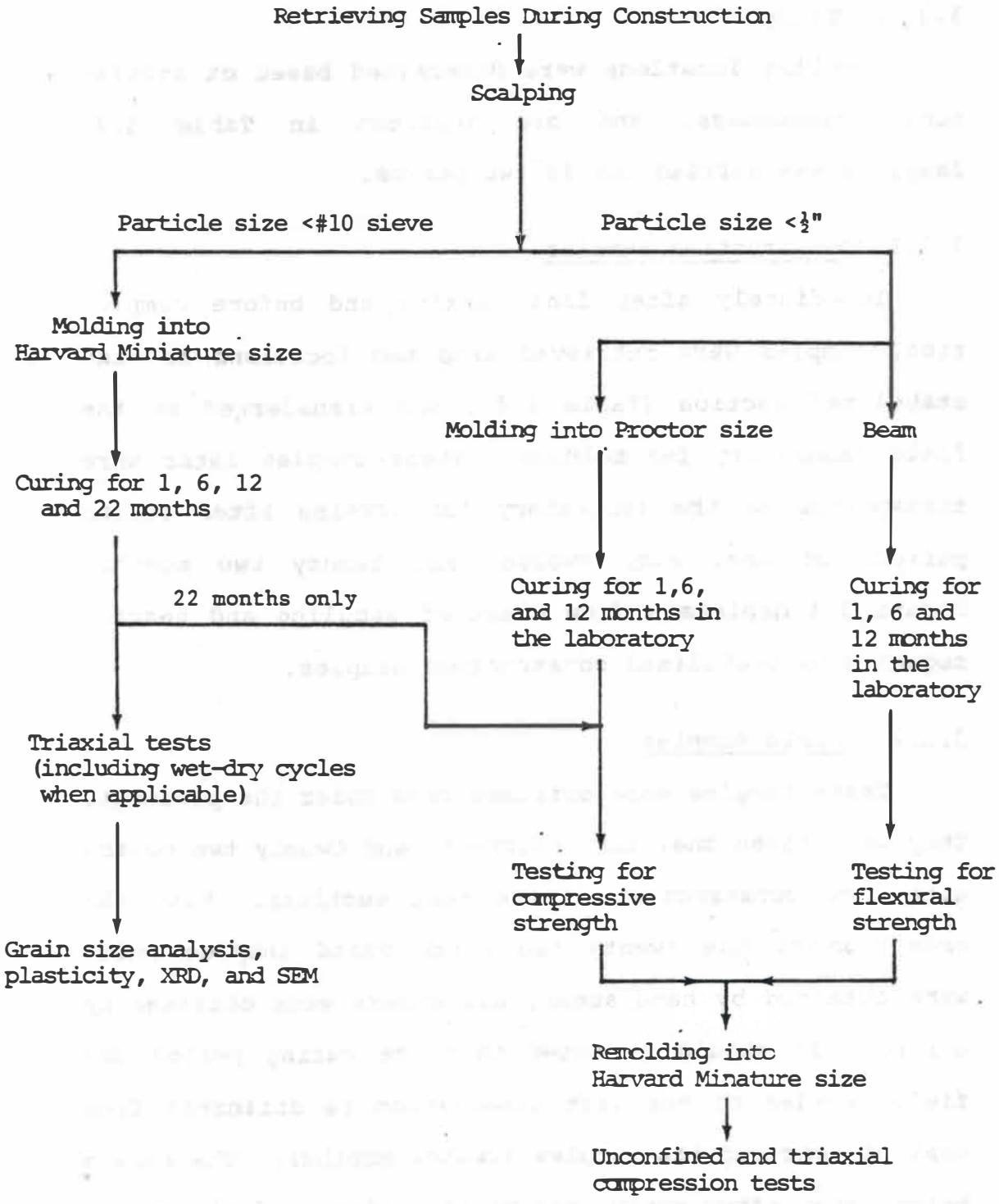

Figure 3.4: Flow chart of sampling and testing sequence of construction samples

To minimize pavement damage one sampling location per section was considered in this phase. The sampling locations of field samples were the same as those of construction samples (Table 3.4). Figure 3.5 depicts sampling and testing sequence of stabilized field samples.

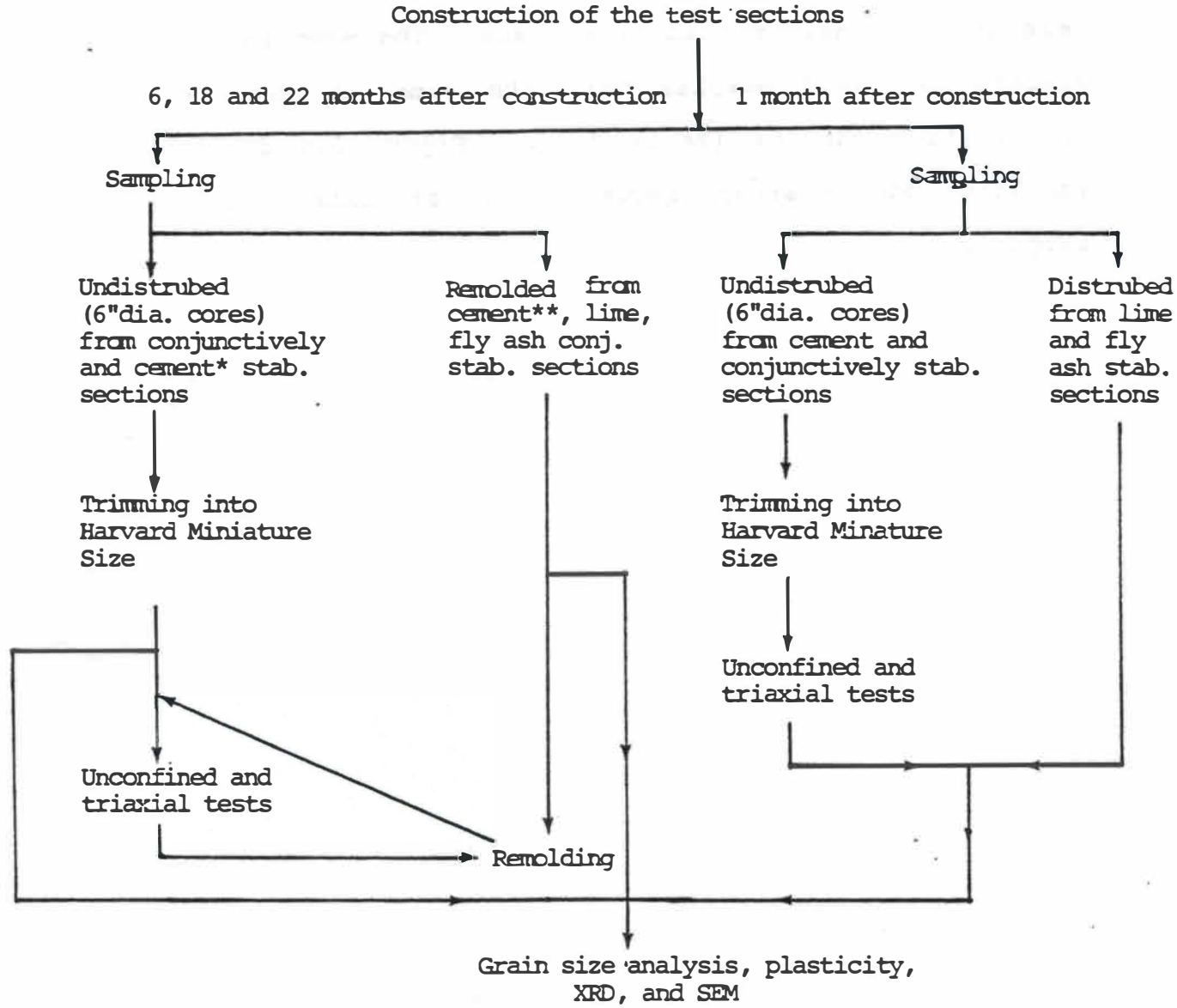

* after 6 months only

** after 18 and 22 months

Figure 3.5: Flow chart of sampling and testing sequence of field samples

CHAPTER IV

EXPERIMENTAL METHODOLOGY

To evaluate the engineering and other significant properties of raw and stabilized shale, standard tests were employed; they are described herein.

4.1 Grain Size Analysis

Grain size distribution of all specimens was determined in accordance with ASTM D422-63(72) (AASHTO Designation T 88-81). Calgon (40 g/l) solution was used as the dispersing agent. They were further dispersed by the Iowa jet apparatus under an air pressure of 10 psi for 5 minutes.

4.2 Atterberg Limits

The liquid limit of the specimens was determined according to ASTM D423-66(72) (AASHTO Designation T 89-81), and the plastic limits were determined in accordance with ASTM D424-59(71) (AASHTO Designation T-90-81).

4.3 Unconfined Compressive Strength

4.3.1 Construction Samples

Specimens for the unconfined compressive strength of construction samples were compacted in Standard Proctor molds using standard compaction effort (3 layers, 25 blows per layer) with the exception of twenty two month cured samples which were compacted into Harvard Miniature size. After the specimens were extracted from the mold, they were wrapped in plastic wrap and transferred to the laboratory for curing at 70°F and 90 to 100 percent relative humidity for one, six, twelve, and twenty two months. At the end of the curing periods, the specimens were unwrapped and tested for unconfined compressive strength.

4.3.2 Field Samples

The field samples, on the other hand, were cored from under the pavement, one, six, eighteen, and twenty two months after construction of the test sections. Due to the brittleness of lime and fly ash stabilized sections, it was not possible to obtain any undisturbed cores. So it was decided to remold the lime and fly ash stabilized field samples in the laboratory using a Harvard miniature mold and then test them. Therefore, all strength values (unconfined and triaxial) of lime and fly ash stabilized field samples reported pertain to

remolded samples. Cement and conjunctively stabilized sections, however, developed enough strength to withstand the coring action and six-inch diameter cores were obtained from these sections. The cores were then trimmed down to the size of a cylinder 1.3 inches in diameter and 2.8 inches in height. This procedure was not followed for the twenty two month cured samples. Since a hand auger was used for sampling, strength determinations were not made.

All the specimens were tested for compressive strength on a Soiltest Model AP-170B compression machine shown in Figure 4.1. The proving ring capacity of the machine was 10,000 pounds. Compressive strength tests were run on one specimen from construction samples and a minimum of two specimens from field samples.

4.4 Triaxial Compression Test

The shear parameters of cohesion (c) and angle of internal friction (ϕ) were evaluated employing triaxial compression. Pore water pressure measurements were not made because in the field the combination of rapid load application and small thickness of base course does not create a critical pore pressure build-up. Therefore, all values of ϕ and c were determined by the total stress method.

Triaxial compression tests were run on a minimum of

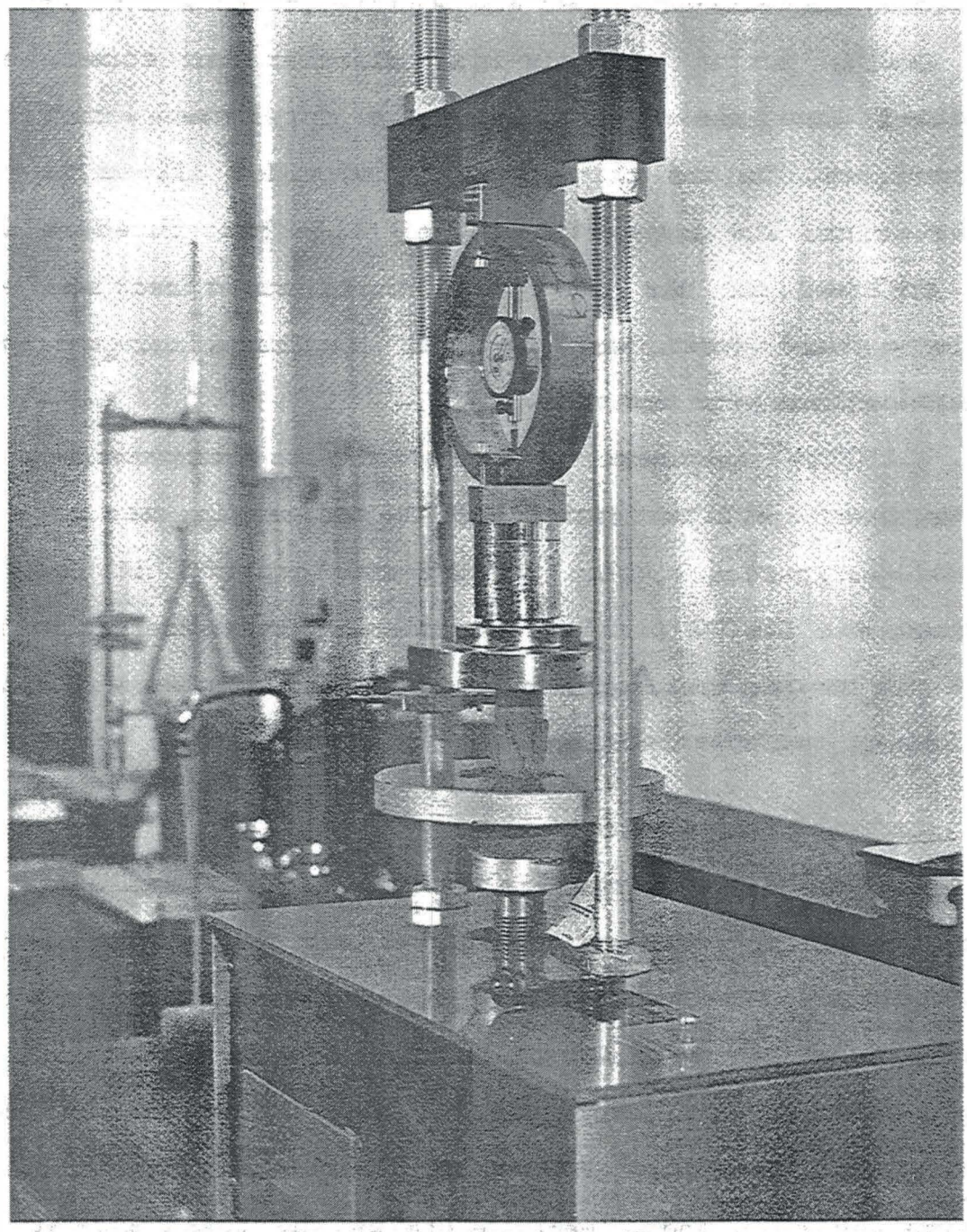

Figure 4.1: Compression strength testing device

two specimens in accordance with the ASTM D2850-70 (AASHTO Designation T 234-74).

4.4.1 Construction Samples

Specimens for the triaxial compression tests were compacted in the Harvard miniature apparatus from the portion of stabilized shale passing the U.S. Standard No. 10 sieve. The specimens were compacted in three layers with a compactive effort of 25 blows per layer using a 20 pound spring loaded press hammer. They were then wrapped in plastic wrap, and transferred to the laboratory for curing at 70°F and 90°F, at 90 to 100 percent relative humidity. At he end of the curing period, specimens were unwrapped and then tested.

4.4.2 Field Samples

Field samples were obtained the same way as for the unconfined compression test (Section 4.3.2). A Clockhouse triaxial machine (Figure 4.2) with a proving ring capacity of 2,000 pounds was used in the tests. The confining pressure was applied through a liquid mixture of glycerine and water. Different failure patterns of the specimens are depicted in Figure 4.3.

4.5 Wet-Dry Cycles

Weathering effects are simulated by subjecting the stabilized shale to cycles of wetting and drying.

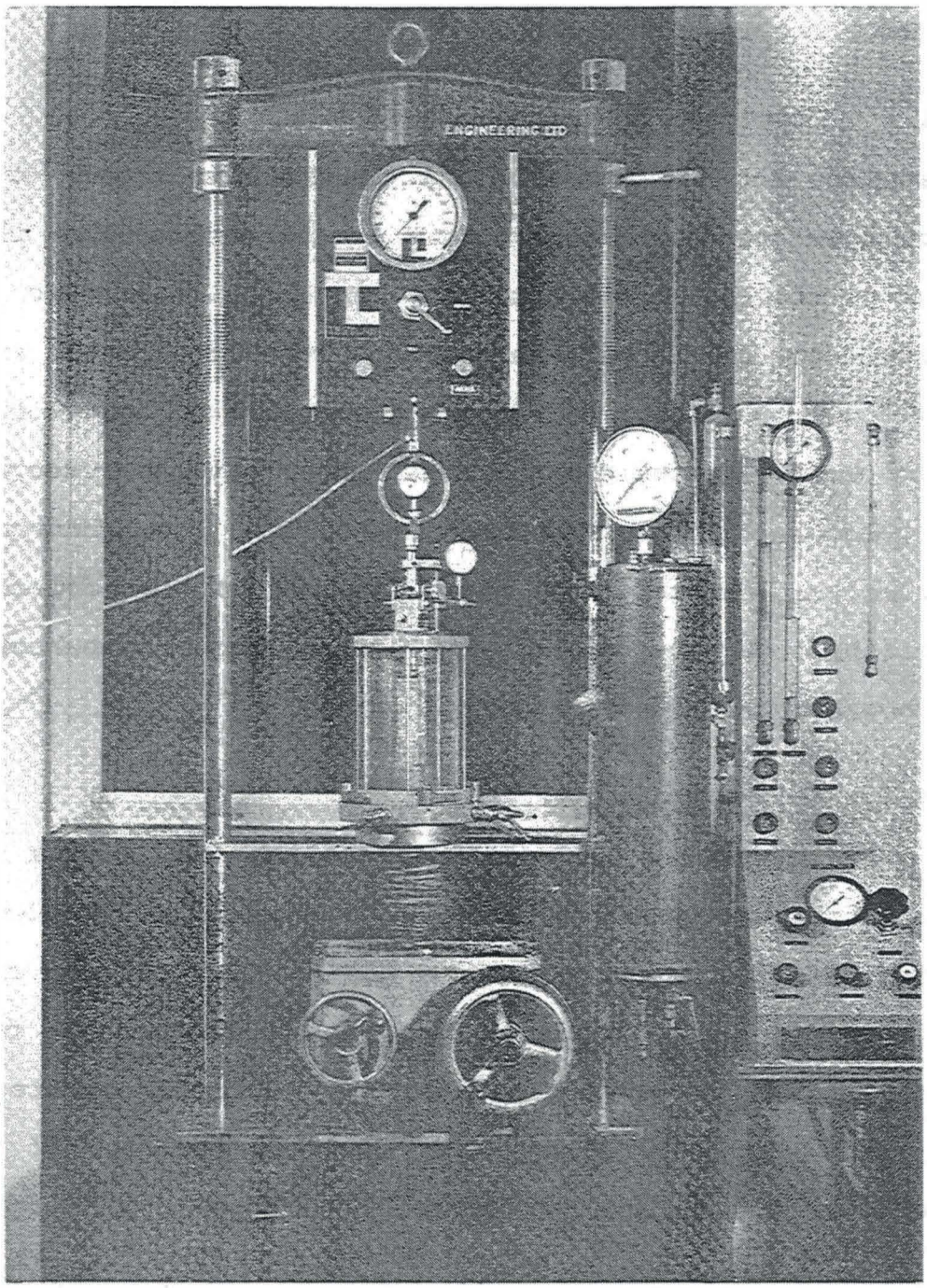

Figure 4.2: Triaxial compression test set up

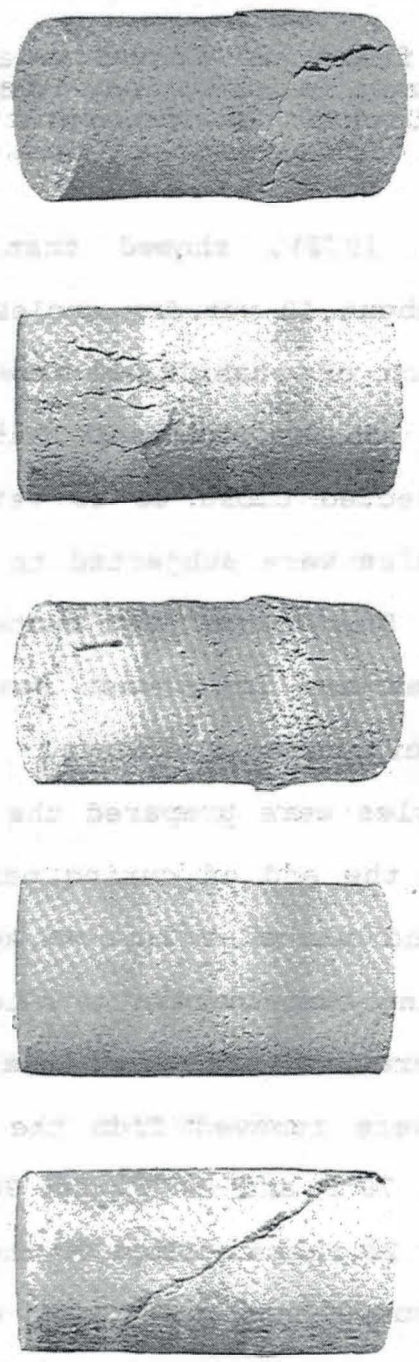

Figure 4.3: Failure patterns of triaxial samples

Laguros and Medhani (1984), defined the wet-dry cycle in the field as

> "A wet-dry cycle in the field is defined as a dry period in a 24 hour interval; rainfall less than 0.1 inches is disregarded unless it is continuous over two 24 hour periods with a total of at least 0.10 inches".

Wet-dry cycle data (Laguros, 1972), showed that Kay County, Oklahoma experiences about 40 wet-dry cycles per year. Between the construction of stabilized base and the placement of the pavement, it was estimated that the stabilized base would be subjected close to 15 wet-dry cycles. The construction samples were subjected to wet-dry cycles in the laboratory. Due to the high number of poor quality specimens the wet-dry cycle test was not performed on the twenty two month cured specimens.

Specimens for wet-dry cycles were prepared the same way as for triaxial test. At the end of curing periods the specimens were unwrapped and placed in an oven set at 140°F for 12 hours. The drying temperature is slightly more than the maximum temperature of open areas of Oklahoma. Then the samples were removed from the oven and put in humidifiers set at 70°F and 90°F, and 90-100 percent relative humidity, for 24 hours. This drying for 12 hours and wetting for 24 hours constituted one cycle (Laguros and Medhani, 1984). At the end of 15 cycles, specimens were tested in a triaxial machine in wet and dry conditions.

4.6 Flexural Strength

To study the effectiveness of stabilization under flexural loads, beams 16L x 4W x 3H inches were molded in the field laboratory as construction samples. The material was passed through U.S. Standard sieve with 1/2 inch opening. A precalculated amount of stabilized shale was forced into a steel mold using a plate for load transfer from a hydraulic jack. The beams were wrapped in plastic wrap and transferred to the laboratory for curing at 70°F, and 90-100 percent relative humidity. No attempt was made to retrieve any beam sample from under the pavement after construction.

At the end of the curing period the beams were unwrapped and tested in accordance with ASTM C78-75 which relates to the flexural strength of concrete using simple beam third point loading. Figure 4.4 shows the loading arrangement and failure mode of stabilized beams.

4.7 Pavement Deflection Measurements

Pavement deflections were measured with the Benkelman beam under a vehicle whose axle load was 18,000 lb. The apparatus is owned by ODOT and was operated by its personnel. The measurements were taken according to AASHTO Designation T256-77.

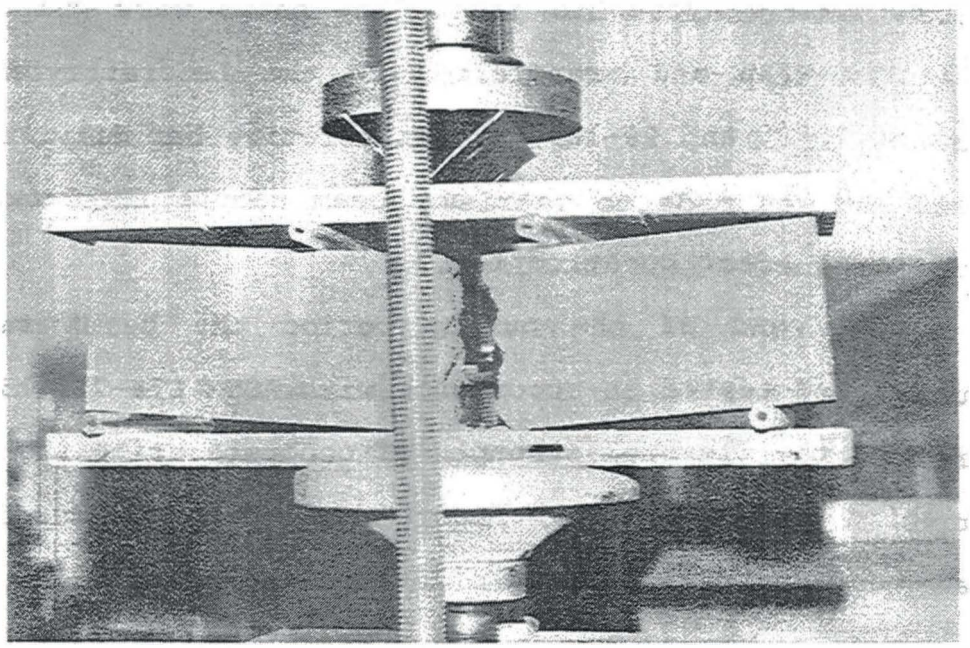

Figure 4.4: Load arrangement and mode of failure of stabilized beams

4.8 Scanning Electron Microscopy and Energy Dispersive Spectroscopy

Following the strength tests broken pieces of the specimens were collected and cut into thin slices. Care was exercised not to damage the failure plane. These specimens were soaked in acetone to halt the hydration process by evaporating the free water in the shale matrix (Laguros and Baker, 1984). The specimens were further dried in an oven at 110°C to remove any excess water and then glued to aluminum stubs with rubber cement. Using a TECHNICS sputter coater the specimens were coated with gold under a vacuum pressure of 110 to 120 millitor (1 millitor = 1μHg) to a depth of approximately 200 Å. The reason for coating with gold was to provide a conductive layer on the specimen surface. After coating the specimens were placed in an ETEC electron microscope with an operating voltage of 20 kv, to obtain photographic exposure of the specimen surface. The photographic packets used were self developing Polaroid type 665. Qualitative energy dispersive spectroscopy (EDS) (elemental analysis) of some of the selected specimens was carried out by a γPGT energy dispersive spectroscope connected to the electron microscope.

4.9 X-Ray Diffraction

To determine the mineralogical composition of raw and stabilized shale X-ray diffraction was utilized.

Material used for analysis was obtained from the specimens collected after strength tests which were treated with acetone and then dried in the oven at 110°C. The material was then ground and passed through U.S. Standard No. 200 sieve. To facilitate detailed analysis, specimens were studied both in random powder and oriented forms explained as follows:

1. Powder packed specimens were put in grooved aluminum slides and pressed by a glass plate. The slides were then put in a Siemens counter tube goniometer (diffractometer) which was operating under 35 kv and 18 ma. The rate of scan was set at 1 degree 2θ per minute. Cu Kα radiation (λ = 1.537 Å) was used. A Siemens KOMPENSOGRAPH X-T was utilized to record the pulses generated by the dector. The chart speed was set at 2 cm per minute. The specimens were scanned from 3° (2θ) to at least 50° (2θ). A number of selected specimens were tested by a Siemens D 500 diffractometer coupled to a LC 500 logic controller by using a PDP 11/23 minicomputer (256K RAM). Excellent agreement was observed with these two diffractometers.
2. Vacuum filtration technique was used to prepare oriented samples in this study. Sodium hexametaphosphate (calgon) was used as the dispersing agent. Optimum dispersion was evaluated by using various

concentrations of calgon (1g/l, 1g/l, 5g/l, 10g/l, 20 g/l) with the different treatments (lime, cement, fly ash, no treatment). The lowest concentration of calgon that effectively dispersed the majority of the samples was chosen as the "optimum"; this concentration was found to be 2 g/l. Dispersion was aided mechanically by air jetting the calgon + water + soil slurry for 10 minutes.

After air jetting was completed the soil slurry was diluted to 800 ml (total volume) in a 1 liter graduated cylinder and quickly remixed. Samples were allowed to settle for different time intervals to check the influence of time on the crystalline composition of the oriented samples. A sedimentation of 1 day was adopted as the "optimum" for all the samples. After the 24-hour sedimentation period the clay suspension was removed from the graduated cylinder and an oriented sample was prepared.

After dispersing the clay fraction, the vacuum filtration step, which produces the oriented specimen, takes only 5 to 10 minutes. Sample thickness can be controlled by overlaying several filtration runs if necessary. Due to the speed at which specimens can be prepared in the vacuum filtration technique, the difference in settling velocities of the various clay minerals, which can cause serious

nonhomogeniety problems in the sedimented slide technique, are negligible (Brindley and Brown, 1980). The specimens were deposited on 0.45 μm millipore filter paper and then transferred to a glass slide or a single crystal sample holder for X-ray analysis. All samples were air dried; some were glycolated and later subjected to heat treatment.

CHAPTER V

PRESENTATION AND DISCUSSION OF TEST DATA

Standard tests were employed to evaluate the engineering behavior of construction and field samples. These tests included moisture-density, grain size analysis, unconfined compressive strength, triaxial compressive strength, cyclic wet-dry, and beam tests. The results of these tests along with those of X-ray diffraction (XRD) and scanning electron microscopy (SEM) are presented and discussed in this chapter.

5.1 Moisture-Density

To ensure proper compaction of the stabilized test section, a Campbell Pacific Nuclear Gauge was used to run moisture-density tests (nuclear method). The results of these tests, which were run by the ODOT personnel, are given in Table 5.1. It is observed that all stabilized sections were compacted in excess of 100 percent of Proctor density. However, the moisture content in all cases fell short of the optimum. The six month data showed that the moisture content increased while the density slightly decreased with the exception of the lime

Table 5.1. Moisture-Density Test Results of Stabilized Test Sections Using Nuclear Apparatus

Test Section	Proctor Density (pcf)	Optimum Moisture Content (%)	During Construction			Six Months After Construction		
			Dry Density (pcf)	Moisture Content %	Percent Compaction	Dry Density (pcf)	Moisture* Content %	Percent Compaction
Control	97.4	23.7	105.1	15.4	108			
Cement	94.8	25.8	103.8	21.0	109	98.4	22.6	104
Lime	93.8	27.6	100.1	22.4	107	102.2	23.0	109
Fly Ash	97.4	23.7	100.3	11.6	103	97.0	23.0	99
Conjunctively Stabilized	91.3	28.0	96.8	20.7	106	96.3	24.2	105

* Determined in the laboratory

stabilized section which showed a small increase in density.

5.2 Grain Size Analysis

Grain size distribution curves of construction and field samples after one month of curing are presented in Figures 5.1 and 5.2, and the corresponding amounts of sand, silt and clay fraction are depicted in Tables 5.2 and 5.3. Grain size analysis data for other curing conditions are shown in Tables A1 and A2 in Appendix A. As evidenced from Figures 5.1 and 5.2, stabilization substantially increased the sand and silt fraction and decreased the clay fraction of the shale. To evaluate the effectiveness of stabilization on the texture of the shale, the numerical parameter aggregation index (AI) is used. This parameter, as defined by Laguros and Jha (1977), gives a numerical value to the degree of aggregation attained as a result of stabilization and it is mathematically expressed as:

$$AI = \frac{\text{Percent nonclay-size material of stabilized shale, } > 2\mu}{\text{Percent nonclay-size material of raw shale, } > 2\mu}$$

Table 5.4 presents the AI values of construction and field samples after one month of curing. AI values for other curing conditions are included in Tables A.1 through A.3 in Appendix A.

All stabilizing agents imparted a high degree of ag-

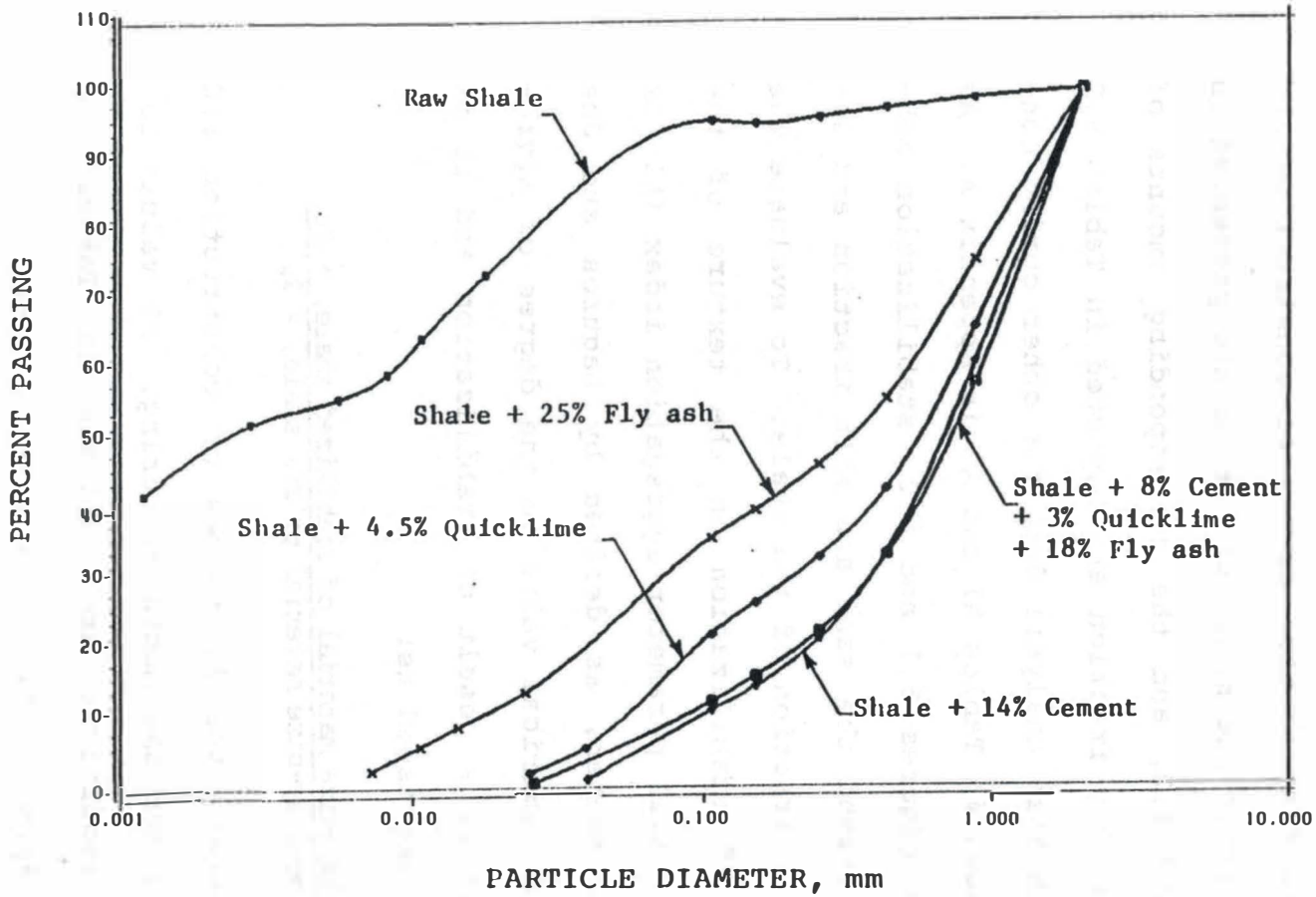

Figure 5.1: Grain size distribution curves of construction samples

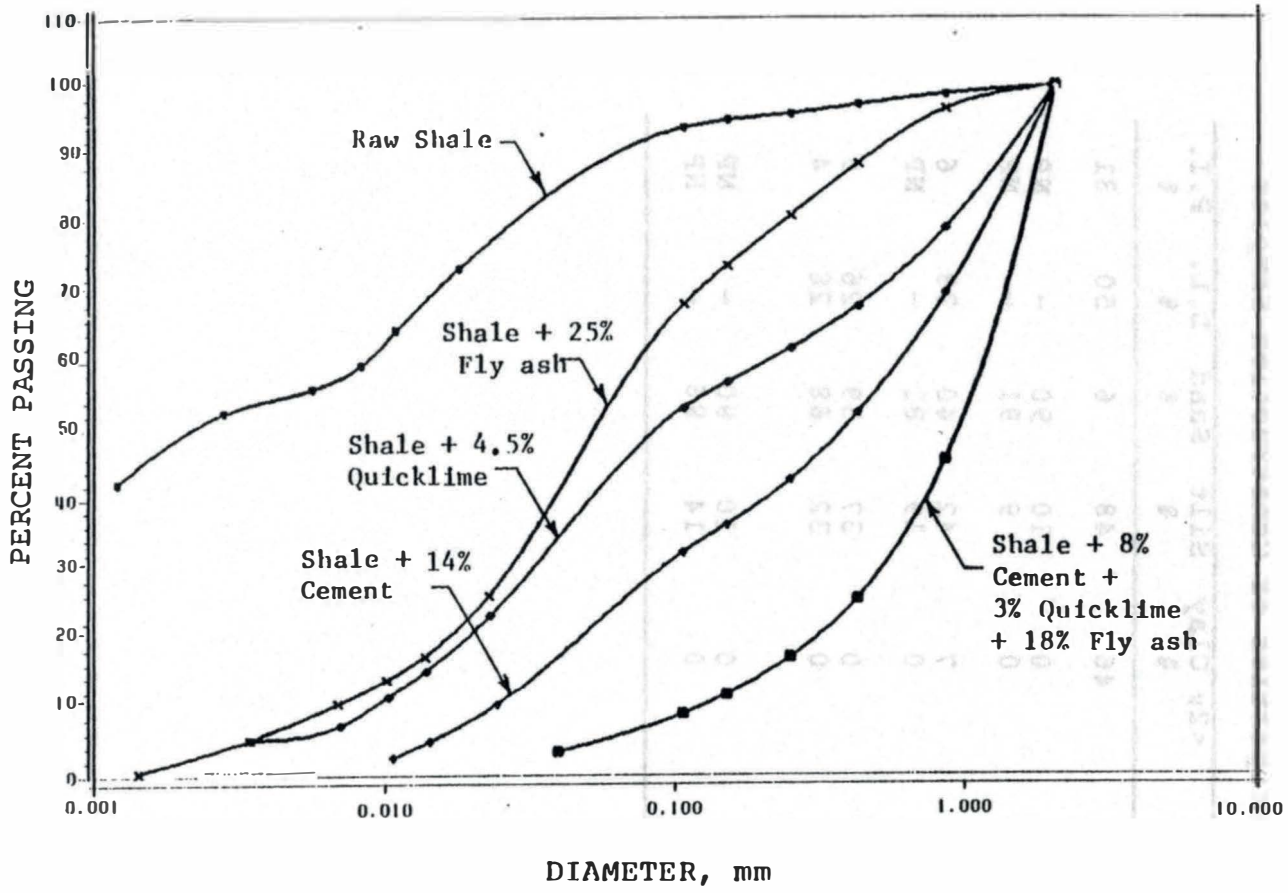

Figure 5.2: Grain size distribution curves of field samples

Table 5.2. Index Properties of Construction Samples

Test Section	Station	<2μ Clay %	Silt %	Sand %	L.L. %	P.I. %
Control	298+05	46	48	6	50	31
Cement Stab.	269+22	0	10	90	-	NP
	272+37	0	9	91	-	NP
Lime Stab.	275+46	7	42	40	38	6
	279+64	0	19	81	-	NP
Fly Ash Stab.	284+60	0	37	59	26	9
	285+36	0	32	68	28	4
Conjuctively Stab.	289+22	0	10	90	-	NP
	292+89	0	14	86	-	NP

Table 5.3. Index Properties of Field Samples

Test Section	Station	<2μ Clay %	Silt %	Sand %	L.L. %	P.I. %
Control	298+05	46	48	6	50	31
Cement Stab.	272+37	0	30	70	-	NP
Lime Stab.	275+46	0	44	37	37	15
Fly Ash Stab.	285+36	5	57	36	40	17
Conjunc-tively Stab.	289+22	0	7	93	-	NP

Table 5.4. Aggregation Index Values of Raw and Stabilized Shale

Test Section	Station	Construction Samples	Field Samples
Control	298+05	1.00	1.00
Cement Stab.	269+22	1.85	-
	272+37	1.85	1.85
Lime Stab.	275+46	1.52	1.85
	279+64	1.85	-
Fly Ash Stab.	284+60	1.85	-
	285+36	1.85	1.72
Conjunctively Stab.	289+22	1.85	1.85
	292+89	1.85	-

gregation (AI = 1.85) to the construction samples, with the exception of lime stabilized shale from Sta. 275+46 which showed an AI = 1.52 and may have been caused by the lower concentration of lime in this particular sample. The degree of aggregation of the field samples as reflected by their AI values were less than their construction counterparts. Cement, lime, and conjunctive stabilization imparted an equal degree of aggregation to the shale, while fly ash stabilization showed a slightly lesser effect compared to the other stabilizing agents.

5.3 Atterberg Limits

Cement, and conjunctive stabilization rendered the shale nonplastic. Lime stabilization reduced the plasticity index from a high value of 31 for raw shale to 6 at Sta. 275+46 and rendered the shale nonplastic at Sta. 279+64. Fly ash stabilization reduced the plasticity index to values below 9.

The effectiveness of stabilization on field samples as reflected by their plasticity indices was not as pronounced as it was on construction samples. Cement and conjunctive stabilization rendered the shale nonplastic. Lime and fly ash stabilization reduced the plasticity index values to 15 and 17, respectively. Plasticity data of construction and field samples after one month of curing are included in Tables 5.2 and 5.3. Data for other

curing periods are presented in Tables A.4 through A.6 in Appendix A.

5.4 Unconfined Compressive Strength

5.4.1 Construction Samples

Dry and immersed strengths of construction samples cured in the laboratory for one, six, twelve, and twenty two months are presented in Figures 5.3 through 5.6. In general, the addition of stabilizing agents increased the unconfined compressive strength values from a low of 16 psi for raw shale, to values ranging from 63 psi to 700 psi. Conjunctive stabilization imparted the highest level of strength to the shale followed by cement, lime, and fly ash stabilization in that order. The variation in strength of specimens from station to station is primarily due to the many variables in construction which make it difficult to have uniform strength values over the entire length of a section.

5.4.1.1 Cement Stabilization. The unconfined compressive strength of cement stabilized shale at Sta. 269+22 ranged from 131 psi (immersed) to 464 psi (dry). Immersion in water for 24 hours reduced the strength of these specimens from an average value of 378 psi to 329 psi. The pattern of the dry strength cannot be fully explained especially since it cannot be duplicated. On the other hand, the strength of specimens from Sta.

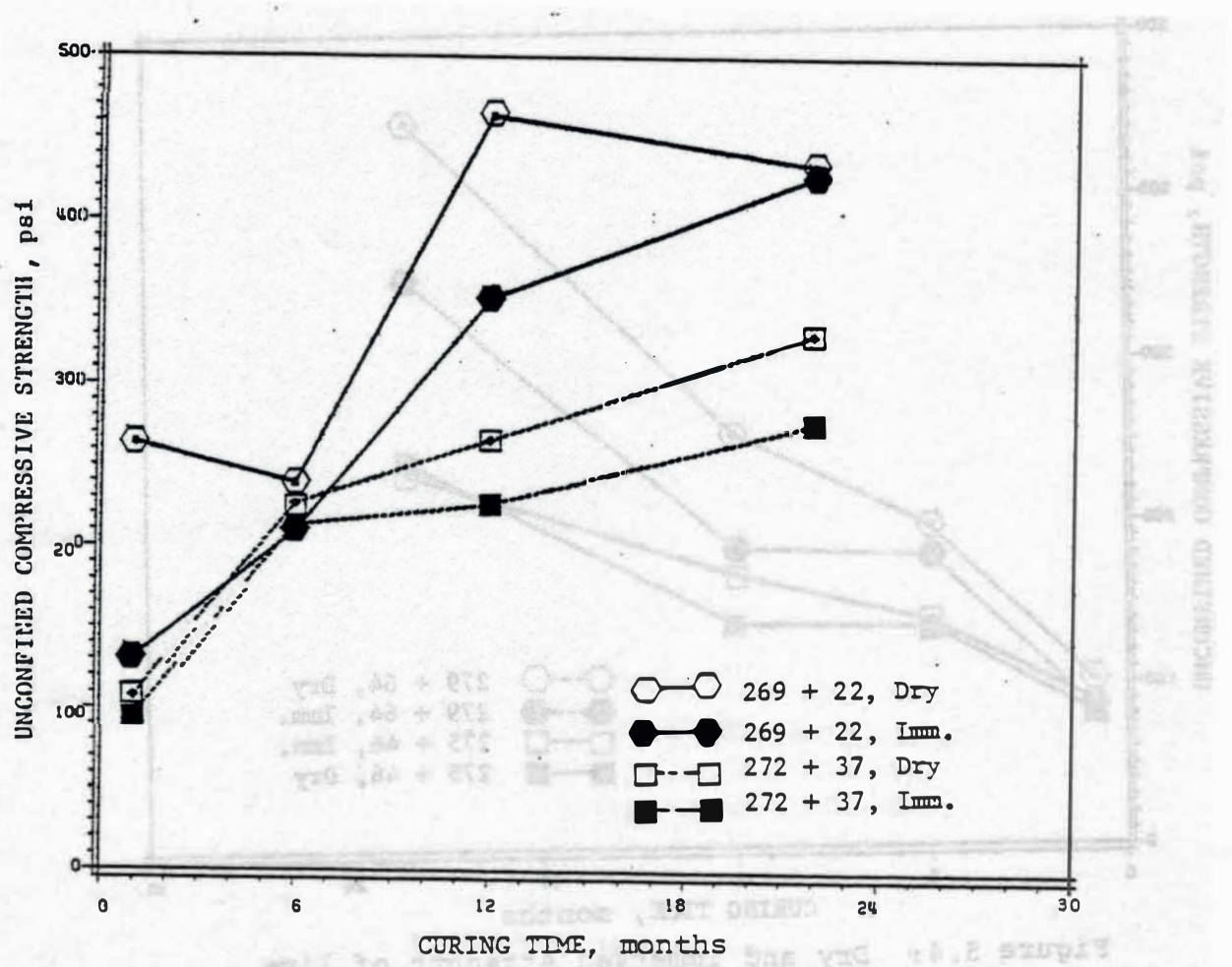

Figure 5.3: Dry and immersed strength of cement stabilized construction samples

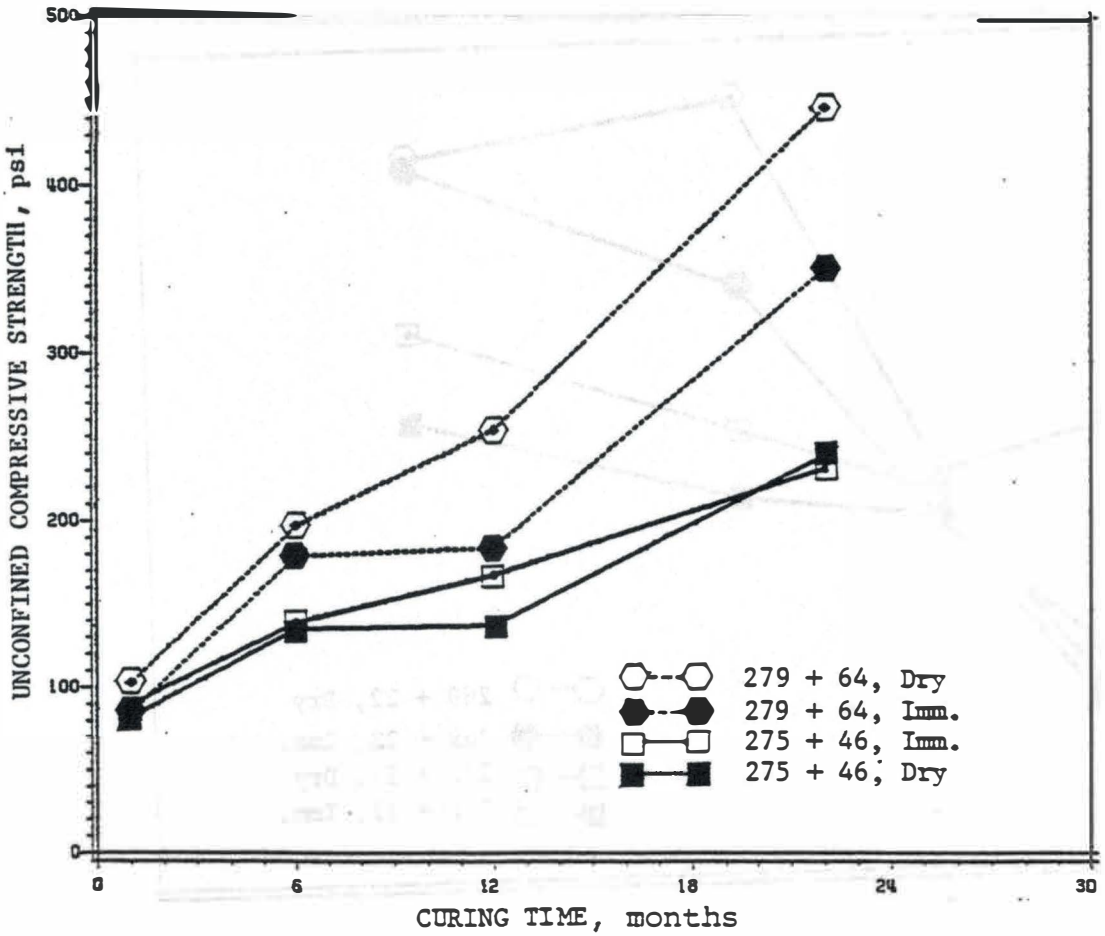

Figure 5.4: Dry and immersed strength of lime stabilized construction samples

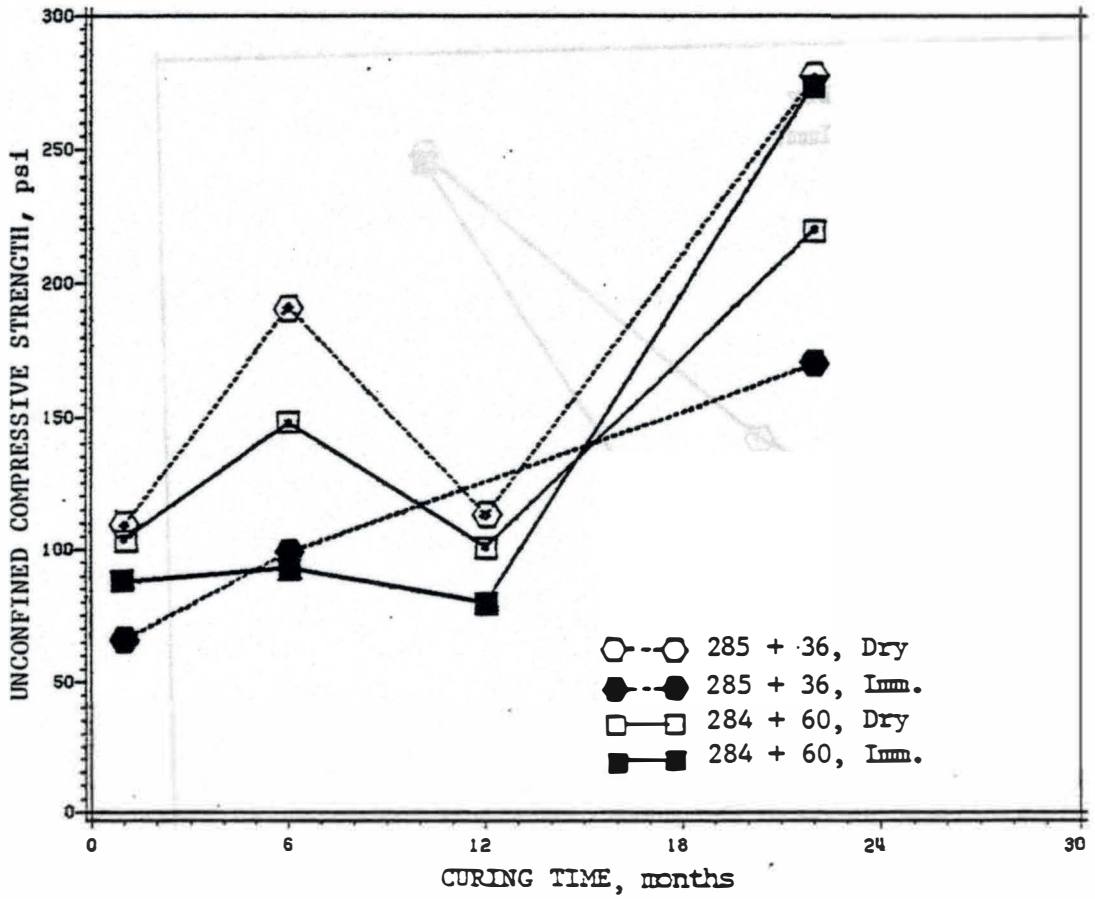

Figure 5.5 Dry and immersed strength of fly ash stabilized construction samples

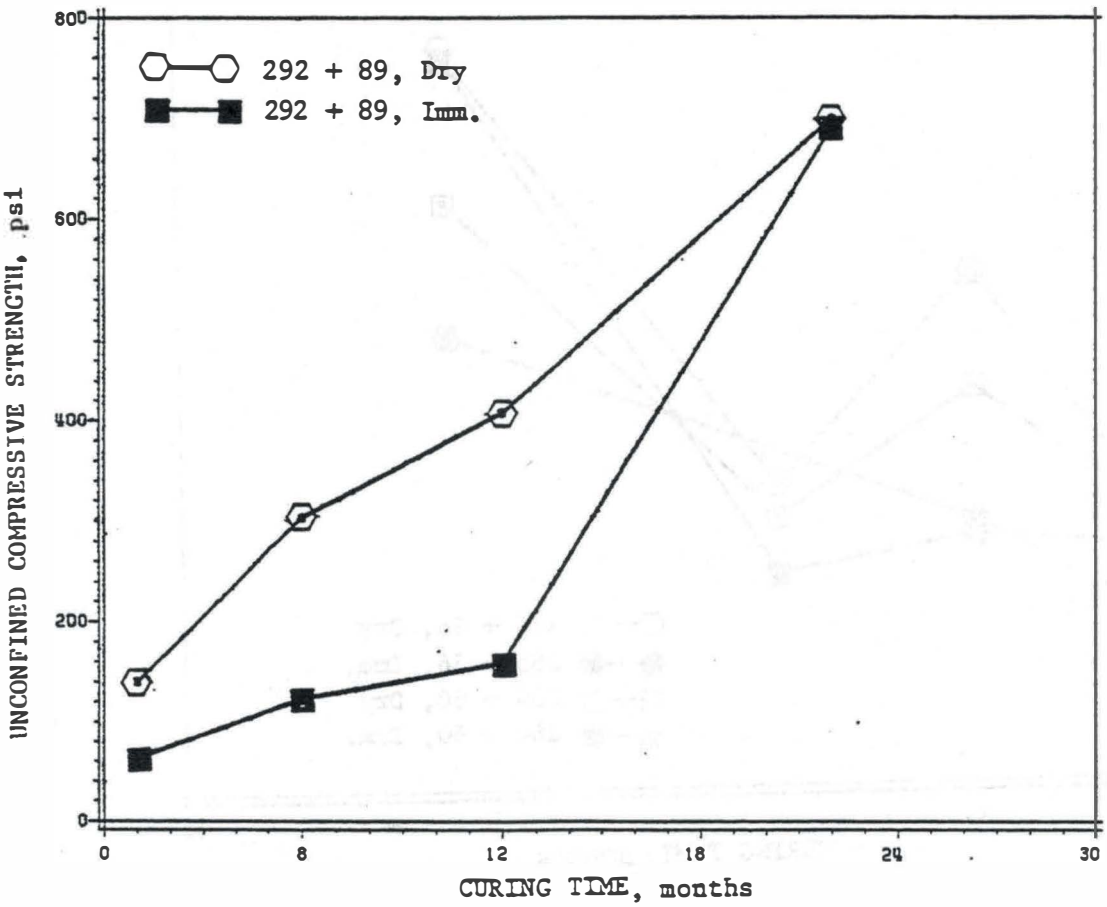

Figure 5.6: Dry and immersed strength of conjunctively stabilized construction samples

272+37 ranged from 95 psi (immersed) to 330 psi (dry). The strength of these specimens was reduced from an average value of 265 psi to 233 psi as a result of immersion in water for 24 hours. Specimens from this station showed a strength increasing pattern with curing time.

5.4.1.2 Lime Stabilization. The unconfined compressive strength of lime stabilized shale was lower than that of cement stabilized shale. Specimens from Sta. 275+46 showed unconfined compressive strength values ranging from 82 psi (immersed) to 239 psi (immersed). Immersion in water for 24 hours reduced the strength of these specimens from an average value of 182 psi to 178 psi. The strength of specimens from Sta. 279+64 ranged from 85 psi (immersed) to 446 (dry). Immersion in water for 24 hours reduced the strength of these specimens from an average value of 315 psi to 249 psi. The unconfined compressive strength of specimens from both stations showed an increasing pattern with curing time.

5.4.1.3 Fly Ash Stabilization. Shale stabilized with fly ash attained levels which were lower than that of lime stabilized shale. Specimens from Sta. 284+60 showed strength values ranging from 80 psi (immersed) to 1275 psi (immersed). The average level of strength upon immersion in water for 24 hours increased from 169 psi to 181 psi. The strength of specimens from Sta. 285+36

ranged from 66 psi (immersed) to 277 psi (dry). The average strength from this station as a result of immersion was reduced from 208 psi to 126 psi. The 12-month immersed strength of samples from this station could not be evaluated because the specimens were cracked before testing.

5.4.1.4 Conjunctive Stabilization. Most specimens from the conjunctively stabilized section developed hair cracks especially those obtained from Sta. 289+22. Specimens obtained from this station after one month of curing showed a strength value of 92 psi (not shown in the figure) in dry conditions which is hardly a representative value. The strength of specimens obtained from Sta. 292+89 ranged from 63 psi (immersed) to 659 psi (dry). Immersion in water for 24 hours reduced the strength of these specimens from an average value of 472 psi to 334 psi.

5.4.2 Field Samples

5.4.2.1 Undisturbed Samples. As mentioned earlier (Section 4.2.3) undisturbed samples could only be obtained from cement and conjunctively stabilized sections. The unconfined compressive strengths of these samples are depicted in Figure 5.7. For reasons explained in Section 4.2.3, no undisturbed samples were obtained from these sections after twenty two months of curing. The data show that conjunctively stabilized shale attained a

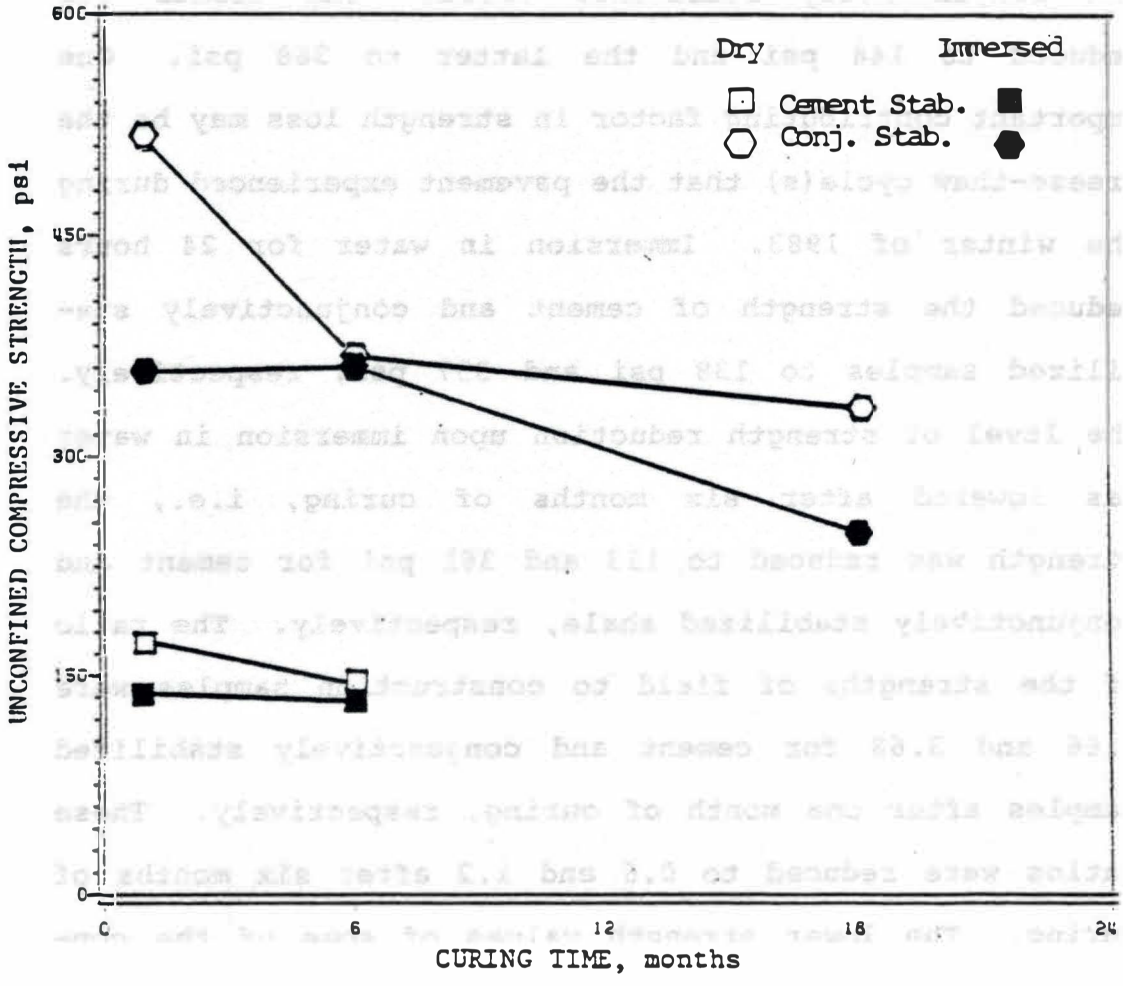

Figure 5.7: Dry and immersed strengths of undisturbed field samples

strength level of 515 psi after one month of field curing while for the same time period, cement stabilized shale showed a strength value of 174 psi. Longer curing periods (six months) reduced the strengths of both cement and conjunctively stabilized shale. The former was reduced to 144 psi and the latter to 368 psi. One important contributing factor in strength loss may be the freeze-thaw cycle(s) that the pavement experienced during the winter of 1983. Immersion in water for 24 hours reduced the strength of cement and conjunctively stabilized samples to 138 psi and 357 psi, respectively. The level of strength reduction upon immersion in water was lowered after six months of curing, i.e., the strength was reduced to 133 and 361 psi for cement and conjunctively stabilized shale, respectively. The ratio of the strengths of field to construction samples were 0.66 and 3.68 for cement and conjunctively stabilized samples after one month of curing, respectively. These ratios were reduced to 0.6 and 1.2 after six months of curing. The lower strength values of some of the conjunctively stabilized construction samples as compared to their field counterparts could be traced to the development of hair cracks in the construction samples which resulted in lower strength values.

5.4.2.2 Remolded Samples. Lime and fly ash stabilized sections did not develop enough strength to withstand the

shear stresses induced from coring, and thus no undisturbed samples could be obtained from these sections. However, it was decided to remold these samples and predict their unconfined compressive strength utilizing the principles of sensitivity and remolded strength. Sensitivity in soil mechanics is defined as "the ratio of the strength of the soil in the undisturbed state to that of the soil in the remolded state" (Spangler and Handy, 1982).

Table 5.5 depicts the remolded strengths and sensitivity of construction and field samples. The remolded specimens could not withstand immersion in water; therefore, they were tested in dry condition. Remolding reduced the strength of all samples to values below 45 psi. After six months of curing the sensitivities of cement, lime, and fly ash stabilized construction samples were about 5 (Table 5.6), while that of conjunctively stabilized construction samples was 13. Cement and conjunctively stabilized field samples showed sensitivities of 8 and 14, respectively. Sensitivity values of lime and fly ash stabilized field sample after six months of curing were interpolated from the sensitivities of cement and conjunctively stabilized field sample and the relationship that exists among the sensitivity value of construction samples. Sensitivities of the eighteen month cured field samples were extrapolated from the sensitivity of

Table 5.5. Remolded Strength (psi) and Sensitivity of Stabilized Samples for the Indicated Curing Periods

Stabilized Test Section	Construction											
	6 months		18 months		22 months		6 months		18 months		22 months	
	Rem. St.	S*	Rem. St.	S*	Rem. St.	S*	Rem. St.	S*	Rem. St.	S*	Rem St.	S*
Cement	44	5	27	-	-	-	18	8	12	13†	-	
Lime	34	4	30	-	16	-	33	4.4**	31	7†	26	
Fly Ash	35	5	32	-	28	-	42	5.5**	8	9†	28	
Conjunctively Stabilized	23	13	23	-	-	-	26	14	9	37		

* S = Sensitivity

** interpolated

† extrapolated

Table 5.6 Shear Parameters of Remolded Samples for the Indicated Curing Periods

Test Section	Construction				Field					
	6 Months		18 months		6 months		18 months		months	
	c	ϕ	c	ϕ	c	ϕ	c	ϕ	c	ϕ
Raw Shale	4	36								
Cement	10	30	8	24	6	31	1	39	*	
Lime	8	31	10	30	14	33	3	36	11	25
Fly Ash	16	21	8	31	12	31	1	18	5	39
Conjunctively Stabilized	6	38	3	36	0	40	8	33	*	

* Because of high strength and brittleness it was not possible to retrieve sufficient amount of sample by a hand auger.

conjuctively stabilized field sample. This procedure could not be followed for the 22 month cured samples, because it was not possible to retrieve enough sample from cement and conjunctively stabilized sections by a hand auger. Utilizing the remolding strength and sensitivity values (Table 5.5), the undisturbed strength of lime and fly ash stabilized field samples were calculated and depicted in Figure 5.8. These values are within the range of strength values of construction samples discussed in sections 5.4.1.2 and 5.4.1.3.

5.5 Triaxial Compression

The shear strength parameters, cohesion (c) and angle of internal friction (ϕ), of raw and stabilized shale were determined from the results of triaxial compression test, using the stress path method. If σ_1 and σ_3 are the major and minor principal stresses, the stress path parameters p and q are given by

$$p = (\sigma_1 + \sigma_3)/2$$

$$q = (\sigma_1 \quad \sigma_3)/2$$

The failure envelope obtained from p-q (Figure 5.9) is referred to as K_f line. The conventional shear strength parameters c and ϕ may be calculated from the following relations:

$$\phi = \sin^{-1} (\tan\alpha)$$

$$c = a/(\cos\phi)$$

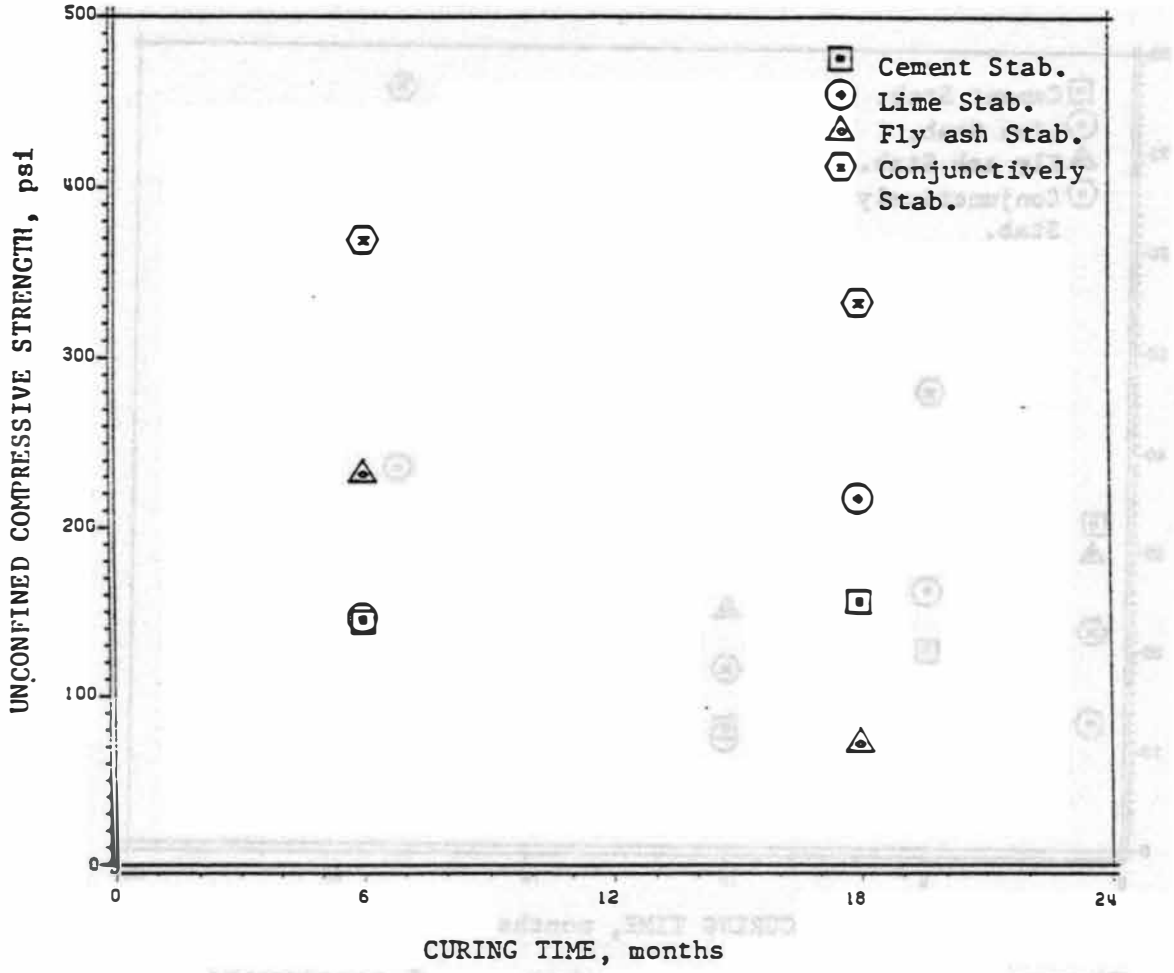

Figure 5.8: Undisturbed strength of stabilized field samples calculated from remolded strength and sensitivity

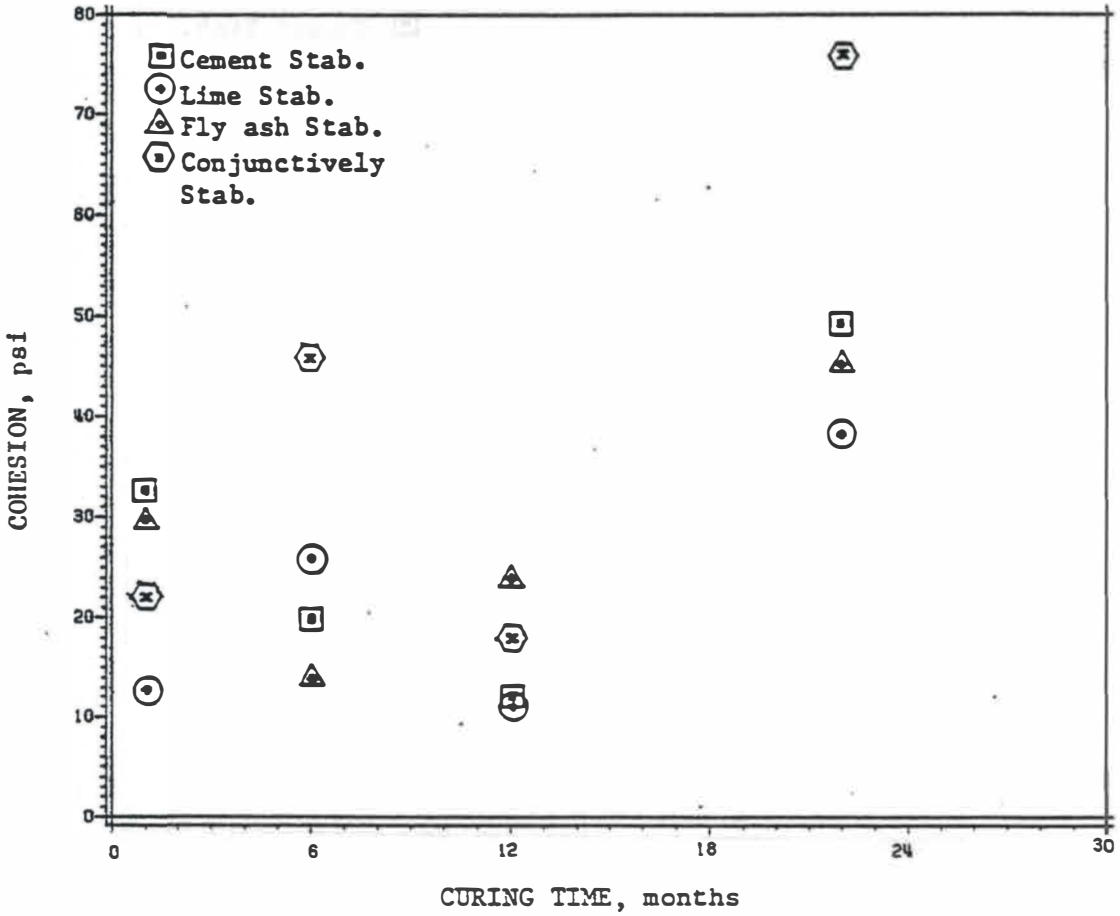

Figure 5.10: Variation of cohesion of construction samples with time (70° F, Dry)

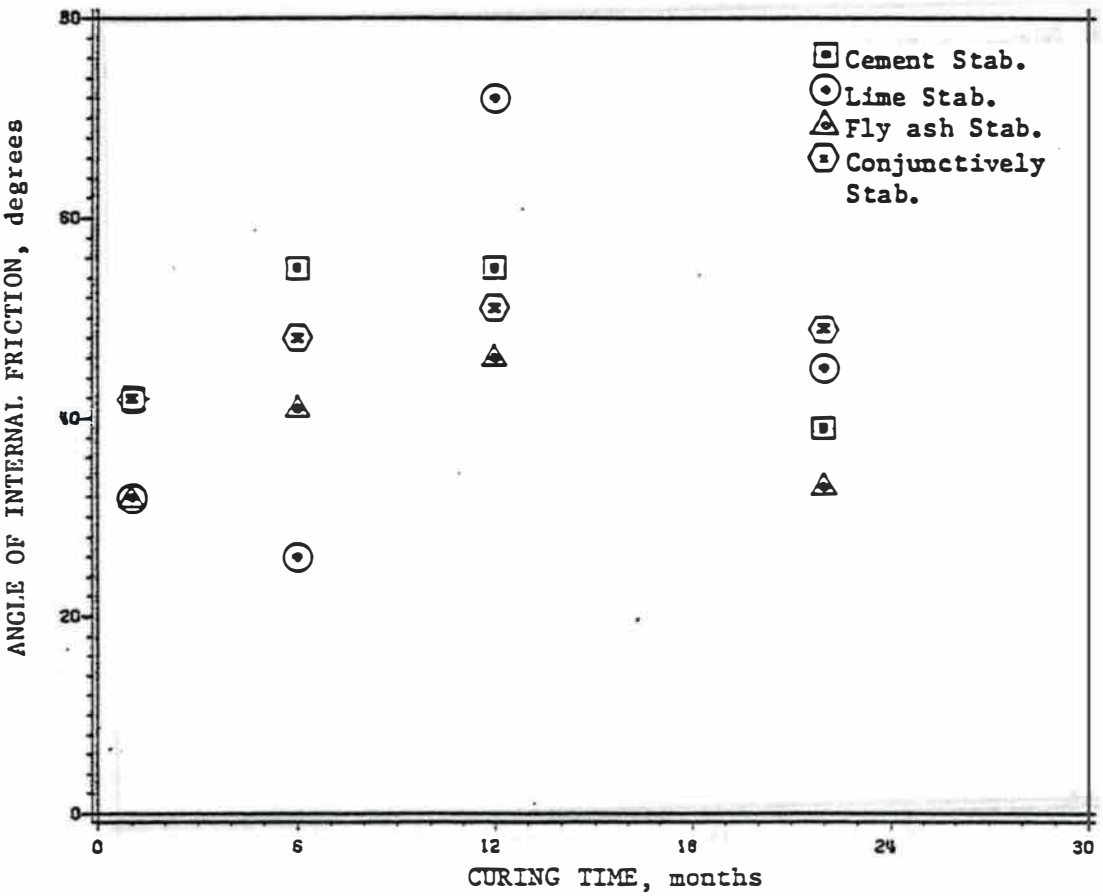

Figure 5.11: Variation of angle of internal friction of construction samples with time (70° F, Dry)

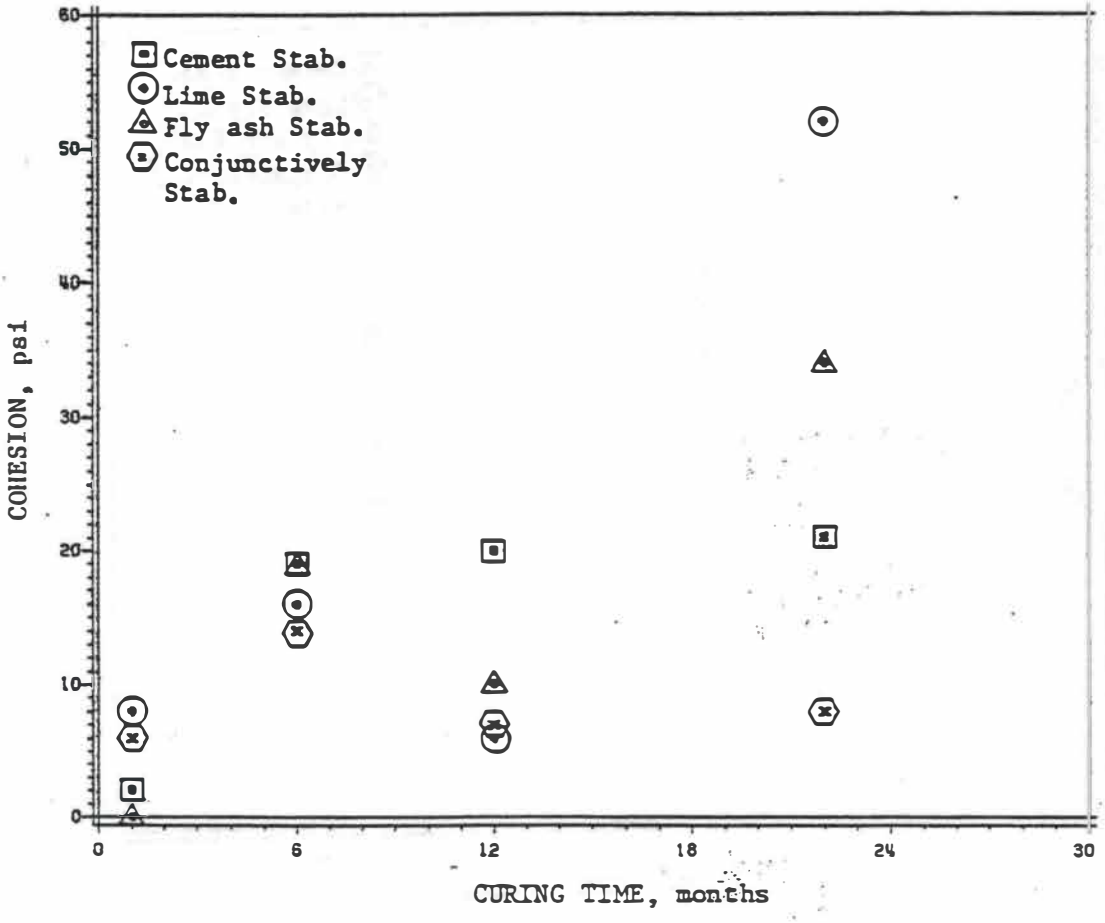

Figure 5.12: Variation of cohesion of construction samples with time (70° F, Imm.)

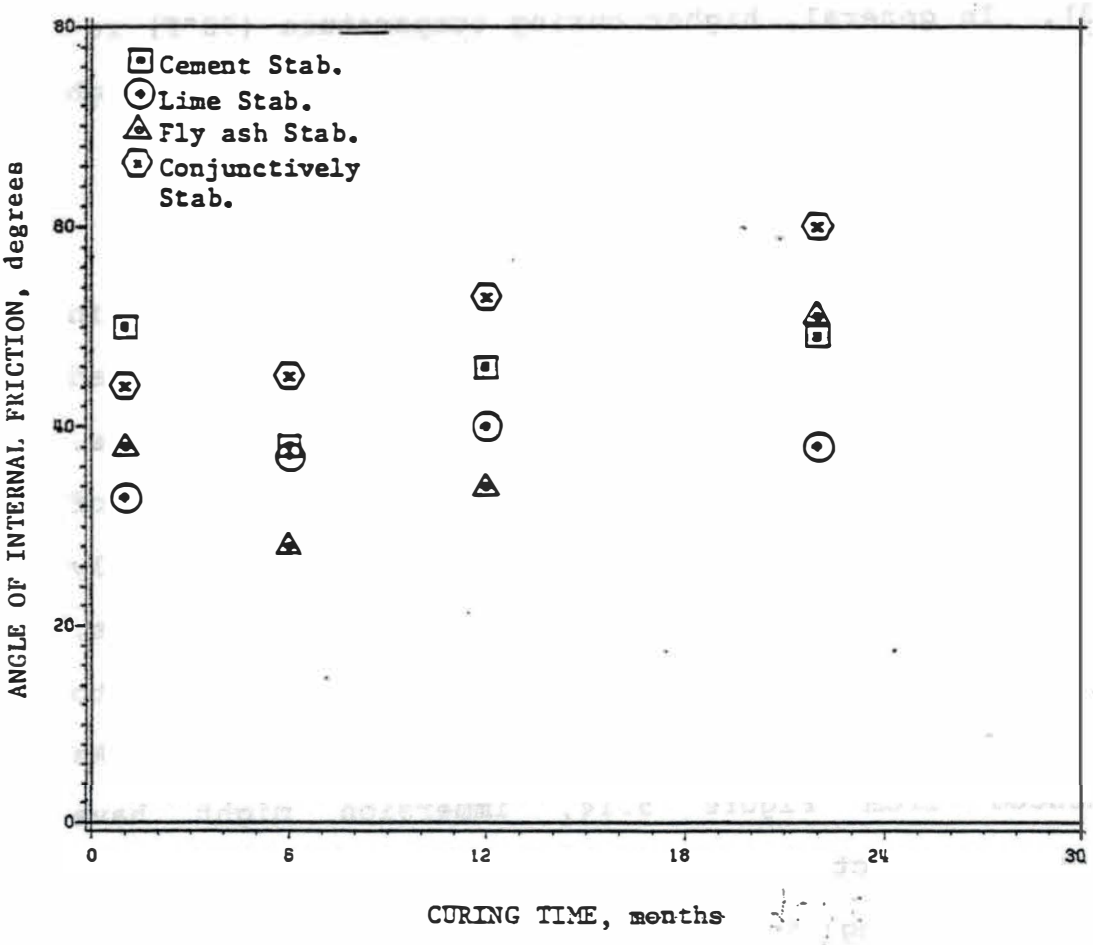

Figure 5.13: Variation of angle of internal friction of construction samples with time (70° F, Inun.)

samples. While no consistent pattern was followed by c values of construction samples as a result of lower curing periods, their ϕ values increased with time. In many cases immersion in water reduced both c and ϕ values of stabilized construction samples (Figures 5.12 and 5.13). In general, higher curing temperature (90°F) resulted in higher c and lower ϕ values (Tables B.1 through B.4, Appendix B).

5.5.2 Field Samples

5.5.2.1 Undisturbed Samples. As mentioned in Section 5.3.2, undisturbed field samples were obtained only from cement and conjunctively stabilized sections. Figures 5.14 and 5.15 present the cohesion and angle of internal friction of undisturbed cement and conjunctively stabilized field samples in dry and immersed conditions. The c values of undisturbed samples ranged from 15 psi to 139 psi and their ϕ values ranged from 18° to 58°. As evidenced from Figure 5.14, immersion might have triggered a reaction between the water and the unreacted cement resulting in an augmentation of the immersed cohesion values of cement stabilized samples.

5.5.2.2 Remolded Samples. The shear parameters of remolded field and construction samples are depicted in Table 5.6. Remolding reduced both c and ϕ values of construction and field samples. In general, remolded

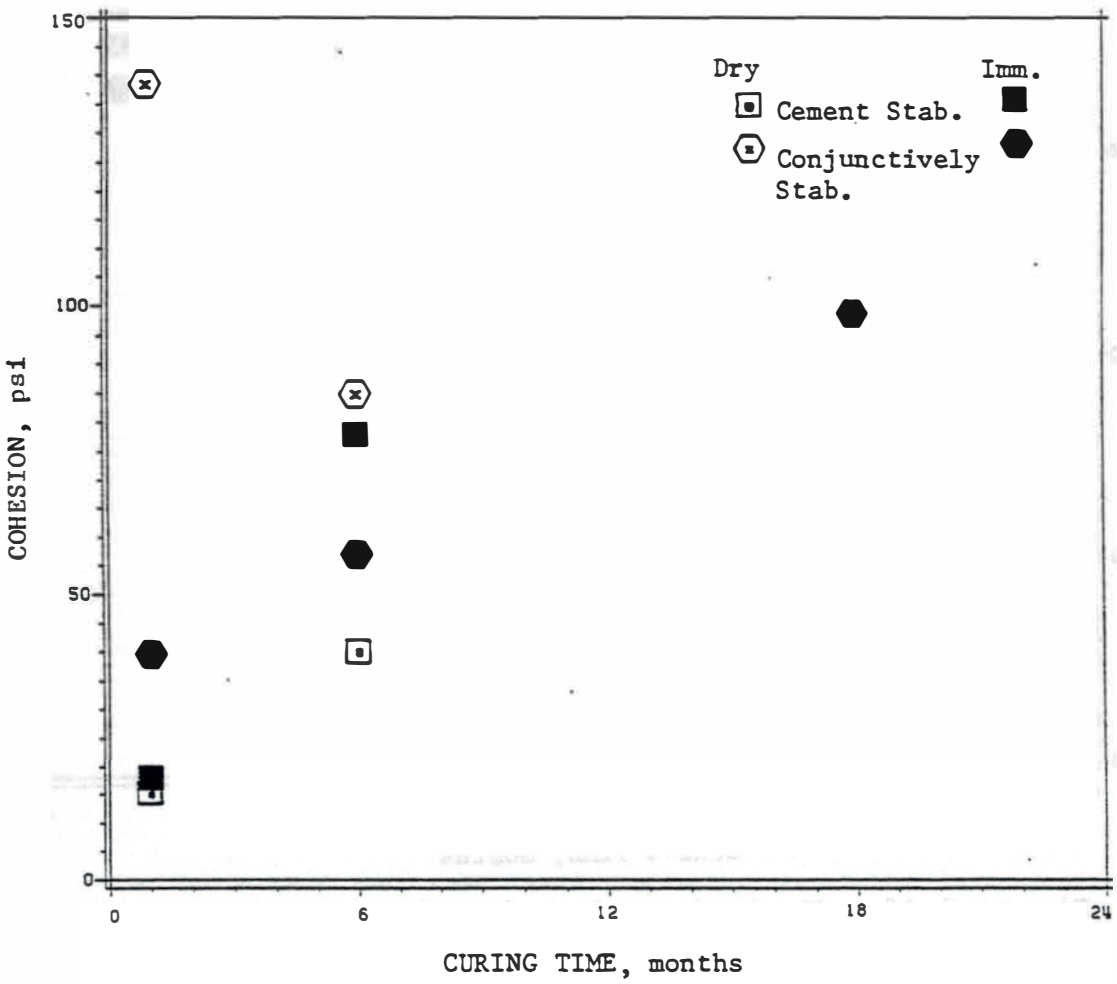

Figure 5.14: Variation of cohesion of cement and conjunctively stabilized field samples with time

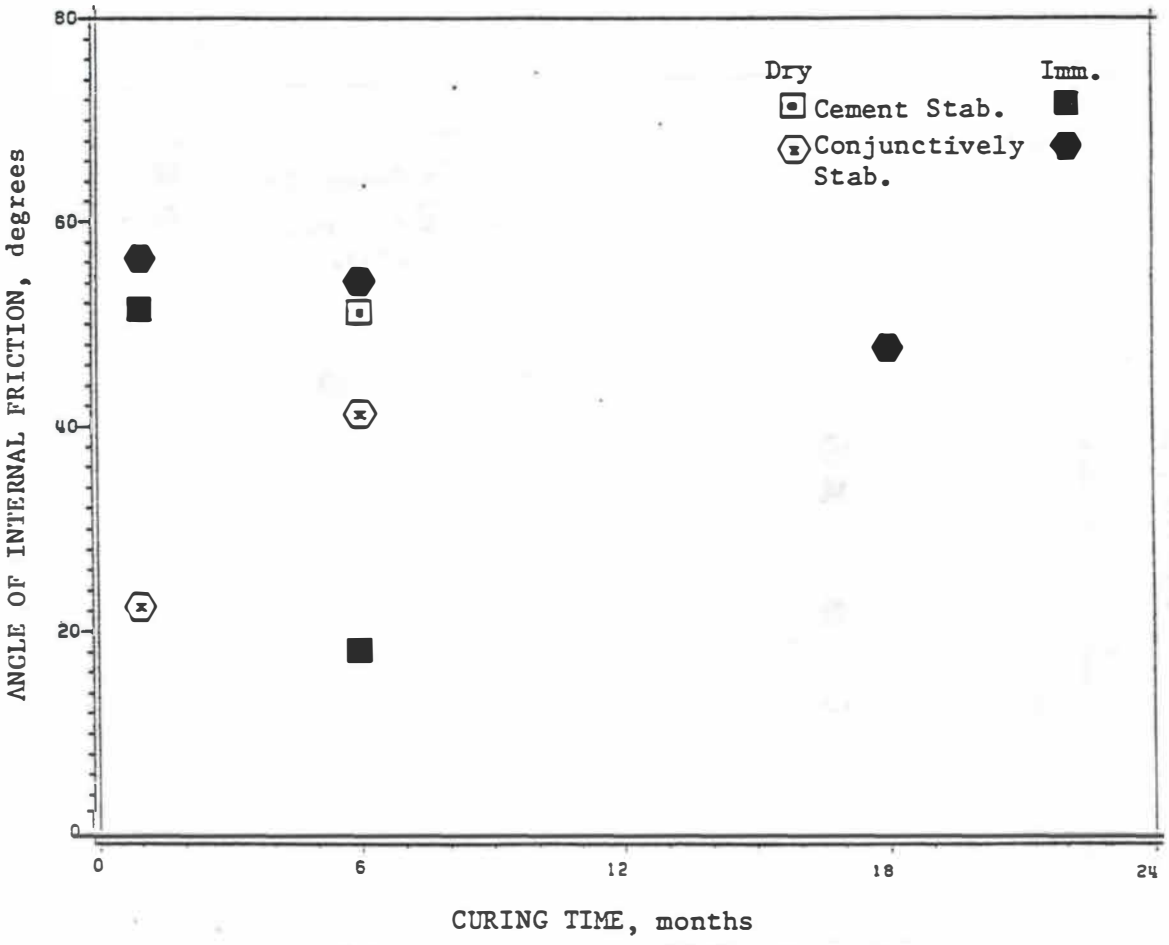

Figure 5.15: Variation of angle of internal friction of cement and conjunctively stabilized field samples with time

construction samples showed higher c and lower ϕ values than their field counterparts.

The maximum design axle load in Oklahoma is 18,000 lb (Yoder and Witczack, 1975). This axle load produces a wheel load of 9,000 lb. Assuming a tire pressure of 100 psi and a loaded area of radius equal to 5.6 inches, the McDowell analytical procedure (1955), gives the maximum shear stress, developed in depths greater than 10 inches (base course), as less than 10 psi provided that there is no sudden acceleration or deceleration. Shear stresses of this magnitude would not cause failure in any of the stabilized shale samples (construction or field) studied in this investigation, even in their remolded condition.

5.6 Wet-Dry Cycles

The shear parameters c and ϕ of stabilized construction samples subjected to 15 wet-dry cycles are presented in Tables 5.7 through 5.10. Each value in these tables is the average of values from two stations.

Cement stabilization increased the angle of internal friction substantially. For example, the average angle of internal friction of cement stabilized specimens was 51°. As a result of wetting and drying it increased to an average value of 61°. Specimens tested in dry conditions showed lower cohesion and higher angle of internal friction than those tested in wet conditions. Specimens

Table 5.7. Shear Parameters of Cement Stabilized Construction Samples After Being Subjected to 15 Wet-Dry Cycles

Curing Time, Months	70°F				90°F			
	Dry		Imm.		Dry		Imm.	
	c	φ	c	φ	c	φ	c	φ
1	8	62	15	68	7	48	20	60
6	39	62	54	52	58	58	145	26
12	16	58	28	49	14	62	8	47

Table 5.8. Shear Parameters of Lime Stabilized Construction Samples After Being Subjected to 15 Wet-Dry Cycles

Curing Time, Months	70°F				90°F			
	Dry		Imm.		Dry		Imm.	
	c	φ	c	φ	c	φ	c	φ
1	0	56	10	54	5	56	46	52
6	53	41	74	26	124	44	12	56
12	69	42	16	54	10	66	1	54

Table 5.9.. Shear Parameters of Fly Ash Stabilized Construction Samples After Being Subjected to 15 Wet-Dry Cycles

Curing Time, Months	70°F				90°F			
	Dry		Imm.		Dry		Imm.	
	c	ϕ	c	ϕ	c	ϕ	c	ϕ
1	11	48	34	48	15	44	32	36
6	54	36	40	30	72	30	22	36
12	58	42	30	17	22	51	40	26

Table 5.10. Shear Parameters of Conjunctively Stabilized Construction Samples After Being Subjected to 15 Wet-Dry Cycles

Curing Time, Months	70°F				90°F			
	Dry		Imm.		Dry		Imm.	
	c	ϕ	c	ϕ	c	ϕ	c	ϕ
1	22	47	8	53	56	46	105	44
6	40	56	10	58	128	43	64	36
12	38	54	59	34	55	51	44	54

cured at 90°F showed higher cohesion and lower angle of internal friction compared to those cured at 70°F.

Lime stabilized specimens, in many cases, showed higher cohesion and lower angle of internal friction than their cement stabilized counterparts. The average c and ϕ values of lime stabilized specimens cured at 70°F and tested dry were 41 psi and 46°, respectively. Specimens tested in wet condition showed slightly lower average c and ϕ (33 psi, 45°). Curing at higher temperature (90°F) increased c and ϕ. The average values of c and ϕ were increased to 46 psi and 55°, respectively.

Fly ash stabilized specimens showed an average c and ϕ values of 41 psi and 42°, respectively, when tested in dry conditions. Both of these parameters were decreased when tested in wet conditions, i.e., c to 35 psi and ϕ to 32°. Specimens cured at 90°F showed slightly lower c and almost the same average ϕ (42°) compared to those cured at 70°F.

The average value of cohesion and angle of internal friction of conjunctively stabilized specimens were 33 psi and 52°, respectively. Both the average c and ϕ were reduced when tested wet. Specimens cured at 90°F showed substantially higher c, slightly lower ϕ values than those cured at 70°F. The average c was increased from 33 psi to 80 psi, while the average ϕ was decreased 52° to 47°.

5.7 Flexural Strength

Upon curing stabilized shale could develop substantial strength which results in increased modulus of elasticity and flexural strength, both of which cause the base course to act like a beam or slab. This section deals with the evaluation of flexural strength of construction and field samples.

The load deflection parameters of construction samples were evaluated by the third point beam loading wherein the beam is loaded to failure and those of field samples were evaluated by utilizing a Benkelman beam. Figure 5.16 presents the load deflection curve of stabilized construction samples and Figure 5.17 depicts the Benkelman beam results 9 months after construction. Load-deflection curves of all stabilizing agents followed almost the same pattern, i.e., at lower loads they followed a curved path with positive slope and at higher loads (50 lbs. and higher), they followed a nearly straight line path, which changed to a curved path near the failure load. For a given load, cement stabilized beams experienced the lowest deflection followed by lime stabilized beams. At loads lower than 50 lbs. fly ash stabilized beams experienced less deflection than their conjunctively stabilized counterparts, while at loads higher than 50 lbs. the reverse is true. This contradicts the results obtained from Benkelman beam measure-

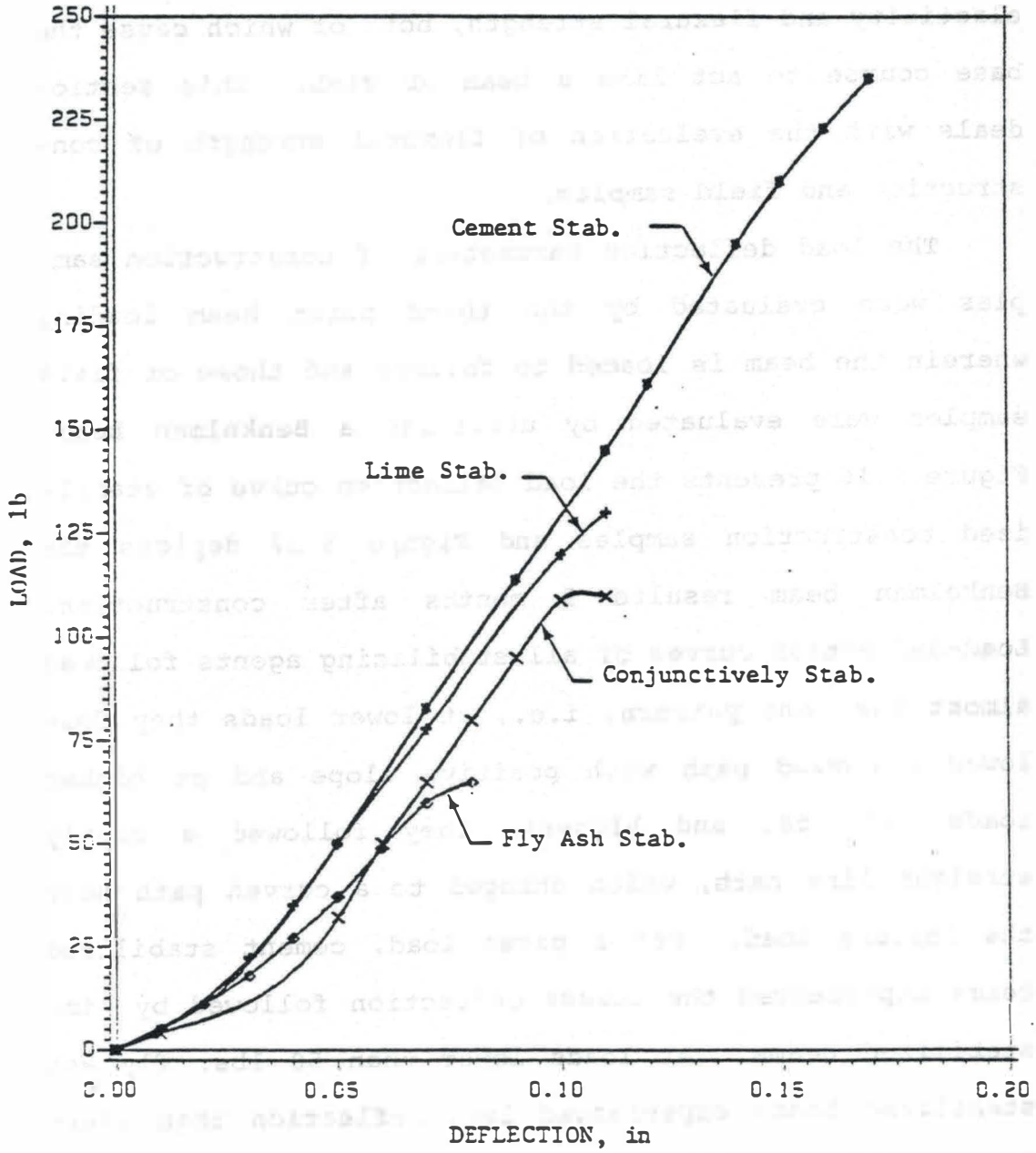

Figure 5.16: Deflection patterns of stabilized beams (construction samples)

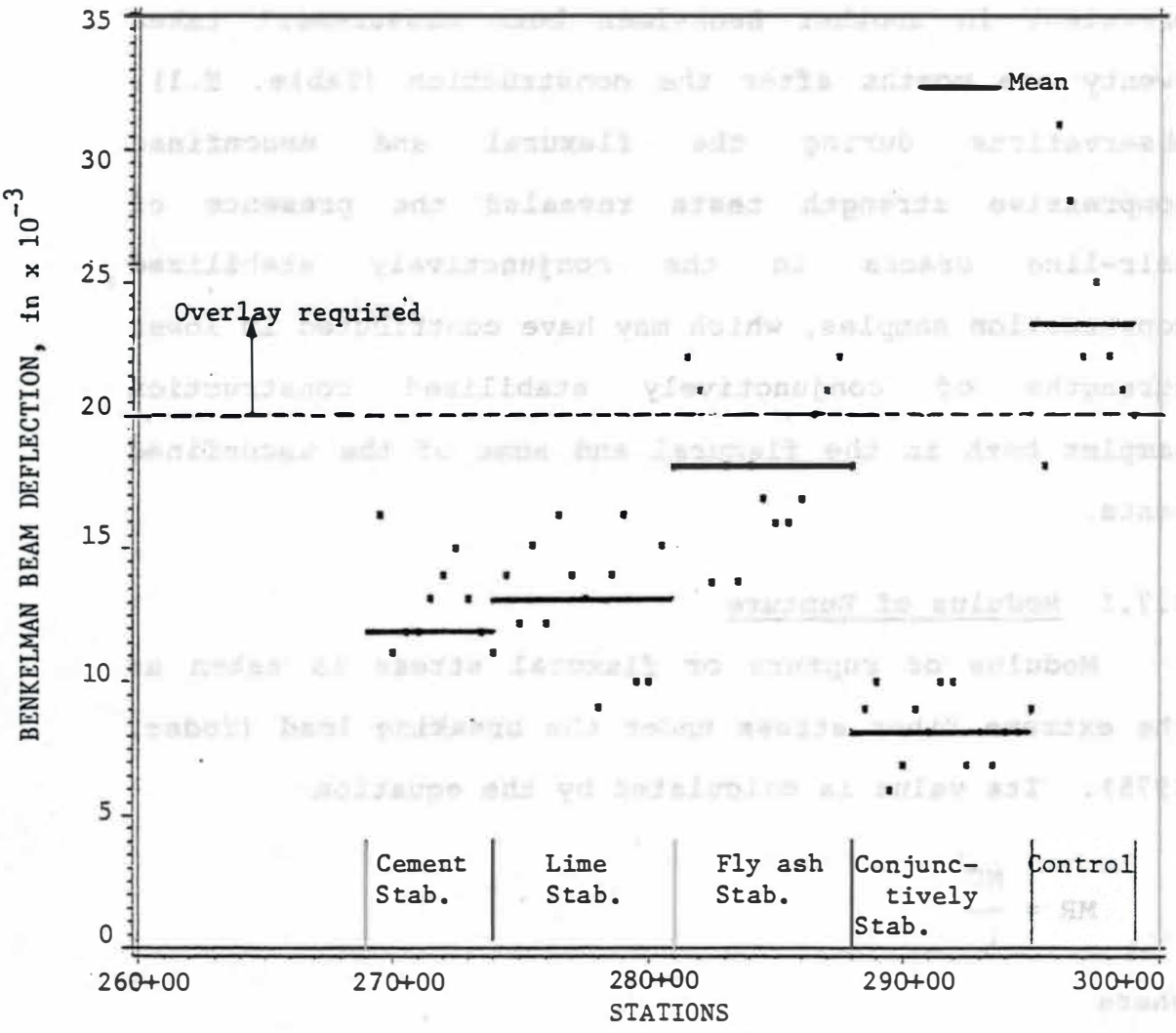

Figure 5.17: Pavement deflection of test sections

ments (Figure 5.17) which show that the average deflection of the conjunctively stabilized section was the lowest of all followed by cement, lime, fly ash stabilized sections, in that order. The same trend was prevalent in another Benkelman beam measurement taken twenty one months after the construction (Table. E.1). Observations during the flexural and unconfined compressive strength tests revealed the presence of hair-line cracks in the conjunctively stabilized construction samples, which may have contributed in lower strengths of conjunctively stabilized construction samples both in the flexural and some of the unconfined tests.

5.7.1 Modulus of Rupture

Modulus of rupture or flexural stress is taken as the extreme fiber stress under the breaking load (Yoder, 1975). Its value is calculated by the equation

$$MR = \frac{MC}{I}$$

where

MR = modulus of rupture, (psi)

C = distance from the neutral axis to extreme fiber, inches

I = moment of inertia, in^4

The modulus of rupture is applicable only within the elastic range of stabilized shale. Table 5.11 depicts the modulus of rupture of stabilized shale. The average modulus of rupture of cement stabilized shale was 76 psi followed by lime 35 psi, fly ash 22 psi and conjunctively stabilized shale 28 psi. Typical MR value for 3000 psi concrete is approximately 500 psi. For the reasons described earlier the MR value for conjunctively stabilized shale may not be realistic. The modulus of rupture of stabilized shale could be predicted from the unconfined compressive strength values by the following linear regression equation:

$$MR = 4.97 + 0.23\ UC \quad (R^2 = 0.61)$$

where

MR = modulus of rupture, (psi)

UC = unconfined compressive strength, (psi)

5.8. Modulus of Elasticity

The flexural moduli of elasticity (E_f) of stabilized shale were calculated from the following equation:

$$E_f = \frac{5\ PL^3}{324\ Y}$$

where

E_f = modulus of elasticity in flexural, psi

I = moment of inertia, in^4

P = load, pounds

Table 5.11. Modulus of Rupture of Stabilized Construction Samples for the Indicated Curing Periods

Stabilized Test Section	Station	1 month Curing	6 month Curing	12 month Curing
Cement	269+22	77	66	125
	272+37	75	38	70
Lime	275+46	28	26	-
	279+64	42	60	44
Fly Ash	284+60	22	6	25
	285+36	21	22	26
Conjunctively Stabilized	289+22	-	66	-
	292+89	28	-	-

L = span length, inches

Y = deflection, inches

The E_f values of stabilized shale (Table 5.12) varied from 3207 to 5559 psi after one month of curing. No consistent pattern could be established between time of curing and modulus of elasticity. In addition, modulus of elasticity in compression (E_c) of stabilized shale from triaxial data (σ_3 = 30 psi) were also calculated and are included in Table 5.12. The modulus of elasticity in compression ranged from 10,999 to 40,000 psi. Among construction samples, cement stabilized specimens showed the highest modulus of elasticity followed by conjunctively, fly ash and lime stabilized specimens. On the other hand, for field samples conjunctive stabilized specimen showed an E_c of 40,000 psi (highest) followed by cement stabilized 12,000 psi.

5.9 Scanning Electron Microscopy

To study the microstructure and void domain characteristics of raw and stabilized shale, use is made of SEM. Micrographs of raw shale, fly ash powder, construction samples cured for one, six, twelve, and twenty two months at 70°F, and those of field samples cured for one, six, eighteen, and twenty two months were obtained. These micrographs were closely analyzed for any change in the microstructure and void domain as a result of stabi-

Table 5.12. Modulus of Elasticity of Stabilized Shale

Stabilized Test Section	Type of Sample	Flexural Modulus of Elasticity (psi)	Compressional Modulus of Elasticity (psi)
Cement	Construction	5474	33,400
	Field	-	12,000
Lime	Construction	4926	10,999
Fly Ash	Construction	2645	24,103
Conjunctively Stabilized	Construction	3207	29,706
	Field	-	40,000

lization. The void domain was analyzed following a procedure developed by Laguros and Jha (1977), a schematic representation of which is given in Figure 5.18.

5.9.1 Raw Shale

The micrograph of raw shale is depicted in Figure 5.19. The particles appear as a blocky arrangement of loosely packed particles. The projected void area was measured and was found to constitute about 17 percent of the total area (Table 5.13).

5.9.2 Fly Ash Powder

Figure 5.20 is a micrograph of fly ash powder as received. The micrograph reveals a preponderance of spherical particles with varying sizes. The surfaces of the spherical particles are relatively smooth and glassy. Also present in the micrograph is an irregular shaped particle which is thought to be a coal fragment which did not fully melt during the firing process.

5.9.3 Cement Stabilization

Micrographs of construction samples stabilized with 14 percent Portland cement are presented in Figure 5.21. After one month of curing, no hydration products in the form of crystal growth could be observed (Figure 5.21a). After six months of curing, Figure 5.18, indicates the formation of blocky aggregates. The twelve month cured

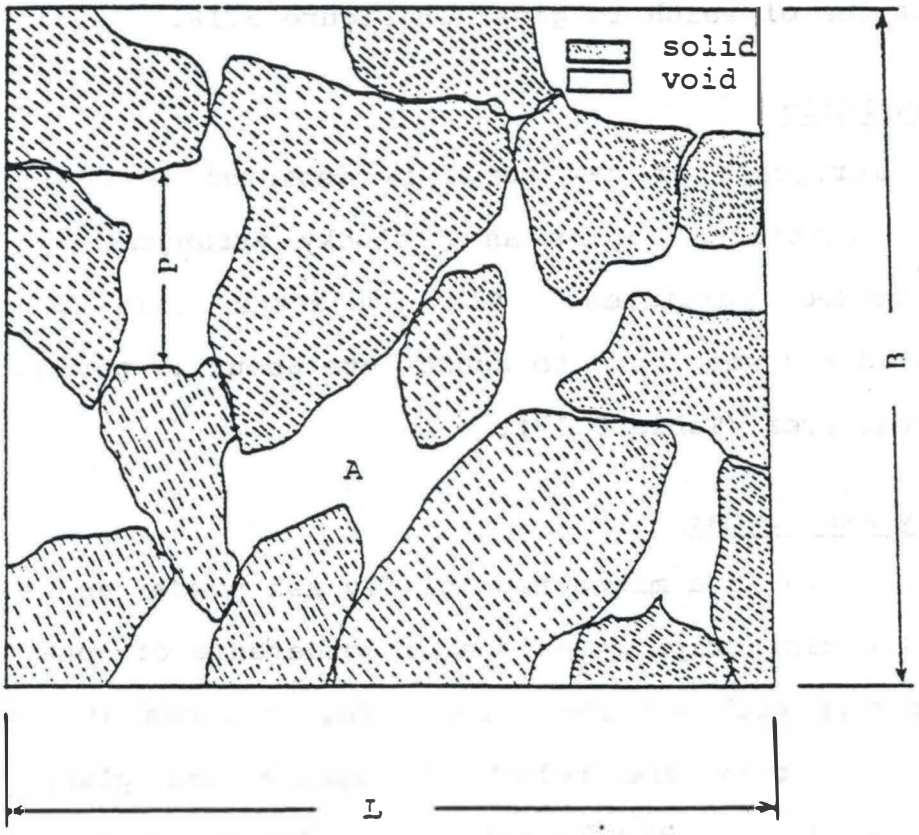

Total area = B x L

$$V = \frac{A}{BxL} \times 100$$

Figure 5.18: Schematic representation of an electron micrograph of a soil mass
(after Laguros and Medhani, 1984)

Table 5.13. Void Area From Micrographs of Raw and Stabilized Shale for Indicated Curing Periods

Test Section	Construction				Field			
	1 mo.	6 mo.	12 mo.	22 mo.	1 mo.	6 mo.	18 mo.	22 mo.
Control	17*							
Cement	1.6	3.7	1.5	1.4	1.3	0	1.3	1.5
Lime	2.9	2.8	4.6	2.0	9	3.2	6.2	3.9
Fly Ash	1.7	2.0	2.2	1.8	1.7	1.5	2.1	1.6
Conjunctively Stabilized	5	2.4	2.5	2.6	2.6	1.5	1.4	1.9

* All values are percent of total area

1 μm ⟷ 3000X

Figure Micrograph of raw shale

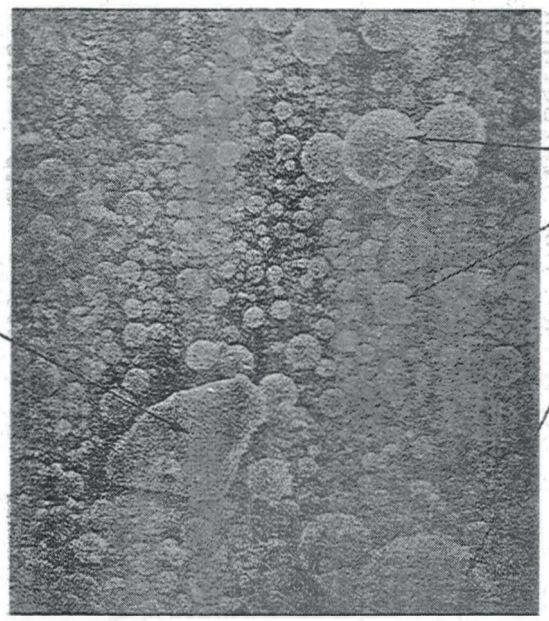

10 μm ⟷ 800X

Figure 5.20: Micrograph of fly ash powder

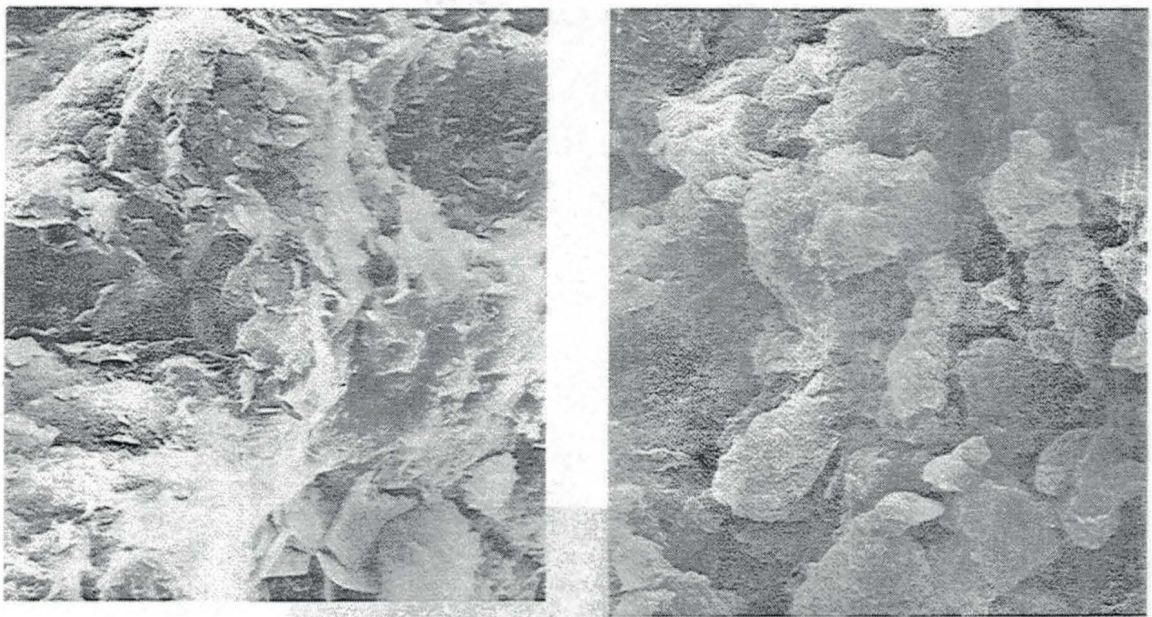

1 μm ⊢ 3000X (a) 1 μm ⊢ 3000X (b)

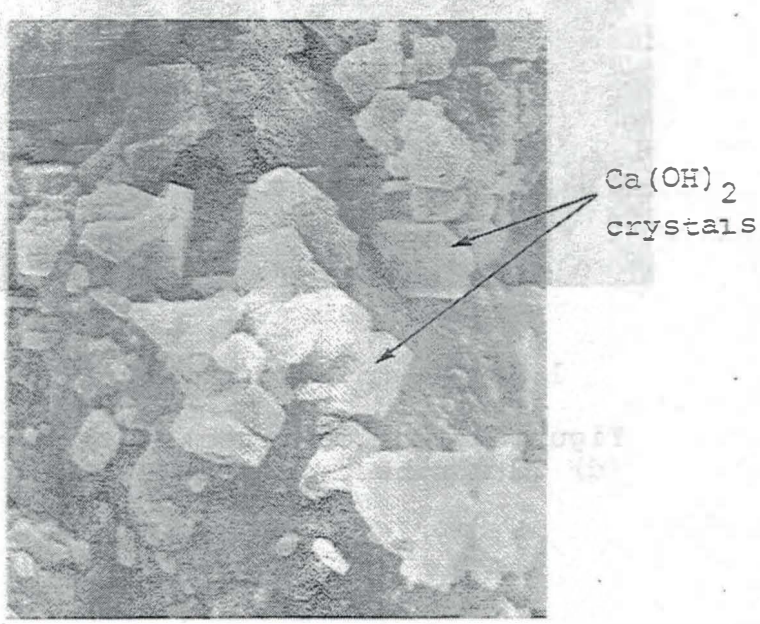

1 μm ⊢ 3000X (c)

Figure 5.21: Micrographs of cement stabilized construction samples

(a) 1 month; (b) 6 months; (c) 12 months

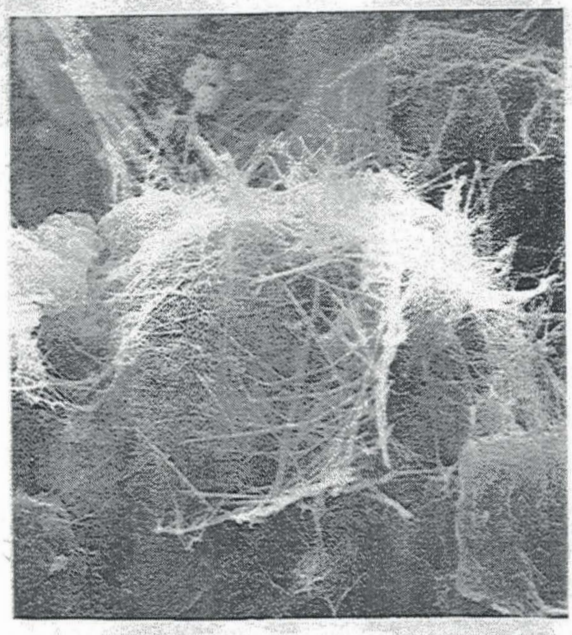

1 μm ⊢⊣ 3000x (d)

Figure 5.21 (continued)
(d) 22 months

specimen (Figure 5.21c) showed hexagonal shaped formations similar to the ones observed by Laguros and Baker (1984). Their EDS (Figure 5.22), along with their hexagonal prismatic shape are indicative of calcium hydroxide crystals. The twenty two month cured specimen (Figure 5.21d) showed the formation of CSH (C = CaO; S = SiO_2; H = H_2O) (tobermorite) spiny crystals.

The micrographs of field samples are shown in Figure 5.23. After one month of curing the micrograph (Figure 5.23a) failed to reveal any crystal formation. However, after six months of curing the hexagonal shaped calcium hydroxide crystals are clearly visible (Figure 5.23b). The twelve and twenty two month cured samples (Figure 5.23c and 5.23d) showed the formation of CSH crystals. The changes in the fabric of shale-cement mixture follows a pattern similar to that observed by Mitchell and ElJack (1965) in their study of soil-cement fabric i.e., the change in the fabric of shale-cement mixture starts from a mixture of discrete soil particles and works its way toward a more homogeneous fabric of indistinguishable components (Figures 5.25b and 5.25c).

The areas of voids of both construction and field samples (Table 5.13) were substantially reduced as a result of cement stabilization. For example, the area of voids of cement stabilized construction and field samples were reduced from 17 percent (raw shale) to 1.6 and 1.3

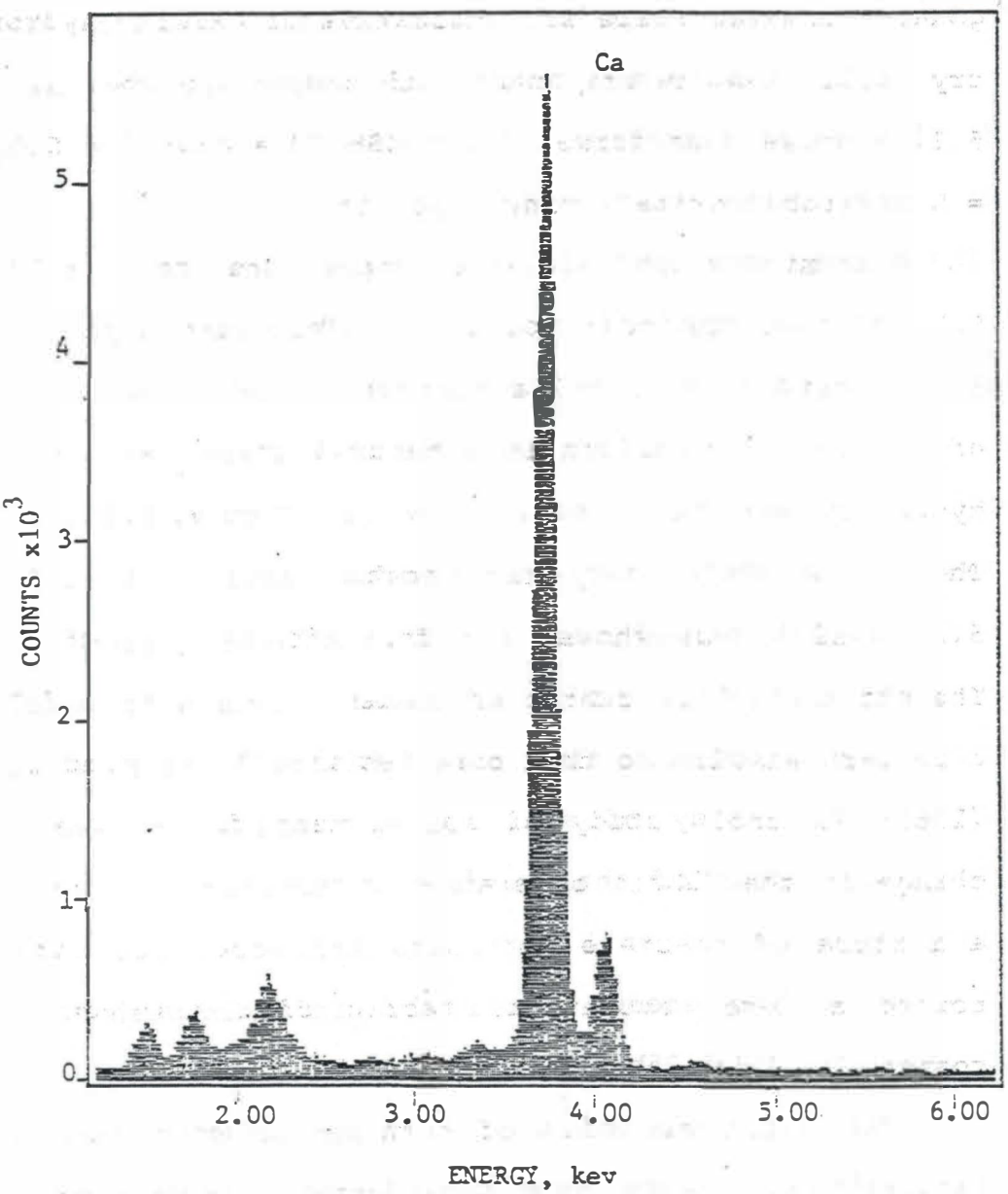

Figure 5.22: EDS of the hexagonal crystals observed in Figure 5.21C

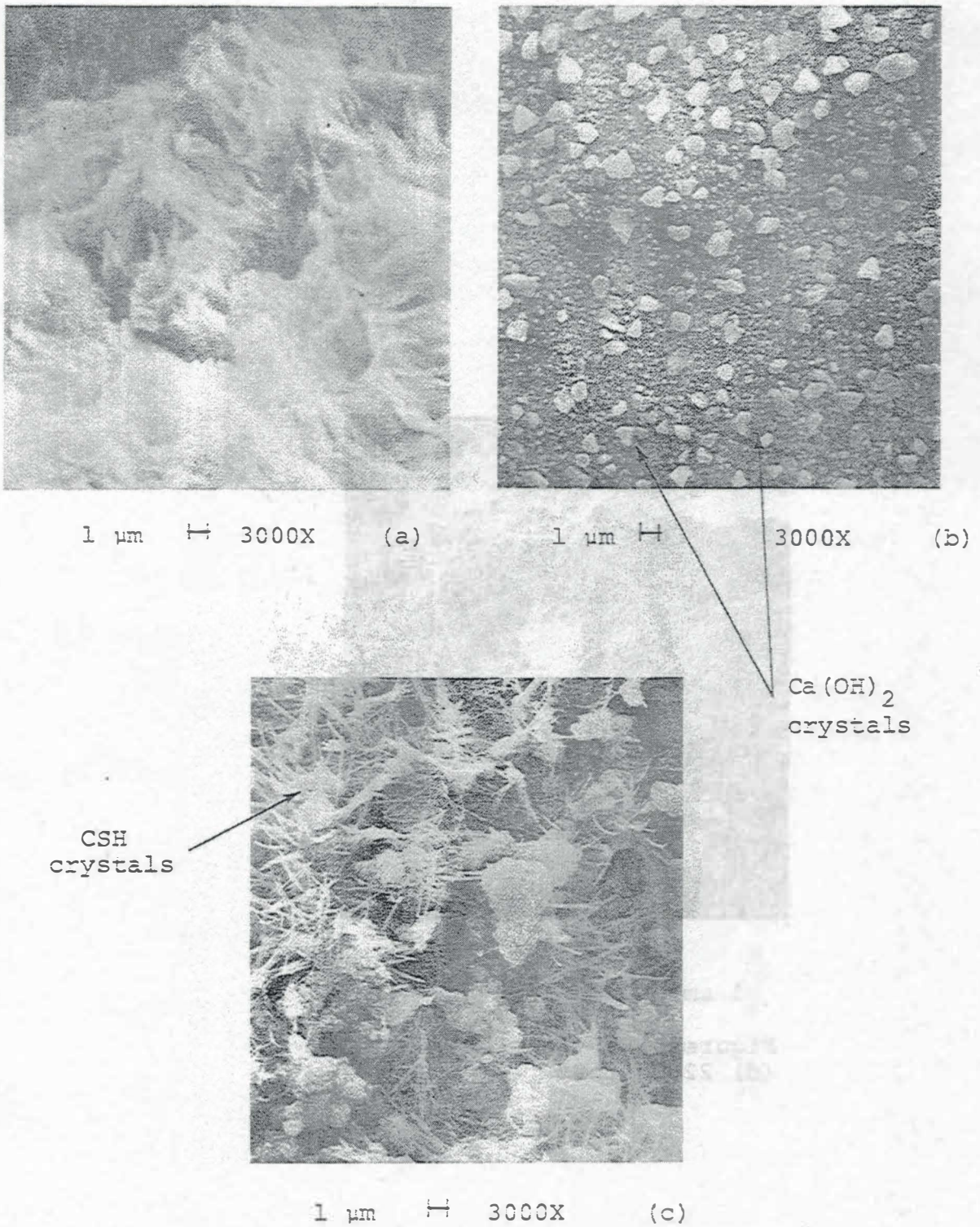

Figure 5.23: Micrographs of cement stabilized field samples

(a) 1 month; (b) 6 months; (c) 18 months

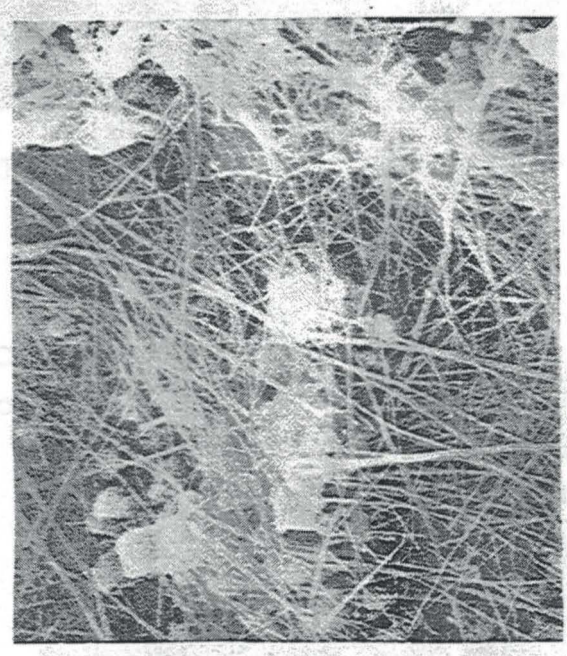

1 µm ⟷ 3000x (d)

Figure 5.23 (continued)
(d) 22 months

percent, respectively. The reduction in the areas of voids as evidenced from Table 5.13 was more pronounced in field samples as compared to construction samples, suggesting denser packing of particles in field samples possibly due to the additional compactive effort expended during the construction of the pavement layer.

5.9.4 Lime Stabilization

Electron micrographs of construction samples stabilized with 4.5 percent quicklime are presented in Figure 5.24, and those of field samples are shown in Figure 5.25. The aggregation of shale particles is discernible in all micrographs, a fact that was also ascertained by the corresponding reduction in their amount of <2μ clay (Table 5.2). The only micrograph which reveals the formation of CSH crystals is the one taken from the twenty two month cured field sample (Figure 5.25d). The void areas in shale fabric were reduced substantially as a result of lime stabilization; for the construction samples they were reduced to 2.9 percent, and for the field samples they were reduced to 9 percent (Table 5.13), indicating better packing for construction samples than field samples. This could be related to the less dispersion of lime throughout the field samples (Figure 5.24) as compared to the construction samples (Figure 5.25).

1 μm ⊢ 3000X (a)

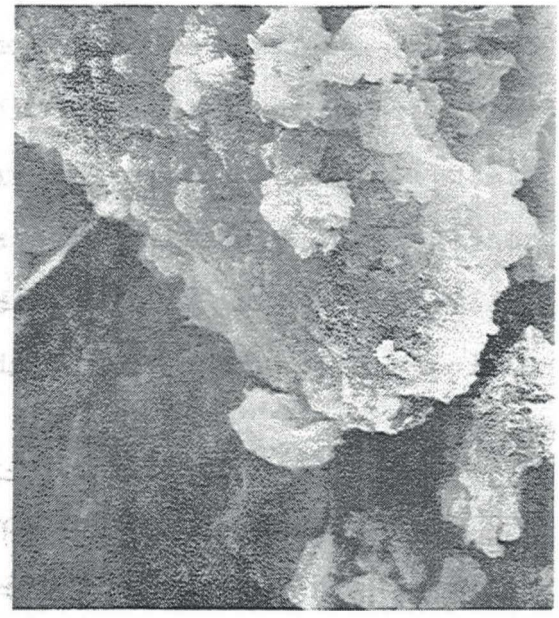

1 μm ⊢ 3000X (b)

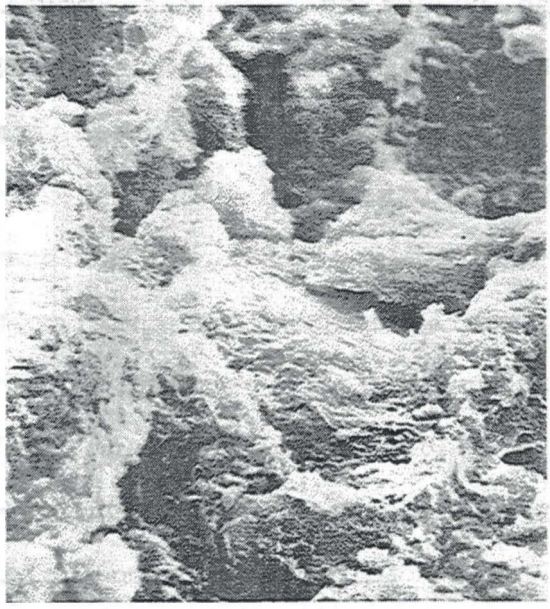

1 μm ⊢ 3000X (c)

Figure 5.24: Micrographs of lime stabilized construction samples

(a) 1 month; (b) 6 months; (c) 12 months

1 μm ⊢ 3000x (d)

Figure 5.24 (continued)
(d) 22 months

1 μm ⊢ 3000X (a)

1 μm ⊢ 3000X (b)

1 μm ⊢ 3000X (c)

Figure 5.25: Micrographs of lime stabilized field samples

(a) 1 month; (b) 6 months; (c) 18 months

1 μm ⊢ 3000x (d)

Figure 5.25 (continued)
(d) 22 months

5.9.5 Fly Ash Stabilization

The major feature in the micrographs of fly ash (25 percent) stabilized construction and field samples is the presence of spherical fly ash particles. Figure 5.26 shows the micrographs of fly ash stabilized construction samples, and Figure 5.27 presents the micrographs of fly ash stabilized field samples. After one month of curing the fly ash particles are heavily coated with hydration products, with some CSH spiny crystals (Figures 5.26a and 5.26a). After six months of curing the amount of CSH crystals is increased substantially with the construction samples (Figure 5.26b) showing more crystal formation than the field samples (Figure 5.27b). After twelve, eighteen, and twenty two months of curing a higher number of CSH crystals are present both in construction and field samples (Figures 5.26c, 5.27c, and 5.27d). Unlike fly ash-cement mixtures in which the spherical (glassy) particles are dissolved with time, in the micrographs of fly ash stabilized shale the spherical particles continue to be present. This could be attributed either to the higher percentage of fly ash or the low amount of water that was used in shale-fly ash stabilization.

The void areas of shale were reduced to 1.7 percent both for construction and field samples as a result of fly ash stabilization (Table 5.13).

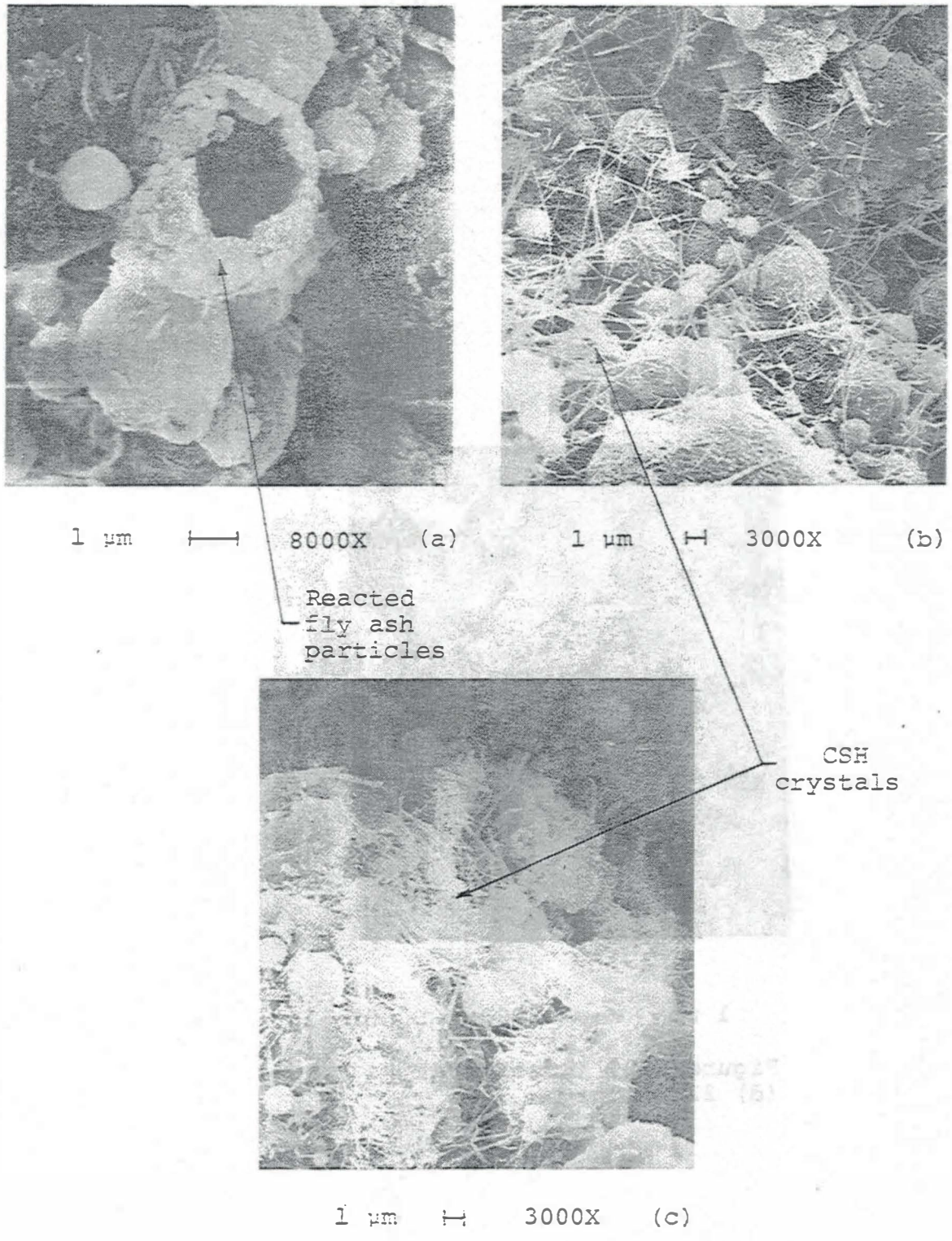

Figure 5.26: Micrographs of fly ash stabilized construction samples

(a) 1 month; (b) 6 months; (c) 12 months

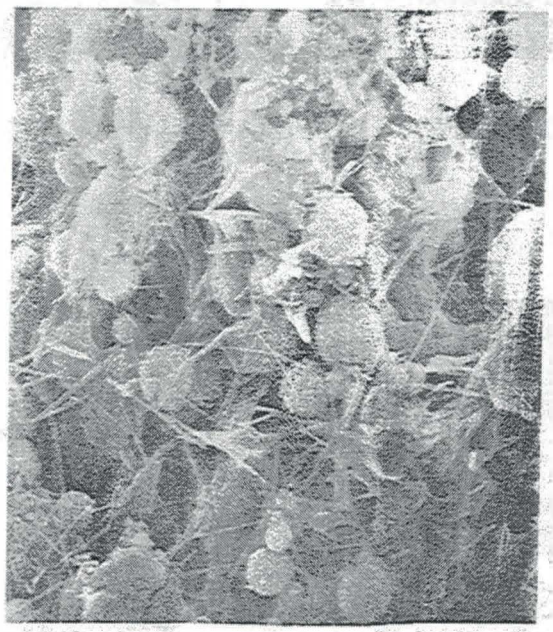

1 μm ⊢ 3000x (d)

Figure 5.26 (continued)
(d) 22 months

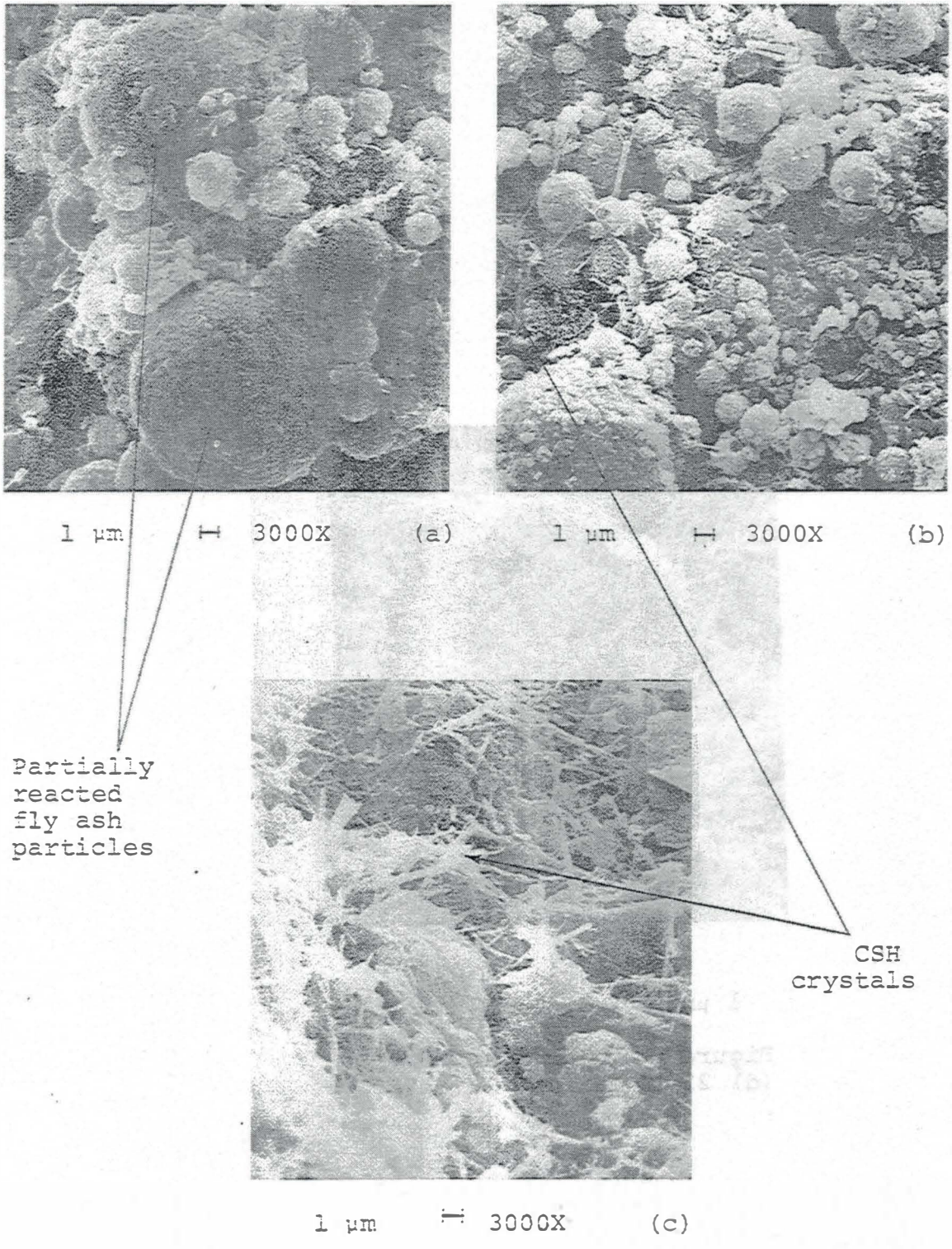

Figure 5.27: Micrographs of fly ash stabilized field samples

(a) 1 month; (b) 6 months; (c) 18 months

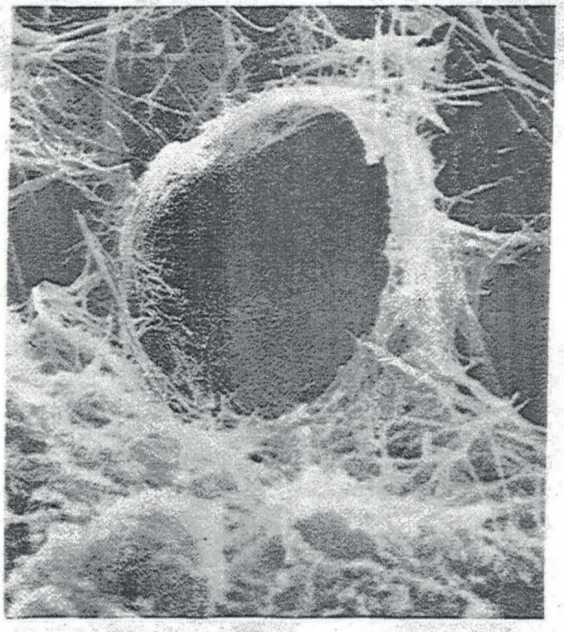

1 µm ⊢ 3000x (d)

Figure 5.27 (continued)
(d) 22 months

5.9.6 Conjunctive Stabilization

The micrographs of conjunctively stabilized construction and field samples are presented in Figures 5.28 and 5.29. The micrograph of construction samples (Figure 5.28a) after one month of curing shows heavy precipitation of calcium hydroxide. Fly ash particles have relatively clean surfaces which suggest the lack of hydration in this particular micrograph. Figure 5.28b reveals some hexagonal crystal formation after six months of curing which was also observed in the cement stabilized shale (Figure 5.21c) and is thought to be calcium hydroxide crystals. After twelve months of curing (Figure 5.28c) the number of spherical particles has been reduced substantially which suggests the consumption of the glassy part of fly ash particles as a result of hydration. The spiny crystals are the CSH type crystals from the tobermorite family.

Micrographs of field samples reveal much more information than their construction counterparts. Figure 5.29a shows the so called "pullout" phenomenon. As the reaction begins, the glassy portion of fly ash is consumed, and crystallized CSH fibers grow inward to fill the space. This is very similar to what Grutzeck et al. (1981), found in their study of the hydration mechanism of high-lime fly ash in Portland cement composites. They reported that, "Bonding of this CSH material to the

1 µm ⊢ 3000X (a)

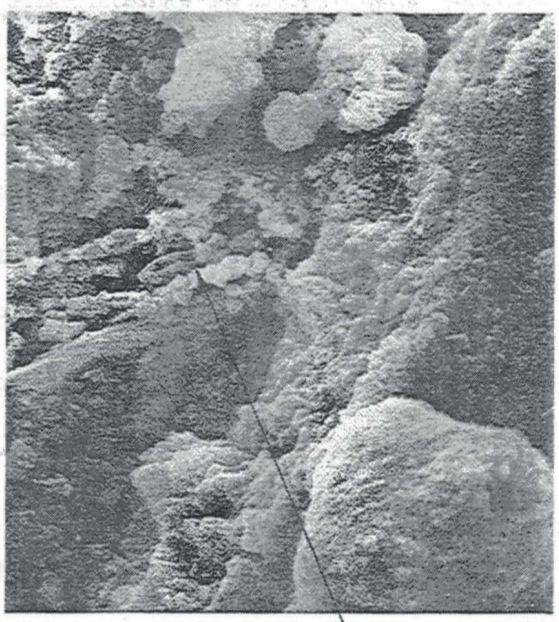

1 µm ⊢ 3000X (b)

1 µm ⊢ 3000X (c)

Figure 5.28: Micrographs of conjunctively stabilized construction samples

(a) 1 month; (b) 6 months; (c) 12 months

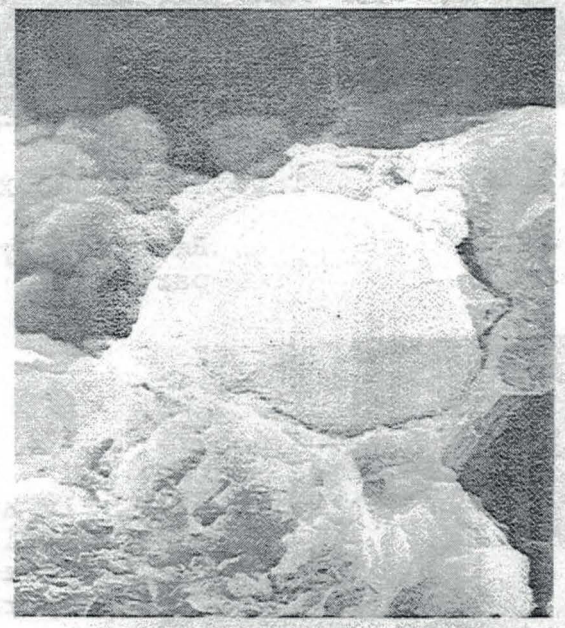

1 µm ⊢ 2000x (d)

Figure 5.28 (continued)
(d) 22 months

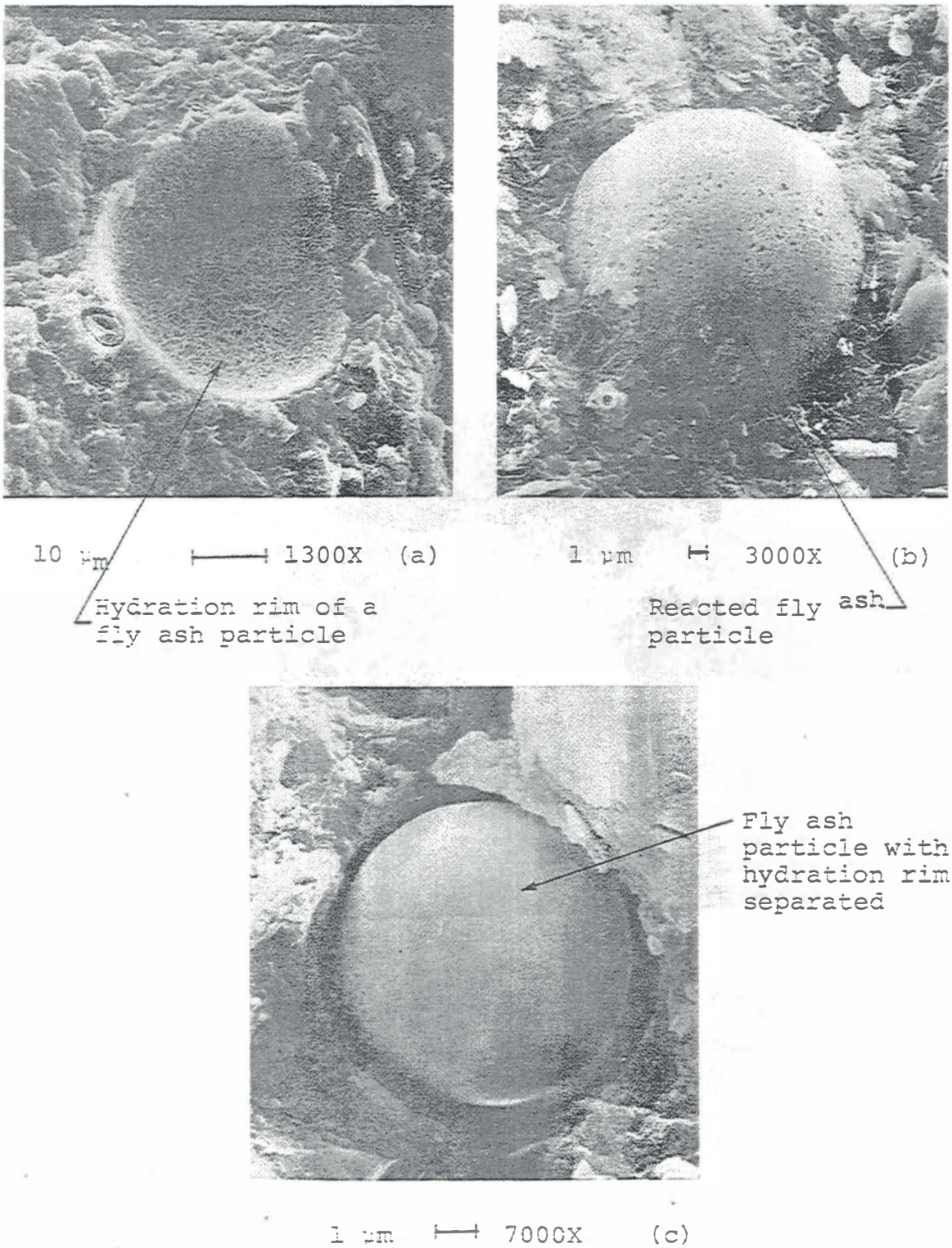

Figure 5.29: Micrographs of conjunctively stabilized field samples (continued)
(a), (b), (c) 1 month

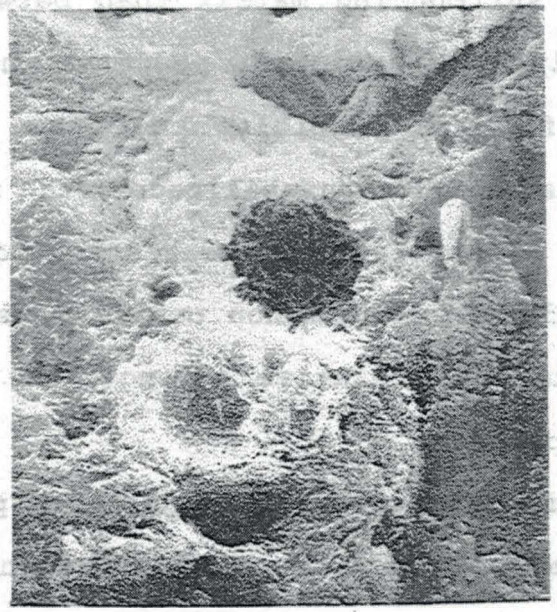

1 µm ⊢ 3000x (c)

Figure 5.29 B (continued)
(d) 22 months

sphere is necessarily weak, and because the fly ash sphere is still quite thick and therefore, strong in tension, the fly ash sphere will pullout of its hydration rim". The CSH material appears to be coating the entire surface of fly ash particle as evidenced from Figure 5.29b. Fly ash particles that have been plucked out of their hydration rim show a very smooth and clean surface (Figure 5.29c) indicating stronger bond between the hydration rim and the surrounding matrix than between the hydration rim and fly ash particles. Separation of the hydration rim from fly ash particles could not be observed in the shale samples stabilized with fly ash alone, an indication of a relatively weak surrounding matrix. Thus, the "pullout" phenomenon could be used as a crude way of measuring the relative strength of fly ash stabilized samples.

As the curing time progresses the "pullout" phenomenon becomes less frequent because of dissolution of fly ash particles and increased strength of surrounding matrix. A reacted cenosphere (hollow particle) is shown in Figure 5.29d in which the entire glassy part of the particle has been changed to reaction products after one month of curing in the field. EDS of this particle (Figure 5.30) showed the presence of aluminum, silica, and calcium suggesting the presence of a calcium aluminum silicate hydrate CASH, which is probably due to the dis-

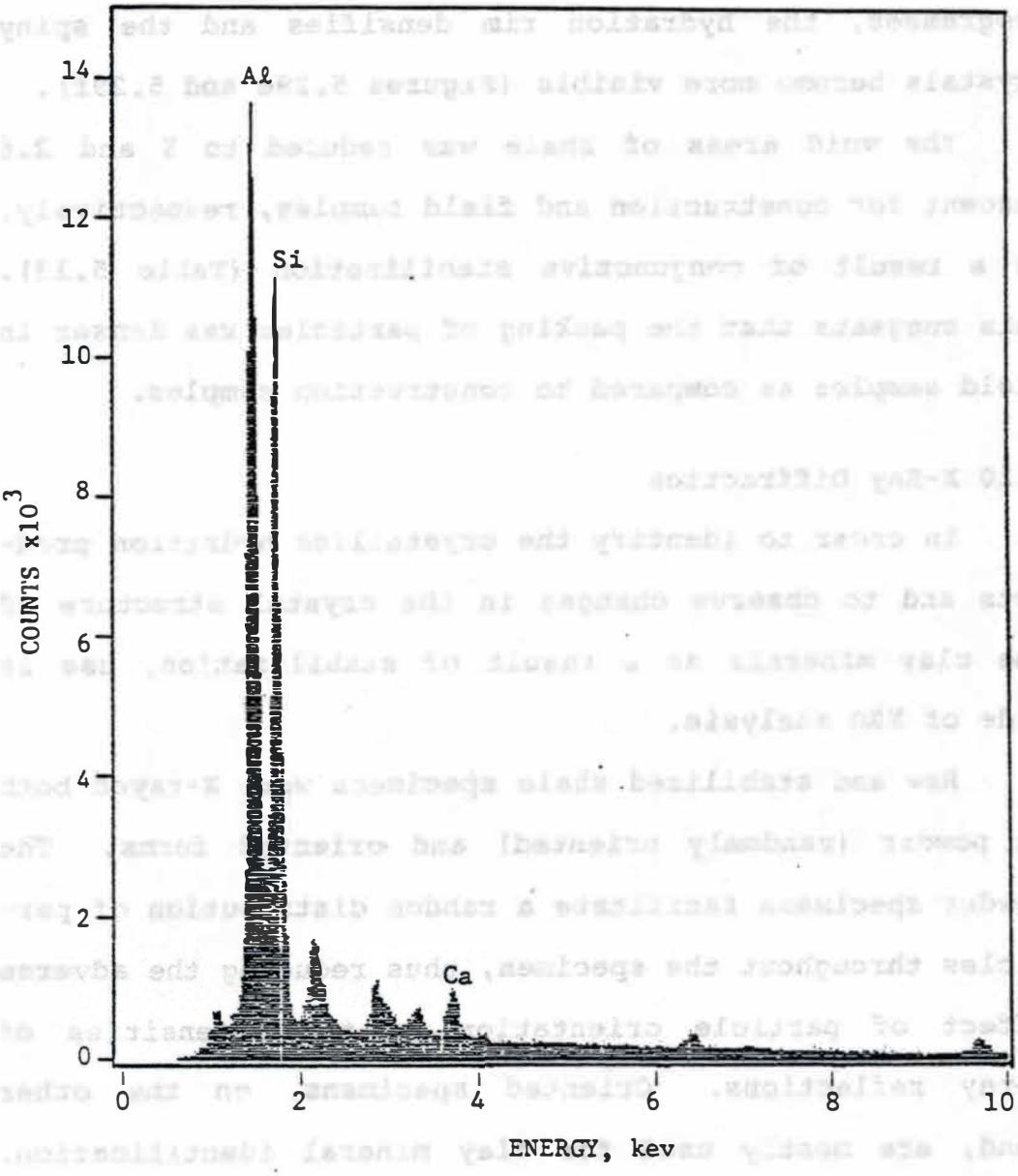

Figure 5.30: EDS of the reacted cenosphere observed in Figure 5.29d

integration of the glass phase. This observation was later confirmed by XRD analysis of conjunctively stabilized shale which showed the possible presence of CASH crystals as a hydration product. As the reaction progresses, the hydration rim densifies and the spiny crystals become more visible (Figures 5.29e and 5.29f).

The void areas of shale was reduced to 5 and 2.6 percent for construction and field samples, respectively, as a result of conjunctive stabilization (Table 5.13). This suggests that the packing of particles was denser in field samples as compared to construction samples.

5.10 X-Ray Diffraction

In order to identify the crystalline hydration products and to observe changes in the crystal structure of the clay minerals as a result of stabilization, use is made of XRD analysis.

Raw and stabilized shale specimens were X-rayed both in powder (randomly oriented) and oriented forms. The powder specimens facilitate a random distribution of particles throughout the specimen, thus reducing the adverse effect of particle orientation in the intensities of X-ray reflections. Oriented specimens, on the other hand, are mostly used for clay mineral identification. Clay minerals are generally platy and acquire a high degree of preferential orientation. In its oriented form

the (001) basal reflection of clay minerals is substantially enhanced, while its (hkl) reflections are diminished or suppressed (Brown, 1961). This property of clay minerals greatly simplifies their identification. To further facilitate clay mineral identification, some selected specimens were subjected to heat treatment and glycolation.

Powder specimens for all stations and curing conditions were X-rayed. Due to the interference of the X-ray peaks of silica, carbonates and feldspars, it was virtually impossible to draw any conclusions from the study of these diffractograms. Therefore, the study was concentrated on the oriented specimens. No major differences between diffractograms of any two stations of the same section were noticed. Therefore, the X-ray diffraction results of only one station per section are presented. Oriented specimens of three curing periods, i.e., after one, six, and twenty two months were subjected to XRD tests. As previously discussed (Chapter III), specimens for X-ray analysis (construction samples) were obtained from the broken parts of Harvard size specimens used for strength tests. These specimens were molded from the stabilized material passing a U.S. Standard sieve No. 10. To study the effect of larger stabilized shale particles on the X-ray reflections, one specimen for each stabilizing agent was prepared from the

broken parts of Proctor size specimens (Proctor specimen) which were cured for six months in the laboratory. The results of the X-ray analyses are presented in this section.

5.10.1 Raw Shale

The raw shale consisted of alpha quartz, a carbonate mineral group (possibly both calcite and dolomite), an unidentifiable feldspar mineral and a clay fraction.

The major clay mineral detected is a mixture of illite and smectite, the former being predominant. The clay is slightly expansive when glycolated. This can be observed in the sharpening of the illite peak at 10 Å and the shifting of the peak in the smectite region (Figure 5.31). Kaolinite is the only other clay mineral present in the raw shale. The presence of kaolinite was verified by heat treatment at 550°C, the temperature at which the crystalline structure of kaolinite is destroyed (Mitchell, 1976). The effect of heat treatment is clearly visible in Figure 5.32.

5.10.2 Clay Mineral Response to Stabilization

Diffractograms of oriented specimens of both field and construction samples were examined for clay mineral response to stabilization. These diffractograms are presented in Figures C.1 through C.18 in Appendix C.

5.10.2.1 Field Samples. Overall, the major clay

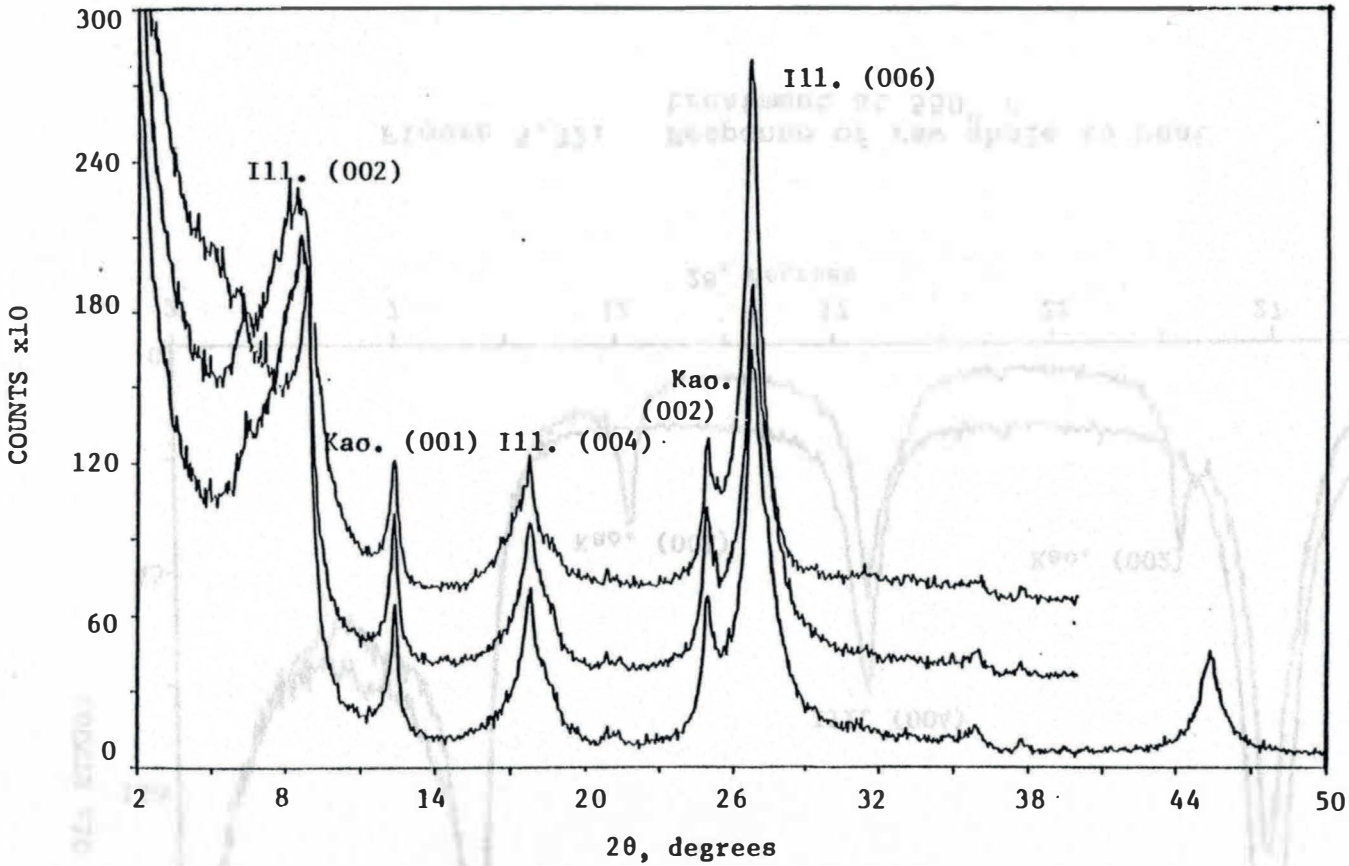

Figure 5.31: Response of raw shale to glycolation

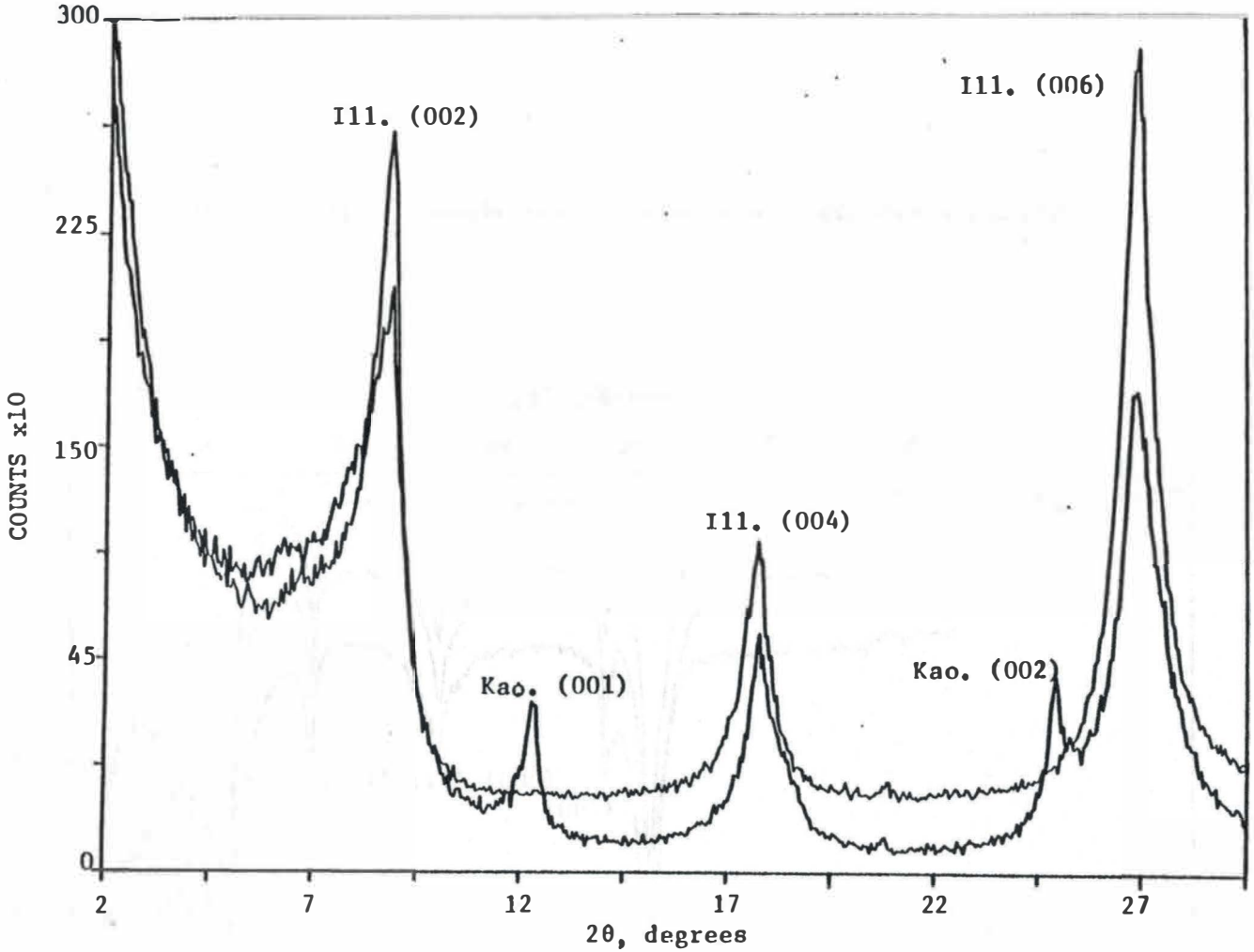

Figure 5.32: Response of raw shale to heat treatment at 550° C

minerals are similar to the ones described under raw shale. Though it is not possible to make any quantitative analysis from oriented diffractograms, for comparison purposes the integrated intensities (area under the peak) of raw and stabilized shale as provided by the Siemens D500 algorithm data are utilized. The complete data are presented in Tables C.1 through C.18, Appendix C, and the data relevant to clay minerals are depicted in Table 5.14.

Cement stabilization reduced the integrated intensities of clay minerals of field samples substantially. After one month of curing, the integrated intensity of illite was reduced to 3 percent and that of kaolinite to 18 percent of that of the raw shale. After six months of curing the illite peak disappeared but there was a slight reduction in kaolinite. After twenty two months of curing the reduction appeared to be less than than of the one and six months curing periods. In addition, non-basal reflections, (hkl), were also present in cement stabilized field samples, which indicates the resistance of cement stabilized field sample to the dispersion process. If the logical sequence is followed:

Table 5.14. Integrated Intensities of Clay Minerals of Field Samples

Test Section	One Month Curing		Six Month Curing		Twenty Two Month Curing	
	Illite	Kaolinite	Illite	Kaolinite	Illite	Kaolinite
Control	49575	3143				
Cement Stab.	1319	555	ND	481	4180	1140
Lime Stab.	1695	469	-	-	17912	2296
Fly Ash Stab.	-	-	175	359	10162	1701
Conjunctively Stab.	2179	417	15385	1344	7689	2098

ND = Not Detected

Presence of non basal reflection

↓

Poor orientation

↓

High shear resistance to dispersive forces

↓

Effectiveness of stabilization,

it may be concluded that dispersion by itself, like plasticity and strength, could be used as a rapid method to assess the effectiveness of stabilization. However, more research is needed to correlate dispersibility with plasticity and strength.

Lime stabilization of field samples showed the same effects on the clay minerals as cement stabilization. The integrated intensity of illite was reduced to 4 percent and that of kaolinite to 15 percent of that of the raw shale. Non-basal reflections (hkl) were present, but in many cases they were weaker than the basal reflection (001) indicating that dispersion is easier in lime stabilized than cement stabilized samples.

Fly ash stabilized field samples, like their cement stabilized counterparts were difficult to disperse. Reduction in the integrated intensity of illite after six months of curing was observed to be 1 percent and that of kaolinite was 12 percent of that of the raw shale. Non-basal reflections were strong in fly ash stabilized specimens indicating resistance to dispersion.

The integrated intensities of illite and kaolinite of conjunctively stabilized samples were reduced to 5 percent and 13 percent of those of the raw shale, after one month of curing, respectively. Longer curing periods (six and twenty two months) appear to cause no more reduction; in fact, the reduction was less, namely, the illite intensity was 31 percent and that of kaolinite 43 percent of those of the raw shale.

5.10.2.2 Construction Samples. Dispersion of construction samples was one of the major problems encountered in oriented specimen preparation.

All of the cement stabilized samples were very difficult to orient. Only the Proctor specimen oriented properly; all the others were poorly oriented and contained a considerable amount of alpha quartz. The clay minerals were essentially the same and glycolation had little influence on the position of the illite peak but it may slightly expand the smectite portion of the clay (see Figure C.5).

The lime stabilized samples were the easiest to disperse and hence could be oriented effectively. Lime stabilized samples (see Figure C.6) were impossible to remove from the filter membrane. XRD analysis for these samples was performed directly on the samples deposited on the filter membranes. The high background in the diffractogram is due to the scattering off from the

filter membrane.

The fly ash stabilized samples were difficult to disperse. Several of the samples produced such a thin filter cake that they could not be transferred from the filter paper for XRD analysis. Thus, Figure C.7 exhibits a very high background because of the scattering off of the filter paper underneath the clay sample. The only sample that could be easily oriented was that obtained from the Proctor specimen. The clay minerals present in the fly ash stabilized samples were essentially the same as those of cement and lime stabilized samples.

Conjunctively stabilized (six months cured) samples were impossible to disperse and orient properly. Thus, the diffractogram of unoriented powder samples is presented (Figure C.8). The major clay minerals present were illite and kaolinite.

From the above discussion it is obvious that only the Proctor specimens were oriented properly. Thus, the presence of larger shale particles (less than 1/2") has a definite effect on the degree of the dispersion effort expended in the preparation of oriented specimens. The fact that the Proctor specimens were dispersed with less effort indicates that stabilization is less effective with larger shale particles as compared to smaller shale particles. This was to be expected because with smaller shale particles, a more intimate mixture of shale and

stabilizing agent is attained as opposed to larger shale particles which are encased and linked to each other with the stabilizing agent forming a honeycomb type of fabric.

To study the relative effectiveness of stabilization on the clay minerals qualitatively, again, the integrated intensities are employed. The reason for choosing the diffractograms of Proctor specimens is that they were properly oriented. The integrated intensities of the clay minerals of construction samples are depicted in Table 5.15. As evidenced from Table 5.15 the integrated intensities of the clay minerals are reduced substantially. Cement stabilization reduced the integrated intensity of illite to 7 percent and that of kaolinite to 35 percent. Lime and fly ash stabilization reduced the intensity of illite to 9 and 3 percent, respectively, and that of kaolinite to 28 and 23 percent, respectively. No comparison could be made with conjunctively stabilized samples because it was impossible to obtain oriented specimens.

5.10.3 Reaction Products

Diffractograms of stabilized shale were closely examined for any new reaction products.

Addition of water to Portland cement results in several hydration products such as CSH, CAH, and $Ca(OH)_2$. However, none of these were observed in the X-ray re-

Table 5.15. Integrated Intensities of Clay Minerals of Construction Samples

Test Section	Illite	Kaolinite
Control	49575	3143
Cement Stab.	3349	1107
Lime Stab.	4583	877
Fly Ash Stab.	1267	723
Conjunctively Stab.	ND	ND*

ND = Not Determined.

flections of cement stabilized specimens. The CSH and CAH crystals either did not form or if they did their X-ray reflections were obscured by the presence of other minerals which made their detection impossible. The major peak of calcium hydroxide at 2.63 Å d-spacing was also absent from all diffractograms of cement stabilized specimens. It is difficult to suggest that calcium hydroxide did not form at all. Electron micrographs of cement stabilized specimens showed the formation of calcium hydroxide crystals. However, because of the small amount of Portland cement (14%) used to stabilize the shale, the amount of calcium hydroxide produced may not be enough to be detected by X-ray diffraction. On the other hand, the calcium hydroxide may have been consumed by some mineral present in the shale possibly by clay minerals, which resulted in the suppression of their X-ray peaks. This phenomenon is very similar to what was postulated by Herzog and Mitchell (1963), who reported that the hardening of clay-cement mixture involves a "primary" reaction in which the usual hydration products of cement are formed, and a "secondary" reaction which is triggered by the $Ca(OH)_2$, a reaction product of "primary" reaction which alters the structure of the clay minerals.

The diffractograms of lime stabilized specimens also failed to show the formation of any reaction product. The main reaction product of quicklime and water, namely

$Ca(OH)_2$ was absent from the diffractogram of all lime stabilized specimens. As discussed in the previous paragraph it may have been consumed by the clay minerals.

Fly ash stabilized field samples and several of the samples subjected to higher curing temperature (90°F) showed the presence of possible hydration products at 12.7 Å, 6.24 Å, 4.16 Å, and 3.04 Å d-spacing. The first three peaks are common to calcium-aluminum-silicate hydrates (CASH) while the 3.04 Å peak is common to calcium carbonate and several calcium silicate hydrates. The 12.7 Å, 6.24 Å, and 4.16 Å appears to be (001) spacings for stratlingite (PDF # 29-285) which belongs to the CASH group.

The reaction product of conjunctively stabilized samples appears to be a CAH group crystal, very similar to tetracalcium aluminate-10-hydrate (PDF's # 14-631 or 14-628). Calcium hydroxide may be present but it is hard to verify it because of overlaps of several lines. The presence of crystalline framework of hydration products was also observed in the electron micrographs of conjunctively stabilized specimens.

CHAPTER VI

COMPARISON OF LABORATORY, CONSTRUCTION AND FIELD DATA

As stated in Chapter I the main thrust of this investigation was aimed at comparing the results of previous laboratory studies (Laguros and Medhani, 1984) to those obtained from the field test sections during and after construction. These comparisons and the relevant discussions are presented in this chapter.

6.1 Gradation and Plasticity

Results of gradation analyses and plasticity tests of laboratory, construction and field samples are depicted in Tables 6.1 through 6.4. In terms of causing aggregation of the fine fraction of shale and reducing its plasticity index, stabilization under all conditions i.e., laboratory, construction and field proved to be effective.

The AI value of cement stabilized shale was increased from 1.00, for raw shale, to 1.83, 1.85 and 1.85 for laboratory, construction and field samples, respectively after one month of curing. This means that

Table 6.1. Properties of Laboratory, Construction, and Field Samples Stabilized with 14 Percent Portland Cement

Type of Sample	Curing Time (months)	<2μ Clay %	Silt %	Sand %	AI	LL %	PI %
Raw		46	48	6	1.00	50	31
Laboratory	1	1	13	86	1.83	-	NP
Construction	1	0	9	91	1.85	-	NP
	6	4	13	83	1.78	-	NP
	12	0	28	72	1.85	-	NP
	22	0	22	78	1.85	-	NP
Field	1	0	30	70	1.85	-	NP
	6	5	30	65	1.76	-	NP
	18	0	17	83	1.85	-	NP
	22	0	33	67	1.85	-	NP

Table 6.2. Properties of Laboratory, Construction, and Field Samples Stabilized with 4.5 Percent Quicklime*

Type of Sample	Curing Time (months)	<2μ Clay %	Silt %	Sand %	AI	LL %	PI %
Raw		46	48	6	1.00	50	31
Laboratory	1	4	18	78	1.78	43	9
Construction	1	7	42	40	1.52	38	6
	6	3	29	68	1.80	-	NP
	12	2	19	79	1.81	-	NP
	22	0	24	76	1.85	-	NP
Field	1	0	44	37	1.85	37	15
	6	8	46	46	1.70	41	7
	18	0	47	53	1.85	37	6
	22	0	30	70	1.85	45	3

* Laboratory samples were stabilized with 6 percent hydrated lime.

Table 6.3. Properties of Laboratory, Construction, and Field Samples Stabilized with 25 Percent Fly Ash

Type of Sample	Curing Time (months)	<2μ Clay %	Silt %	Sand %	AI	LL %	PI %
Raw		46	48	6	1.00	50	31
Laboratory	1	6	30	64	1.74	39	12
Construction	1	0	32	68	1.85	28	4
	6	2	35	63	1.81	30	3
	12	2	36	62	1.81	32	2
	22	0	42	58	1.85	-	NP
Field	1	5	57	36	1.72	40	17
	6	12	58	30	1.63	37	16
	18	3	52	45	1.80	40	17
	22	2	55	43	1.81	37	9

Table 6.4. Properties of Laboratory, Construction, and Field Samples Stabilized with 8 Percent Cement + 3 percent Quicklime* + 18 Percent Fly Ash

Type of Sample	Curing Time (months)	<2μ Clay %	Silt %	Sand %	AI	LL %	PI %
Raw		46	48	6	1.00	50	31
Laboratory	1	0	12	8	1.85	-	NP
Construction	1	0	10	90	1.85	-	NP
	6	0	7	93	1.85	-	NP
	12	4	25	71	1.78	-	NP
	22	0	28	72	1.85	-	NP
Field	1	0	7	93	1.85	-	NP
	6	14	26	60	1.59	-	NP
	18	0	19	81	1.85	-	NP
	22	-	-	-	-	-	-

* The amount of lime for laboratory samples was 4 percent hydrated lime

laboratory, construction, and field samples attained almost the same degree of aggregation of the fine fraction. The shale was rendered non-plastic in all cases as a result of cement stabilization.

Stabilization with lime increased the AI value of laboratory samples to 1.78 which was higher than construction samples (1.52), and lower than field samples (1.85). The latter value may have been caused by an undue concentration of lime in this particular sample. The plasticity index of shale was reduced from 31 percent for raw shale to 9, 6 and 15 percent, respectively, for laboratory, construction and field samples.

Fly ash stabilization also increased the AI values substantially. Laboratory samples showed an AI value of 1.74 which was lower than that of the construction samples (1.85) and slightly higher than their field counterparts (1.72). Plasticity index values of fly ash stabilized shale were 12, 4 and 17 percent, respectively, for laboratory, construction and field samples.

The AI of conjunctively stabilized shale was the same (1.85) for both laboratory and construction samples, followed by 1.78 for field samples. Conjunctive stabilization rendered the shale non-plastic in all cases.

The unexpected higher AI of construction samples compared to laboratory samples in some cases may be attributed to the fact that during specimen preparation of

construction samples, the material was passed through the U.S. Standard sieve No. 10 which may have resulted in a higher concentration of the stabilizing agent which was finer than the pulverized shale. Also the fraction retained on the sieve contained clay lumps which were discarded. The combination of these two factors may have caused an undue increase in AI and decrease in P.I. Further proof of the effect of these factors was observed in the preparation of oriented specimens for XRD (see Section 5.10.2.2) wherein construction samples showed higher resistance to dispersive forces thus making it impossible to orient properly.

6.2 Unconfined Compressive Strength

The immersed strength which represents a more severe test condition is selected as a basis of comparison of unconfined compressive strength, with the exception of raw shale, lime and fly ash stabilized remolded field samples which could not withstand immersion in water, and thus their predicted field strength calculated from remolded strength in dry test condition is chosen for comparison. Table 6.5 presents the unconfined compressive strengths of laboratory, construction, and field samples; and Table 6.6 depicts the ratios of the strengths of construction to laboratory and field to laboratory samples.

The data in Table 6.5 show that cement stabilized

Table 6.5. Unconfined Compressive Strength (psi) of Raw and Stabilized Shale for the Indicated Curing Period

Stabilized Test Section	Laboratory		Construction				Field			
	1 mo.	6 mos.	1 mo.	6 mos.	12 mos.	22 mos.	1 mo.	6 mos.	18 mos.	22 mos.
Control	73		16				16			
Cement Stab.	300	545	113	211	290	352	138	133	-	**
Lime Stab.	71	126	84	157	160	294	-	143*	217*	-
Fly Ash Stab.	132	134	77	96	80	222	-	231*	72*	-
Conjunctively Stab.	437	721	63	123	159	612	357	361	248	-

* Predicted undisturbed strength

** Could not be predicted because of insufficient amount of sample for remolded strength

Table 6.6. Strength Ratios of Stabilized Samples for the Indicated Curing Periods

Stabilized Test Section	*R_1		*R_2	
	1 month	6 months	1 month	6 months
Cement	0.38	0.39	0.46	0.24
Lime	1.18	1.25	-	1.15†
Fly Ash	0.58	0.72	-	1.72†
Conjunctively Stabilized	0.14	0.17	0.82	0.50

* $R_1 = \frac{\text{Strength of construction samples}}{\text{Strength of laboratory samples}}$

$R_2 = \frac{\text{Strength of field samples}}{\text{Strength of laboratory samples}}$

† Predicted undisturbed strength

laboratory samples have higher strength levels than their construction and field counterparts. The strength ratio of field to laboratory samples was 0.46 (Table 6.6) which is within the range of values reported by Wang (1968), and Robert and Schoeneman (1965). While lime stabilized laboratory samples showed slightly lower strength than their construction counterparts, fly ash stabilized laboratory samples attained higher levels of strength than their construction counterparts. The conjunctively stabilized laboratory samples attained higher strength levels than their construction and field counterparts.

In general, as the controlled conditions become less strict from the laboratory to the construction to the field samples, the effectiveness of stabilization as manifested by strength is slightly reduced.

6.3 Cohesion and Angle of Internal Friction

The shear parameters c and ϕ, as determined from the triaxial test, are presented in Table 6.7 and 6.8. The data suggest that cement stabilization laboratory samples showed higher cohesion than their construction and field counterparts after one month of curing; however, the value of ϕ was almost equal for all types of cement stabilized samples. Both c and ϕ of the lime stabilized laboratory samples were higher than their construction counterparts. The same trend is prevalent for fly ash

Table 6.7. Shear Parameters c (psi) and ϕ (degrees) of Stabilized Shale for the Indicated Curing Periods

Test Section	Laboratory				Construction				Field			
	1 month		6 months		1 month		6 months		1 month		6 months	
	c	ϕ	c	ϕ	c	ϕ	c	ϕ	c	ϕ	c	ϕ
Raw	4	36										
Cement	33	50	-	-	2	50	19	38	18	51	78	18
Lime	14	41	16	50	8	33	16	37	-	-	14*	33*
Fly Ash	28	43	14	60	0	38	19	28	-	-	12*	31*
Conjunctively Stabilized	31	61	-	-	6	44	14	45	40	56	57	54

Table 6.8. Ratios of Cohesion and Angle of Internal Friction of Stabilized Shale for the Indicated Curing Period

Stabilized Test Section	$^{*}RC_1$		$^{*}R\phi_1$		$^{*}RC_2$		$^{*}R\phi_2$	
	1 month	6 months	1 month	6 months	1 month	6 months	1 month	6 months
Cement	0.06	-	1.0	-	0.54	-	1.02	-
Lime	0.57	1	0.8	0.74	-	1[†]	-	0.80[†]
Fly Ash	0	1.36	0.88	0.47	-	0.43[†]	-	0.72[†]
Conjunctively Stabilized	0.19	-	0.66	-	1.29	-	0.84	-

* $RC_1 = \frac{c \text{ of construction samples}}{c \text{ of laboratory samples}}$, $RC_2 = \frac{c \text{ of field samples}}{c \text{ of laboratory samples}}$

$R\phi_1 = \frac{\phi \text{ of construction samples}}{\phi \text{ of laboratory samples}}$, $R\phi_2 = \frac{\phi \text{ of field samples}}{\phi \text{ of laboratory samples}}$

† Remolded samples

and conjunctively stabilized samples, except for the cohesion of conjunctively stabilized field samples which was higher than that of the laboratory samples, after one month of curing.

The ratio of the cohesion of stabilized construction to laboratory samples ranged from 0 to 1.36 and that of field to laboratory samples ranged from 0.43 to 1.29. For the corresponding ϕ values the ratios ranged from 0.66 to 1.0 and 0.72 to 1.02, respectively (Table 6.8).

6.4 Moduli of Elasticity

The flexural modulus of elasticity (E_f) and compressional modulus of elasticity (E_c) of laboratory, construction, and field samples are presented in Table 6.9. E_f values of cement stabilized laboratory and construction were very close to each other. The ratio of E_f of construction to laboratory samples was 1, while the ratio of their E_c values was 0.61. The ratio of the E_c values of cement stabilized field to laboratory sample was 0.22. Lime stabilized samples showed a different pattern i.e., the E_f of laboratory samples was lower than E_f of construction samples, while the reverse was true for E_c. The ratio of E_f of construction to laboratory samples was 1.18, and the ratio of their E_c was 0.62 which is approximately the same as that of cement stabilized samples (0.61).

Table 6.9. Comparison of Moduli of Laboratory to Construction and Field Samples

Test Section	Type of Sample	Flexural Modulus of Elasticity, E_f (psi)	* RE_f	Compressional Modulus of Elasticity (psi)	* RE_c
Cement	Laboratory	5504		54545	
	Construction	5474	0.99	33400	0.61
	Field	-		12000	0.22
Lime	Laboratory	4178		17708	
	Construction	4926	1.18	10999	0.62
	Field	-	-	-	-
Fly Ash	Laboratory	3877		22989	
	Construction	2645	0.68	24103	1.05
	Field	-	-	-	-
Conjunctively Stabilized	Laboratory	5839		48889	
	Construction	3207	0.55	29706	0.61
	Field	-	-	40000	0.82

* $RE_f = \frac{E_f \text{ Construction samples}}{E_f \text{ Laboratory samples}}$

$RE_c = \frac{E_c \text{ Construction or field samples}}{E_c \text{ Laboratory samples}}$

Fly ash stabilized laboratory samples showed higher E_f and lower E_c than their construction counterparts. The ratio of E_f of construction to laboratory samples was 0.68, and the ratio of their E_c was 1.05.

Finally, the ratio of E_f of conjunctively stabilized construction to laboratory was 0.55. The ratio of E_c of construction to laboratory was 0.61 and that of field to laboratory samples was 0.82 which suggests that conjunctively stabilized field samples attain higher modulus of elasticity than the construction samples.

6.5 Scanning Electron Microscopy

The projected area of voids as measured from the micrographs of raw and stabilized samples is a qualitative measure of the degree of aggregation of the particles and by extension an indicator of the degree of packing which takes place. Therefore, the projected area of voids is used to compare the effectiveness of stabilization. Table 6.10 depicts the void areas of raw and stabilized laboratory, construction, and field samples.

Cement stabilization reduced the void areas substantially. Laboratory samples showed a void area of 1.4 percent of the total area as compared to 1.6 percent and 1.3 percent for construction and field samples, respectively, indicating an almost equal degree of packing of particles in the samples. Longer curing periods (six

Table 6.10. Void Area From Micrographs of Raw and Stabilized Shale for the Indicated Curing Period, Percent of Total Area

Test Section	Type of Sample	1 month	6 months
Control	Laboratory	14	-
	Field	17	-
Cement Stab.	Laboratory	1.4	-
	Construction	1.6	3.7
	Field	1.3	0
Lime Stab.	Laboratory	2.2	2
	Construction	2.9	2.8
	Field	9	3.2
Fly Ash Stab.	Laboratory	2.1	0.6
	Construction	1.7	2
	Field	1.7	1.5
Conjunctively Stab.	Laboratory	1.1	1.1
	Construction	5	2.4
	Field	2.6	1.5

months) increased the void area of construction samples and decreased that of the field samples.

This was not unexpected because the field samples were further compacted by the placement of pavement layers and the construction samples showed some swelling as part of humid curing.

Lime stabilization reduced the void areas of laboratory samples to 2.2 percent of total area and those of construction and field samples to 2.9 and 9 percent of the total area. This indicated that packing of particles in laboratory samples was denser than their construction and field counterparts. Longer curing periods reduced the void areas to 2, 2.8, and 3.2 percent, respectively, for laboratory, construction, and field samples.

Fly ash stabilized samples showed void areas of 2.1, 1.7, and 1.7 percent for laboratory, construction, and field samples, respectively, indicating almost the same degree of packing of particles in laboratory, construction and field samples. While longer curing periods (six month) reduced the percent void areas of laboratory and field samples to 0.6 and 1.5, no significant change was observed with those of construction samples.

The area of voids of conjunctively stabilized laboratory samples was 1.1 percent and those of construction and field samples were 5 and 2.5 percent, respectively. Laboratory samples did not experience any change upon

longer curing periods, but the area of voids of construction and field samples were reduced to 2.4 and 1.5 percent, respectively. Packing of particles was denser in laboratory samples followed by field and construction samples in that order.

6.6 X-Ray Diffraction

A quantitative comparison of XRD data of laboratory and field samples is impossible because of a number of reasons such as different diffraction equipment, different diffractogram scales, and different sample preparation techniques. Therefore, in this section all comparisons are made from a qualitative point of view.

Unlike laboratory samples in which the kaolinite peak disappeared from the diffractogram of lime, cement, and conjunctively stabilized samples, the kaolinite peak was present in the diffractogram of all construction and field samples. This indicates that laboratory stabilization was more effective in destroying and/or masking of kaolinite crystal. The 10 Å illite peak, although present in the diffractograms of laboratory, construction, and field samples, was substantially reduced in intensity.

As far as reaction products are concerned, cement and lime stabilized laboratory samples showed the formation of different forms of hydrated and unhydrated calci-

um silicates, but diffractograms of construction and field samples failed to detect any new crystal formation as a result of lime and cement stabilization.

Fly ash stabilized laboratory specimens produced tetracalcium aluminum silicate hydrate, calcium aluminum silicate, calcium silicate hydrate and tricalcium silicate. However, only one possible form of calcium aluminum silicate hydrate (stratlingite) was identified as the reaction product of fly ash stabilized construction and field samples.

Conjunctively stabilized laboratory samples also produced reaction products that could not be found in the diffractograms of construction and field samples. Only tetracalcium aluminate-19-hydrate was observed in the diffractogram of construction and field samples which was not observed in laboratory samples.

It appears that the favorable laboratory controlled mixing, sample preparation, and curing conditions produce reaction products that are not formed or cannot be detected in the field because of poor pulverization, lack of an intimate mix, poor distribution of stabilized agent into the shale, and lack of controlled curing conditions. However, the last item, namely curing conditions, may not be as critical as the other factors because construction samples which were cured under laboratory conditions behaved like their field counterparts.

6.7 Visual Observations

Periodic visual observations of the stabilized test section indicated their performance to be excellent. The last two observation (July 1985 and May 1986) showed some slight rutting of the test sections which was more obvious in the control section, as expected. The rut depth ranged from 0 to 0.2 in. over the length of test sections (Table E.1). To this date the ride quality is excellent.

The supporting abilities of the stabilized sections was in excess of 20,000 lb. with the exception of one measurement out of fourteen in the fly ash stabilized section which was slightly lower than 20,000 lb. (Table E.1).

CHAPTER VII

CONCLUSIONS AND RECOMMENDATIONS

7.1 Conclusions

The purpose of this study was to investigate the stabilization of shale with Portland cement, lime, fly ash and the use of all three conjunctively, in a field test section in Ponca City, Kay County, Oklahoma. Based on the data obtained from various tests on samples obtained during the construction (construction samples) and those obtained after the construction (field samples), and comparing them to those obtained from laboratory prepared samples (laboratory samples) the following conclusions are drawn:

1. Some inconsistent patterns in the engineering behavior of construction and field samples was observed. These inconsistencies are primarily due to many construction variables such as lack of thorough distribution of stabilizing agent through the shale, difficulties in having an intimate mix, and the lack of a uniform water distribution through the mix. The other possible source of inconsisten-

cies may be related to the human error during the preparation of stabilized samples for testing.

2. Compaction of all test sections was in excess of 100 percent of Proctor density, but the moisture contents were lower than optimum.
3. Cement, lime, fly ash and conjunctive stabilization were effective in ameliorating the texture and plasticity of the shale by reducing the amount of clay size particles and the plasticity index. In terms of the degree of aggregation, both construction and field samples showed AI values which were in close agreement with each other.
4. Cement and conjunctive stabilization rendered the shale non-plastic. Lime stabilized construction and field samples showed PI values of 6 and 15 percent, respectively. Fly ash stabilization reduced the PI to 4 and 17 percent for construction and field samples, respectively.
5. The unconfined compressive strength of all construction, and cement and conjunctively stabilized field samples increased substantially as a result of stabilization. The ratio of the strength of field to laboratory cement stabilized sample was 0.46 and that of conjunctively stabilized samples was 0.82.
6. Undisturbed samples could not be obtained from lime and fly ash stabilized sections. However, their

undisturbed field strengths were predicted from their sensitivity and remolded strength which were in the range of values obtained from their construction counterparts.

7. Immersion in water for 24 hours reduced the unconfined compressive strength of all samples. The average loss in strength upon immersion in water was 8, 18, 26, and 58 percent, respectively, for cement, lime, fly ash and conjunctively stabilized construction samples. The strengths of cement and conjunctively stabilized field samples were reduced by 21 and 30 percent, respectively.
8. In general, cohesion and angle of internal friction of construction and field samples were increased as a result of stabilization.
9. Wetting and drying cycles increased the cohesion and angle of internal friction of construction samples.
10. Stabilization increased the modulus of rupture of stabilized shale. The modulus of rupture of stabilized shale was found to be related to the unconfined compressive strength by the linear regression equation:

$$MR = 4.97 + 0.23\ UC$$

11. Electron micrographs of stabilized construction and field samples revealed substantial decrease in the void areas, indicating a dense packing of particles.

Energy dispersive spectroscopy indicated the presence of calcium hydroxide crystals, in the micrographs of cement and conjunctively stabilized samples. It also indicated the presence of a calcium-silicate-hydrate as a reaction product of conjunctively stabilized samples.

12. Qualitative X-ray diffraction studies of construction and field samples indicated a substantial decrease in the integrated intensities of clay minerals as a result of stabilization. An interesting observation made during oriented sample preparation for XRD was the resistance of the specimens to dispersive force. The cement and fly ash stabilized samples were found to be very difficult to disperse and orient indicating strong stabilizing effect of those admixtures in a micro scale. Non-basal reflections, (hkl), were quite strong in some of the cement and fly ash stabilized samples and sometimes as strong as the oriented, (001), reflections. Reflections other than (001) were also present in the lime stabilized and conjunctively stabilized samples but the (001) lines were very much stronger than the other reflections indicating that the latter were easier to break apart during the dispersion process.
13. No hydration products in the form of crystal growth

were detected by the diffractograms of cement and lime stabilized samples. However, diffractograms of fly ash stabilized samples revealed the possible formation of stratlingite, a calcium-aluminum silicate hydrate, and the conjunctively stabilized samples showed the possible presence of a compound similar to tetracalcium aluminate-19-hydrate.

14. Laboratory samples showed more beneficiation (amelioration) followed by construction and field samples in that order. In other words, as the controlled conditions become less strict from the laboratory, to the construction to the field samples, the effectiveness of stabilization is slightly reduced. However, construction and field samples were at an acceptable performance level strongly indicating that field stabilization is an effective solution to the use of expansive shale.

7.2 Recommendations

While the field stabilization of expansive shale met with some degree of success, there are still some unanswered questions that need further research. The following are some of the areas for which further research is recommended:

1. The long term effectiveness of field stabilization during the life of the pavement needs to be studied.

This could be accomplished by supplementing periodic visual observations with some field coring after 4, 8, and 10 years. The cores should be tested for plasticity, strength, XRD, and SEM.

2. The brittleness of cores obtained from fly ash stabilized section may have been caused by excessive amounts of fly ash used. In future studies, investigation of smaller amounts is recommended.
3. Another solution to combat brittleness may be in the conjunctive use of lime and fly ash in the field. The use of lime helps to mollify or "break" the shale structure, and thus provides an intimate mixture of lime-shale-fly ash. Thus, the shale-lime-fly ash reaction is enhanced.
4. Perform cost analyses of the mix designs so that the most cost-effective mode of stabilization be determined.

REFERENCES

Ahlberg, H.L. and Barenberg, E.J. (1963), "The University of Illinois Pavement Test Track - A Tool for Evaluating Highway Pavements," Highway Research Record, No. 13, pp 1-21.

Ahlberg, H.L. and Barenberg, E.J. (1965), "Pozzolanic Pavement," Engineering Experiment Station, Bulletin 473, University of Illinois, Urbana, IL.

Alexander, M.L. (1976), "A Review of the Performance of Lime Treated Roadways in California," Final Report CA-DOT-TL-3324-1-76-14, FHWA/RD/M-0337.

American Association of State Highway and Transportation Officials (1982), "Standard Specifications for Transportation Materials and Methods of Sampling and Testing," AASHTO Designation: M 145-73, 13th ed., Washington D.C.

American Society for Testing and Materials (1973), "1973 Book of ASTM Standards," Part 10, Pa.

Anessi, T.H. (1970, "Strength and Consolidation Properties of Raw and Stabilized Oklahoma Shales", Ph.D. Dissertation, University of Oklahoma, Norman, Oklahoma, Unpublished.

Baker, M. and Laguros, J.G. (1984), "Reaction Products in Fly Ash Concrete," Symposium Proceedings, Material Research Society, pp. 73-83.

Bramao, L., Cady, J.G., Hendricks, S.B. and Swerdlow, M. (1952), "Criteria for the Characterization of Kaolinte, Halloysite, and a Related Mineral in Clays and Soils," Soil Science, Vol. 73, pp. 273-287.

Brindley, G.W. and Brown, G. (1980), "Crystal Structure of Clay Minerals and Their X-Ray Identification," Mineralogical Society, London.

References (continued

Brown, G. (1961) ed., "X-ray Identification and Crystal Structure of Clay Minerals", Mineralogical Society, London.

Burnet, B., Murtha, M.J. and Harnby, N. (1984), "Co-utilization of Pulverized Coal Ash and Flue Gas Scruber Sludge," Ashtech '84, Second International Conference on Ash Technology and Marketing, Barbican Centre, London.

Chu, Y.T. (1977), "Engineering Behavior of Pavement Materials: State of the Art," U.S. Station, Final Report No. FAA-RD-77-37, WES TR S-77-9.

Dallaire, G. (1973), "Dallas-Ft. Worth: World's Largest, Best Planned Airport," Civil Engineering, pp. 53-58.

Davidson, D.T. and Handy, R.L. (1960), "Lime and Lime-Pozzolan Stabilization," In: Woods, K.B., ed., Highway Engineering Hand Book, McGraw-Hill, pp. 21-98-21-108.

Diamond, S. (1981), "The Characterization of Fly Ashes," Materials Research Society Symposium N, Annual Meeting, pp. 12-23.

Diamond, S. and Kinter, E.B. (1965), "Mechanisms of Soil-Lime Stabilization - An Interpretive Review," Research Record, No. 92, pp. 83-102.

Diamond, S., White, J.L. and Dolch, W.L. (1963), "Transformation of Clay Minerals by Calcium Hydroxide Attack," and Minerals, 12th National Conference, Atlanta, Georgia, pp. 359-379.

Eades, J.L., Nichols, F.P., Jr. and Grim, R.E. (1963), "Formation of New Minerals with Lime Stabilization as Proven by Field Experiments in Virginia," Research, Bulletin No. 335, pp. 31-39.

Felt, E.J. and Abrams, M.S. (1957), "Strength and Elastic Properties of Compacted Soil-Cement Mixtures," American Society for Testing and Materials, Special Technical Publication No. 206.

George, K.P. and Davidson, D.T. (1963), "Development of a Freeze-Thaw Test for Design of Soil-Cement," Research Record, No. 36, pp. 77-96.

References (continued)

Glenn, R.G. and Handy, R.L. (1963), "Lime-Clay Mineral Reaction Products," Highway Research Record, No. 29, pp. 70-82.

Grutzeck, M.W., Roy, D.M., and Scheetz, B.E. (1981), "A Hydration Mechanism of High-Lime Fly Ash in Portland Cement Composites," Material Research Society Symposium N, Annual Meeting, pp. 92-101.

Herrin, M. and Mitchell, M. (1961), "Lime Soil Mixes," Highway Research Board, Bulletin No. 304, pp. 99-138.

Herzog, A. and Mitchell, J.K. (1963), "Reactions Accompanying Stabilization of Clay with Cement," Highway Research Record, No. 36, pp. 146-171.

Highway Research Board Committee on Soil-Cement Stabilization, (1959), "Definition of Terms Relating to Soil-Portland Cement Stabilization," Highway Research Abstracts, Vol. 29, No. 6, pp. 28-29.

Hoover, J.M., Huffman, R.T. and Davidson, D.T. (1962), "Soil Stabilization Field Trials, Primary Highway 117, Jaspar County, Iowa," Highway Research Board, Bulletin No. 357, pp. 41-68.

Humbert, R.P., and Shaw, B.T. (1941), "Studies of Clay Particles with the Electron Microscope: I. Shape of Clay Particles," Soil Science, Vol. 52, pp. 481-487.

Jackson, M.L., Mackie, W.Z. and Pennington, R. P. (1946), "Electron Microscope in Soil Research," Proceedings of the Soil Science Society of America, Vol. 11, pp. 57-63.

Joshi, R.C., Duncan, D.M. and McMaster, H.M. (1975), "New and Conventional Engineering Use of Fly Ash," Transportation Engineering Journal, ASCE Proceedings, Vol. 101, No. TE4, pp. 791-806.

Kelly, O.J. and Shaw, B.T. (1942), "Studies of Clay Particles with the Electron Microscope: III. Hydrodynamic Considerations in Relation to the Shape of Particles," Proceedings of the Soil Science Society of America, Vol. 7, pp. 58-68.

References (continued)

Kinter, E.B., Wintermyer, A.M. and Swerdiow, M. (1952), "Electron Microscopy of Soil Clays and Related Materials," Public Roads, Vol. 27, No. 5, pp. 89-100.

Kumar, S. (1974), "A Study of the Effects of Simulated Weathering and Repeated Loads on Four Lime Stabilized Oklahoma Shales", Ph.D. Dissertation, University of Oklahoma, Norman, Oklahoma, Unpublished.

Laguros, J.G. (1972), "Predictability of Physical Changes of Clay Forming Materials in Oklahoma," Report No. ODOT 68-03-2, OURI 1677, University of Oklahoma, School of Civil Engineering and Environmental Science, Norman, Oklahoma.

Laguros, J.G., Davidson, D.T., Handy, R.L. and T.Y. Chu (1956), "Evaluation of Lime for Stabilization of Loess," ASTM Proceedings, Vol. 56, pp. 1301-1315.

Laguros, J.G. and Jha, K. (1977), "Stabilization of Oklahoma Shales," Report No. ODOT 73-04-2, ORA 158-602, University of Oklahoma, School of Civil Engineering and Environmental Science, Norman, Oklahoma.

Laguros, J.G. and Medhani, R. (1984), "Stabilization of Oklahoma Shales, Field Implementation Phases," Final Report ODOT 79-09-2 (Item 2185), ORA 158-867, The University of Oklahoma.

Laguros, J.G. and Medhani, R. (1984), "Fly Ash in Soil Stabilization," Ashtech '84, Second International Conference on Ash Technology and Marketing, Barbican Centre, London.

Loughborough, T.F. (1948), "Performance of Soil-Cement Roads in Virginia," Virginia Highway Bulletin, Vol. 14, No. 11, pp. 3-6.

Lund, O.L. and W.J. Ramsey (1959), "Experimental Lime Stabilization in Nebraska," Highway Research Board, Bulletin No. 231, pp 24-59.

Maclean, D.J. (1956), "Consideration Affecting the Design and Construction of Stabilized-Soil Road Bases," Journal, Institute of Highway Engineers, London, Vol. 3, No. 9, p. 16.

References (continued)

Marshall, C.E., Humbert, R.P., Shaw, B.T. and Caldwell, O.G. (1942), "Studies of Clay Particles with the Electron Microscope: II. The Fractionation of Beidellite, Nontronite, Magnesium Bentonite, and Attapulgite," Soil Science, Vol. 54, pp. 149-158.

Mateos, M. (1964), "Stabilization of Soils with Fly Ash Alone," Highway Research Record, No. 52, pp. 59-65.

McDonald, E.B. (1970), "Experimental Stabilization of Pierre Shale," Highway Research Record, Bulletin No. 315, pp. 14-28.

McDowell, C. (1959), "Stabilization of Soils with Lime, Lime-Fly Ash and Other Lime Reactive Materials," Highway Research Board, Bulletin No. 231, pp. 60-66.

McDowell, C. (1966), "Evaluation of Soil-Lime Stabilization Mixtures," Highway Research Record, Bulletin No. 139, pp. 15-24.

McDowell, C. (1955), "Wheel-Load Stress Computations Related to Flexible Pavement Design," Highway Research Board, Bulletin No. 114, pp. 1-20.

Mills, W.H., Jr. (1935), "Road Base Stabilization with Portland Cement," Engineering New Record, Vol. 115, No. 22, pp. 751-753.

Mills, W.H., Jr. (1936), "Stabilizing Soil with Portland Cement, Experiments by South Carolina Highway Department," Highway Research Board, Proceedings, Vol. 16, pp. 322-347.

Mills, W.H., Jr. (1940), "Condition Survey of Soil-Cement Roads," Highway Research Board, Proceedings, Vol. 20, pp. 812-820.

Mills, W.H., Jr. (1941), "Condition Survey of Soil-Cement Roads," Highway Research Board, Proceedings, Vol. 21, pp. 482-492.

Minnick, L.J. (1967), "Reaction of Hydrated Lime with Pulverized Coal Fly Ash," Proceedings: Fly Ash Utilization Symposium, U.S. Bureau of Mines Information, Circular No. 8348.

Minnick, L.J. and Williams, R. (1956), "Field Evaluation of Lime-Fly Ash-Soil Compositions for Roads," Highway Research Board, Bulletin No. 129, pp. 83-99.

References (continued)

Mitchell, J.K. (1976), "Fundamentals of Soil Behavior," John Wiley & Sons, New York.

Mitchell, J.K. and ElJack, S.A. (1965), "The Fabric of Soil Cement and Its Formation," Clay and Clay Minerals, 14th National Conference, pp. 297-305.

Mitchell, J.K. and Freitag, D.R. (1959), "A Review and Evaluation of Soil-Cement Pavements," Journal of the Soil Mechanics and Foundation Division, ASCE Proc., pp. 49-73.

Moh, Za-Chieh (1965), "Reaction of Soil Minerals with Cement and Chemicals," Highway Research Record, No. 86, pp. 39-61.

National Cooperative Highway Research Program, Synthesis of Highway Practice, No. 37 (1976).

Noble, D.F. (1967), "Reactions and Strength Development in Portland Cement-Clay Mixture," Highway Research Record, No. 198, pp. 39-56.

Ormsby, W.C. and Kinter, E.B. (1973), "Strength Development and Reaction Products in Lime-Montmorillonite-Water Systems," Public Roads, Vol. 37, No. 4, pp. 136-148.

Postek, Michael T., et al. (1980), "Scanning Electron Microscopy," A student's handbook, Ladd Research Industries, Inc. 1980.

Redus, J.F. (1958), "Study of Soil-Cement Base Courses on Military Airfields," Highway Research Board, Bulletin No. 198, pp. 13-19.

Reid, C.R. (1948), "Report of Committee on Soil-Cement Roads," Highway Research Board, Bulletin No. 14, pp. 12-17.

Robert, S.E. and Schoeneman, E.P. (1965), "Soil-Cement Construction Using Loess Soil," Highway Research Record, No. 86, pp. 62-72.

Sloane, R.L. (1964), "Early Reaction Determination in Two Hydroxide-Kaolinite Systems by Electron Microscopy and Diffraction," Clay and Clay Minerals, 13th National Conference, pp. 331-339.

References (continued)

Spangler, M.G., and Handy, R.L. (1973), "Soil Engineering", Harper & Row, New York.

Stamp, R.J. and Smith, I.E. (1984), "Pulverized Fuel Ash-Waste Material or Mineral Resource?", Ashtech '84, Second International Conference on Ash Technology and Marketing, Barbican Centre, London.

Stewart, R.L., Fletcher, O.S. and Chu, T.Y. (1971), "Stabilization of Piedmont Soils for Use as Base Material on Secondary Road Projects," Highway Research Record, No. 351, pp. 21-34.

Thompson, M.R. (1966), "Lime Reactivity of Illinois Soils", Journal of the Soil Mechanics and Foundation Division, ASCE Proceedings, Vol. 92, No. SM5, pp. 67-92.

Thompson, M.R. (1968), "Lime-Treated Soils for Pavement Construction," Journal of the Highway Division, ASCE Proceedings, Vol. 94, No. HW2, pp. 191-217.

Thompson, M.R. (1975), "Soil-Lime Mixtures for Construction of Low-Volume Roads," Transportation Research Board, Special Report No. 160, pp. 149-165.

United States Department of Agriculture, Soil Conservation Service (1967), "Soil Survey for Kay County, Oklahoma," U.S. Government Printing Office, Washington, D.C.

Wang, M.C. (1968), "Stress and Deflections in Cement-Stabilized Soil Pavements," Ph.D. Dissertation, University of California, Berkeley.

Willis, E.A. (1947), "Experimental Soil-Cement Base Course in South Carolina," Public Roads, Vol. 25, No. 1.

Yoder, E.J. and Witczak, M.W. (1975), "Principles of Pavement Design," John Wiley & Sons, New York.

APPENDIX A

GRAIN SIZE AND PLASTICITY DATA OF STABILIZED SHALE

Table A.1. Index Properties of Construction Samples Cured at 70°F, and 90-100 Percent Relative Humidity for the Indicated Curing Periods

Test Section	Station	1 month				6 months				12 months				22 months			
		<2μ Clay	Silt	Sand	AI	<2μ Clay	Silt	Sand	AI	<2μ Clay	Silt	Sand	AI	<2μ Clay	Silt	Sand	AI
Control	298+05	46	48	6	1.00	46	48	6	1.00	46	48	6	1.00	46	48	6	1.00
Cement Stab.	269+22	0	10	90	1.85	5	5	90	1.76	0	20	80	1.85	3	41	56	1.80
	272+37	0	9	91	1.85	4	13	83	1.78	0	28	72	1.85	0	22	78	1.85
Lime Stab.	275+46	7	42	40	1.52	3	29	68	1.8	2	19	79	1.81	0	24	76	1.85
	279+64	0	19	81	1.85	0	20	80	1.85	2	35	63	1.81	1	34	65	1.83
Fly Ash Stab.	284+60	0	37	59	1.85	6	33	61	1.74	0	36	64	1.85	0	33	67	1.85
	285+36	0	32	68	1.85	2	35	63	1.81	2	36	62	1.81	0	42	58	1.85
Conjunctively Stab.	789+22	0	10	90	1.85	0	7	93	1.85	4	25	71	1.78	0	28	72	1.85
	292+89	0	14	86	1.85	0	11	89	1.85	2	22	76	1.81	0	27	71	1.81

All values are in percent except AI

Table A.2. Index Properties of Construction Samples Cured at 90°F, and 90-100 Percent Relative Humidity for the Indicated Curing Periods

Test Section	Station	1 month				6 months				12 months				22 months			
		<2μ Clay	Silt	Sand	AI	<2μ Clay	Silt	Sand	AI	<2μ Clay	Silt	Sand	AI	<2μ Clay	Silt	Sand	AI
Control	298+05	46	48	6	1.00	46	48	6	1.00	46	48	6	1.00	46	48	6	1.00
Cement Stab.	269+22	0	10	90	1.85	2	6	92	1.81	0	12	88	1.85	-	-	-	-
	272+37	0	12	88	1.85	0	21	79	1.85	0	7	93	1.85	0	22	78	1.85
Lime Stab.	275+46	5	37	48	1.76	2	24	74	1.81	0	28	72	1.85	0	21	79	1.85
	279+64	0	22	78	1.85	0	14	86	1.85	0	29	71	1.85	0	33	67	1.85
Fly Ash Stab.	284+60	0	42	54	1.85	1	36	63	1.83	5	21	74	1.76	0	37	62	1.85
	285+36	0	35	61	1.85	1	44	55	1.83	4	30	66	1.78	0	39	61	1.85
Conjunctively Stab.	289+22	0	0	100	1.85	0	7	93	1.85	0	8	92	1.85	0	20	80	1.85
	292+89	0	10	90	1.85	0	7	93	1.85	0	20	80	1.85	0	27	73	1.85

All values are in percent except AI

Table A.3. Index Properties of Field Samples for the Indicated Curing Period

Test Section	Station	1 month				6 months				18 months				22 months			
		<2μ Clay	Silt	Sand	AI	<2μ Clay	Silt	Sand	AI	<2μ Clay	Silt	Sand	AI	<2μ Clay	Silt	Sand	AI
Control	298+05	46	48	6	1.00												
Cement Stab.	272+37	0	30	70	1.85	5	30	65	1.76	0	17	83	1.85	0	33	67	1.85
Lime Stab.	275+46	0	44	37	1.85	8	46	46	1.7	0	47	53	1.85	0	30	70	1.85
Fly Ash Stab.	285+36	5	57	36	1.72	12	58	30	1.63	3	52	45	1.80	2	55	43	1.81
Conjunctively Stab.	289+22	0	7	93	1.78	14	26	60	1.59	0	19	81	1.85				

Table A.4. Plasticity Tests Results of Construction Samples Cured at 70°F, and 90-100 Percent Relative Humidity for the Indicated Curing Periods

Test Section	Station	1 month		6 months		12 months		22 months	
		LL	PI	LL	PI	LL	PI	LL	PI
Control	298+05	50	31	50	31	50	31	50	31
Cement Stab.	269+22	-	NP	-	NP	-	NP	-	NP
	272+37	-	NP	-	NP	-	NP	-	NP
Lime Stab.	275+46	38	6	-	NP	-	NP	-	NP
	279+64	-	NP	-	NP	-	NP	-	NP
Fly Ash Stab.	284+60	26	9	31	10	31	9	34	NP
	285+36	28	4	30	3	32	2	34	NP
Conjunctively Stab.	289+22	-	NP	-	NP	-	NP	-	NP
	292+89	-	NP	-	NP	-	NP	-	NP

Table A.5. Plasticity Tests Results of Construction Samples Cured at 90°F, and 90-100 Percent Relative Humidity for the Indicated Curing Periods

Test Section	Station	1 month		6 months		12 months		22 months	
		LL	PI	LL	PI	LL	PI	LL	PI
Control	298+05	50	31	50	31	50	31	50	31
Cement Stab.	269+22	-	NP	-	NP	-	NP	-	NP
	272+37	-	NP	-	NP	-	NP	-	NP
Lime Stab.	275+46	41	4	-	NP	-	NP	-	NP
	279+64	-	NP	-	NP	-	NP	-	NP
Fly Ash Stab.	284+60	27	9	29	4	33	9	-	NP
	285+36	26	3	30	2	30	2	-	-
Conjunctively Stab.	289+22	-	NP	-	NP	-	NP	-	NP
	292+89	-	NP	-	NP	-	NP	-	NP

Table A.6. Plasticity Tests Results Field Samples for the Indicated Curing Periods

Test Section	Station	1 month		6 months		18 months		22 months	
		LL	PI	LL	PI	LL	PI	LL	PI
Control	298+05	50	31						
Cement Stab.	272+37	-	NP	-	NP	-	NP	-	NP
Lime Stab.	275+46	37	15	41	7	37	6	45	3
Fly Ash Stab.	285+36	40	17	37	16	40	17	37	9
Conjunctively Stab.	289+22	-	NP	-	NP	-	NP	-	-

APPENDIX B

TRIAXIAL AND UNCONFINED COMPRESSIVE STRENGTH TESTS DATA OF CONSTRUCTION SAMPLES

Table B.1. Shear Parameters of Cement Stabilized Construction Samples

Curing Time, Months	70°F				90°F			
	Dry		Imm.		Dry		Imm.	
	c	ϕ	c	ϕ	c	ϕ	c	ϕ
1	33	42	2	50	18	50	7.5	50
6	20	55	19	38	27	49	60	40
12	12	55	20	46	12	51	21	34
22	49	39	21	49	11	64	29	52

c = psi

ϕ = degrees

Table B.2. Shear Parameters of Lime Stabilized Construction Samples

Curing Time, Months	70°F				90°F			
	Dry		Imm.		Dry		Imm.	
	c	ϕ	c	ϕ	c	ϕ	c	ϕ
1	13	32	8	33	56	23	22	40
6	26	26	16	37	44	36	15	42
12	11	72	6	40	56	36	23	41
22	38	45	52	38	94	34	42	51

Table B.3. Shear Parameters of Fly Ash Stabilized Construction Samples

Curing Time, Months	70°F				90°F			
	Dry		Imm.		Dry		Imm.	
	c	ϕ	c	ϕ	c	ϕ	c	ϕ
1	30	32	0	38	26	40	37	7
6	14	41	19	28	48	33	9	32
12	24	46	10	34	30	42	12	34
22	45	33	34	51	26	46	27	40

Table B.4. Shear Parameters of Conjunctively Stabilized Construction Samples

Curing Time, Months	70°F				90°F			
	Dry		Imm.		Dry		Imm.	
	c	ϕ	c	ϕ	c	ϕ	c	ϕ
1	22	42	6	44	92	32	32	44
6	46	48	14	45	27	62	16	58
12	18	51	7	53	14	63	62	44
22	76	49	8	60	84	40	88	35

Table B.5. Shear Parameters* of Undisturbed Field Samples

Test Section	1 Month Curing				6 Month Curing				18 Month Curing			
	Dry		Imm.		Dry		Imm.		Dry		Imm.	
	c	ϕ	c	ϕ	c	ϕ	c	ϕ	c	ϕ	c	ϕ
Raw Shale	4	36										
Cement	15	51	18	51	40	51	78	18	-	-	-	-
Conjuctively Stabilized	139	22	40	56	85	41	57	54	-	-	98	48

* c - psi

ϕ - degrees

Table B.6. Unconfined Compressive Strength (psi) of Cement Stabilized Field Samples

Curing Period (months)	Specimen No.	Dry	Average	Imm.	Average
1	1	187		107	
	2	136		169	
	3	199	174	-	138
6	1	158		180	
	2	131	144	86	133
* 18	-	-	-	-	-
** 22	-	-	-	-	-

* The quality of samples were not good enough to withstand trimming.

** Hand auger was used for sampling, therefore no sample could be obtained.

Table B.7. Unconfined Compressive Strength (psi) of Conjunctively Stabilized Field Samples

Curing Period (months)	Specimen No.	Dry	Average	Imm.	Average
1	1	560		430	
	2	449		309	
	3	535	515	332	357
6	1	263		533	
		434		340	
		386	368	231	361
*18	1	333	333	248	248
**22	-	-	-	-	-

* The amount of sample obtained from the field was not enough to test more than one sample.

** Hand auger was used for sampling, therefore no sample could be obtained.

Table B.8. Unconfined Compressive Strength (psi) of Construction Samples for the Indicated Curing Periods

Test Section	Station	*1 month		*6 months		*12 months		**22 months	
		Dry	Imm.	Dry	Imm.	Dry	Imm.	Dry	Imm.
Control	298+22	16	-						
Cement Stab.	269+22	264	131	239	209	464	353	434	428
	272+37	108	95	226	213	266	226	330	276
Lime Stab.	275+46	90	82	139	135	168	137	231	239
	279+64	103	85	197	179	254	184	446	350
Fly Ash Stab.	284+60	104	88	148	93	101	80	220	275
	285+36	109	66	191	99	113	***	227	170
Conj. Stab.	289+22	92	94	***	***	***	***	700	691
	292+89	140	63	304	123	408	159	659	533

* Test run on one Proctor-size sample.

** Test run on at least two Harvard Minature-size samples.

*** Samples were broken before testing.

APPENDIX C

X-RAY DIFFRACTOGRAMS AND DIFFRACTION DATA

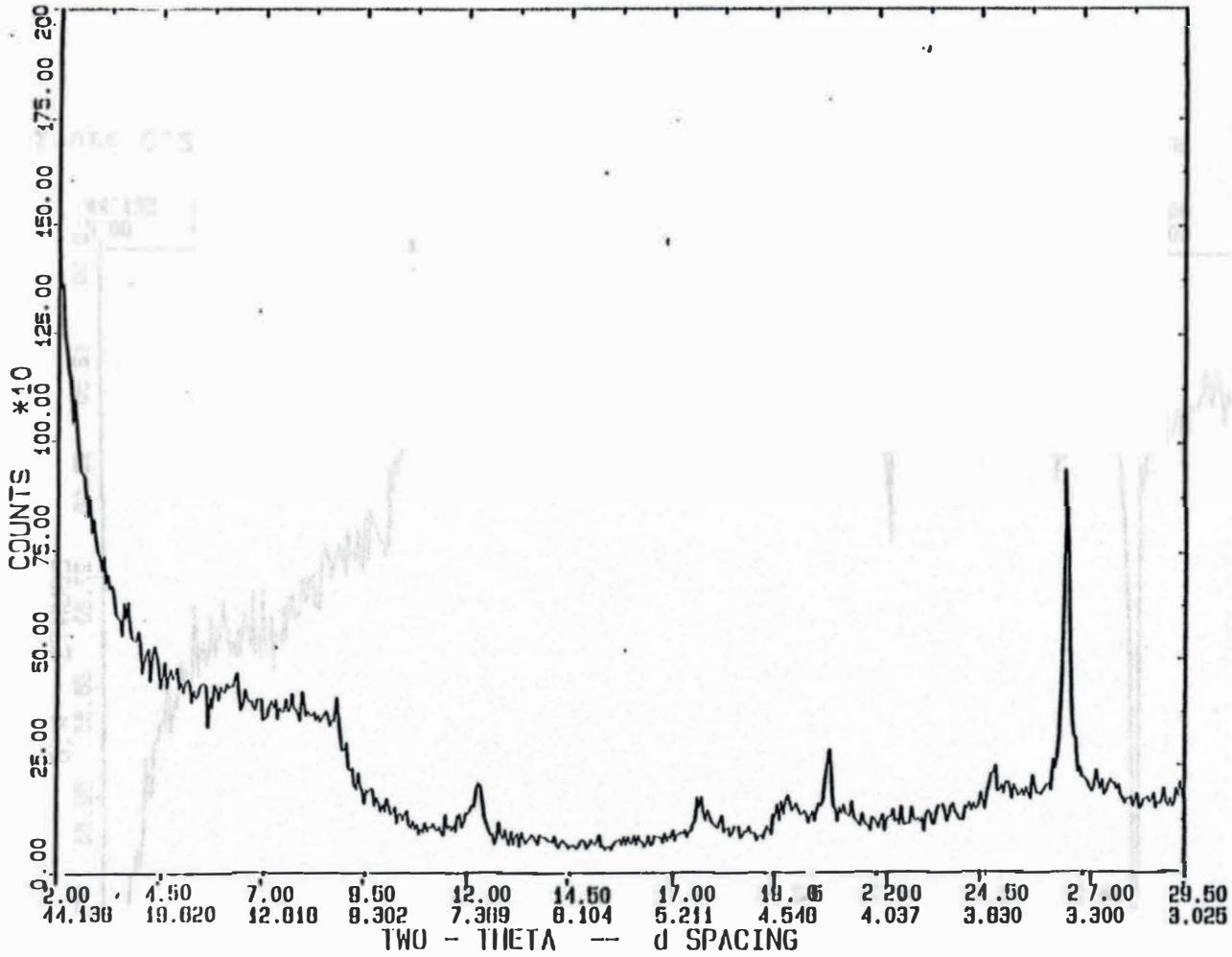

Figure C.1: X-ray diffractogram of cement stabilized field samples (6 months, oriented)

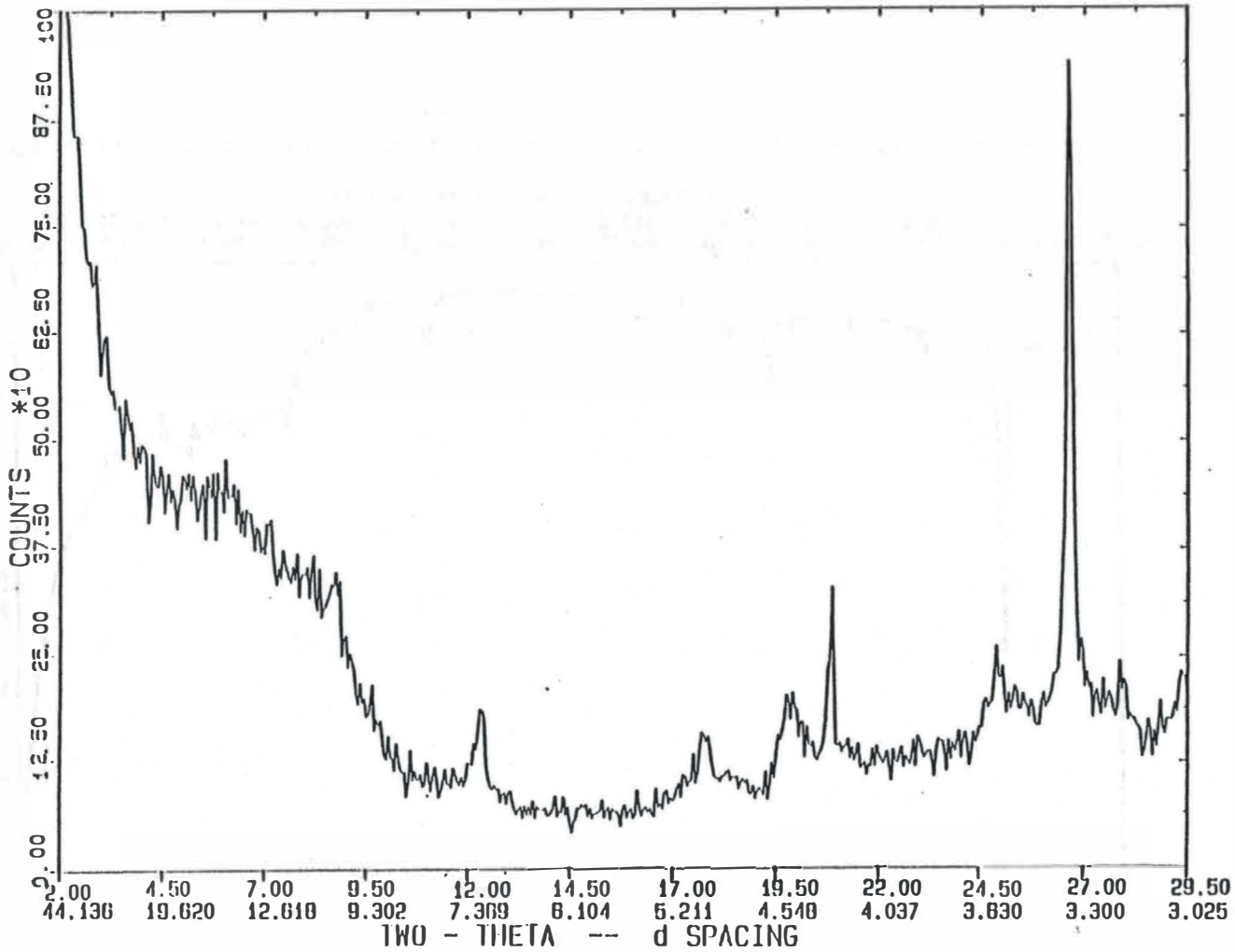

Figure C.2: X-ray diffractogram of lime stabilized field samples (6 months, oriented)

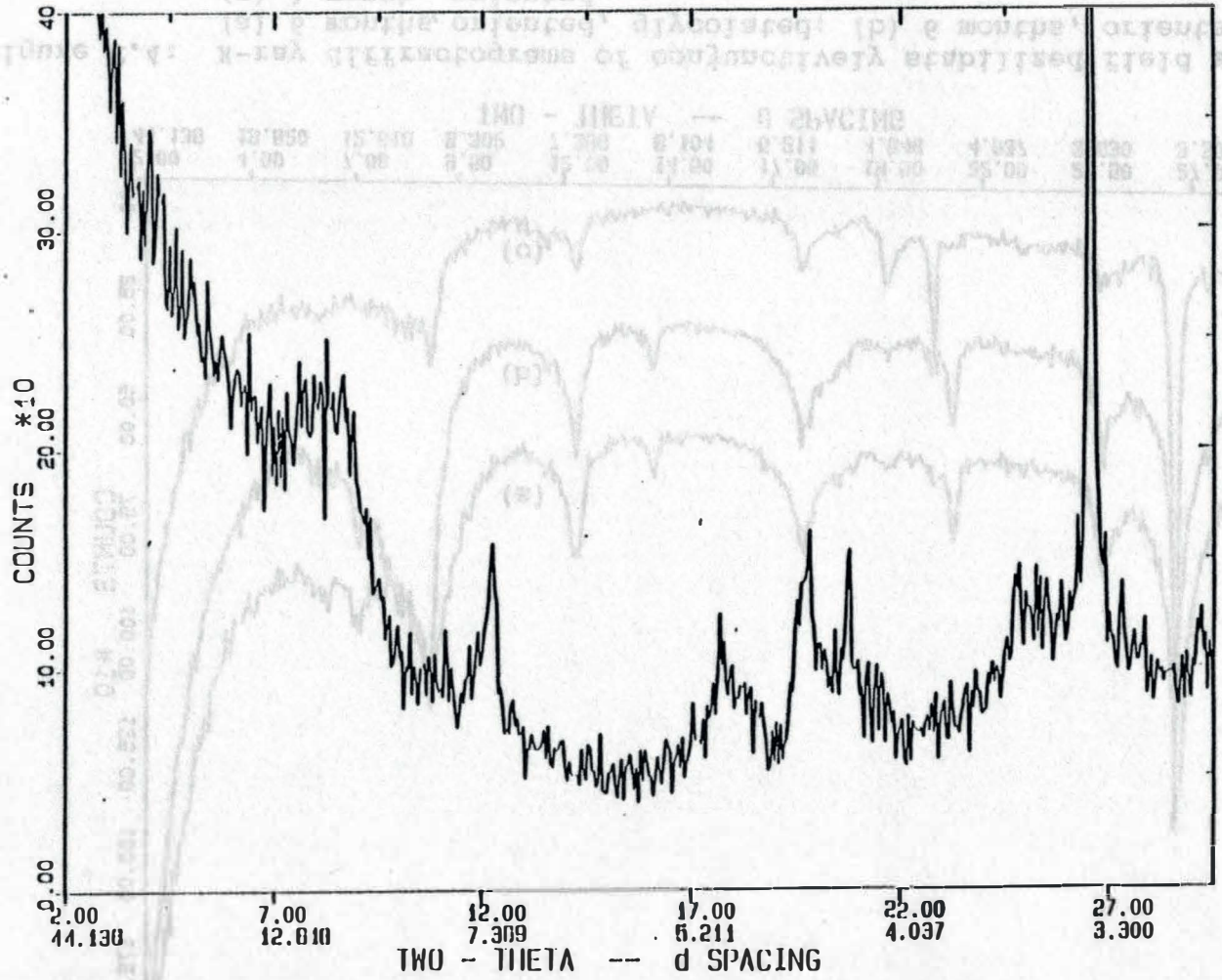

Figure C.3: X-ray diffractogram of fly ash stabilized field samples (6 months, oriented)

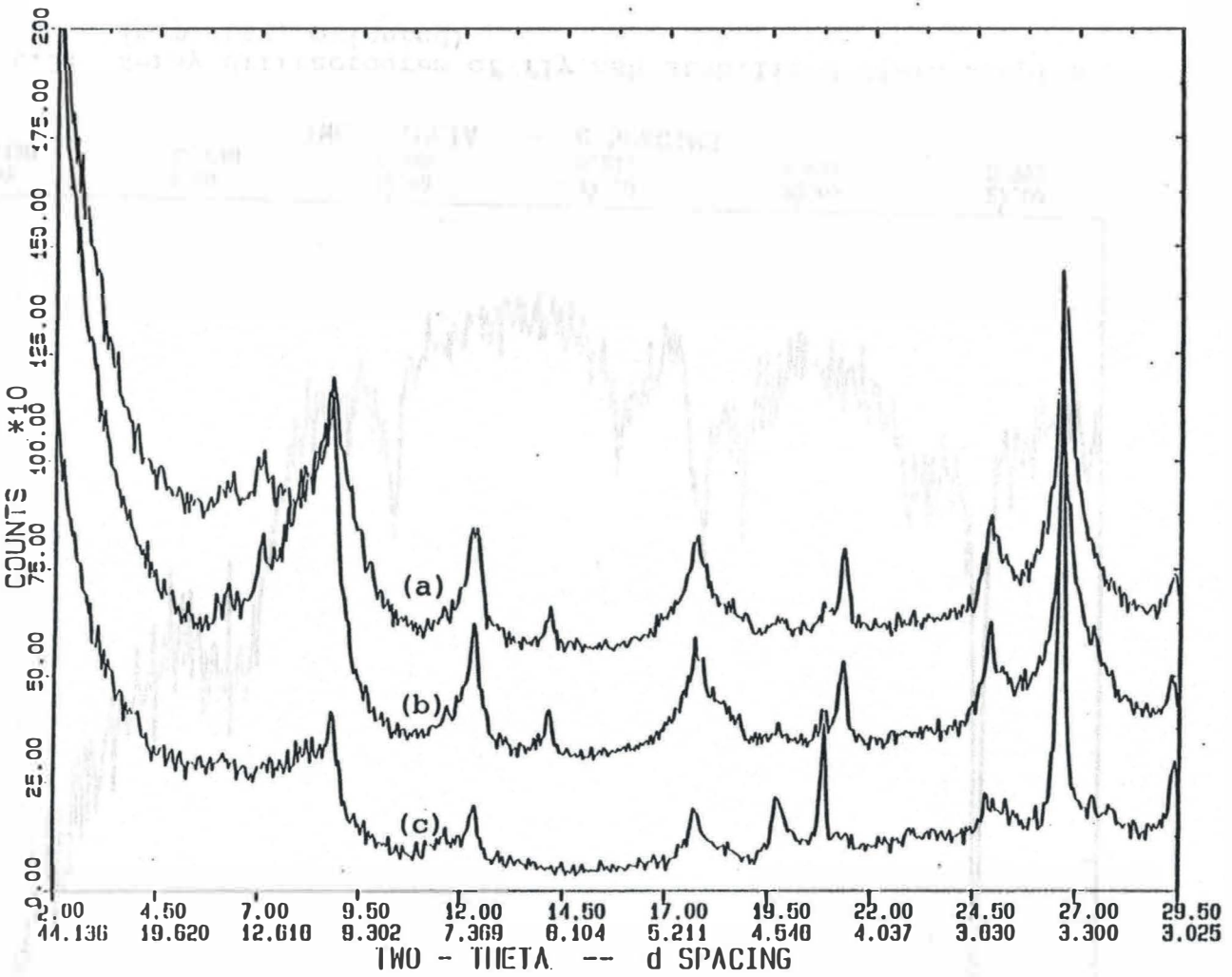

Figure C.4: X-ray diffractograms of conjunctively stabilized field samples. (a) 6 months, oriented, glycolated; (b) 6 months, oriented; (c) 1 month, oriented

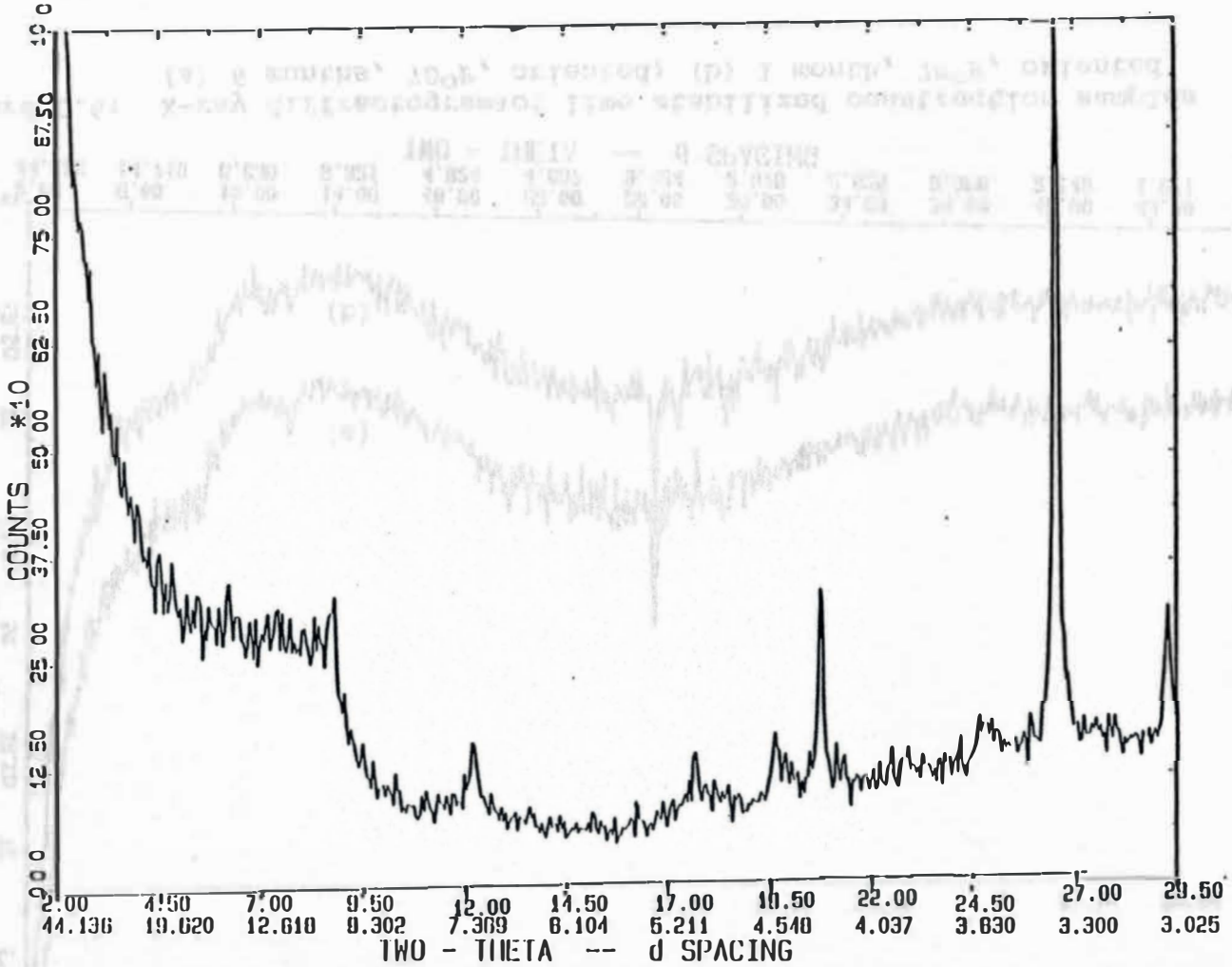

Figure C.5: X-ray diffractogram of cement stabilized construction samples (6 months, 70°F, oriented)

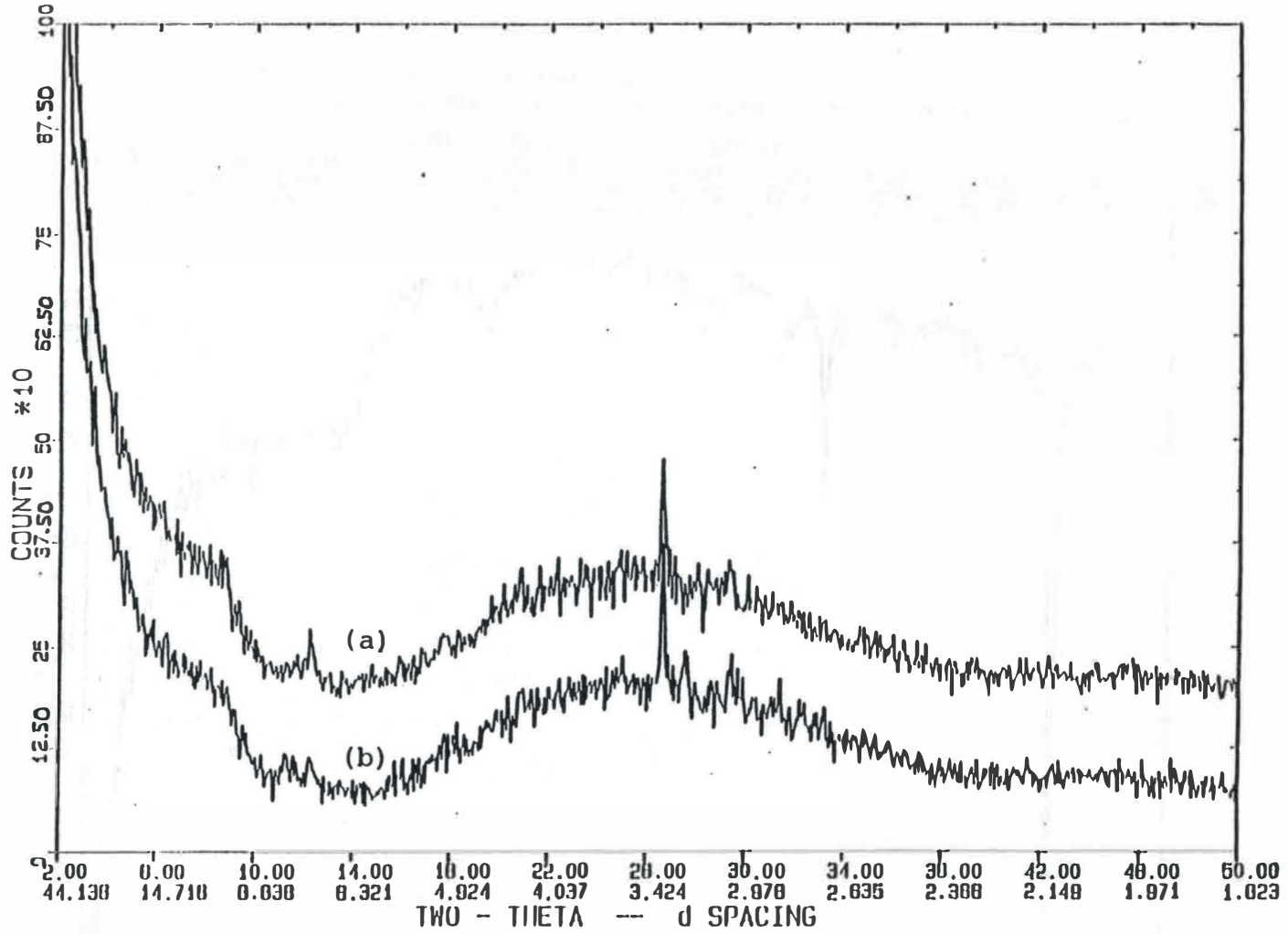

Figure C.6: X-ray diffractograms of lime stabilized construction samples (a) 6 months, 70°F, oriented; (b) 1 month, 70°F, oriented

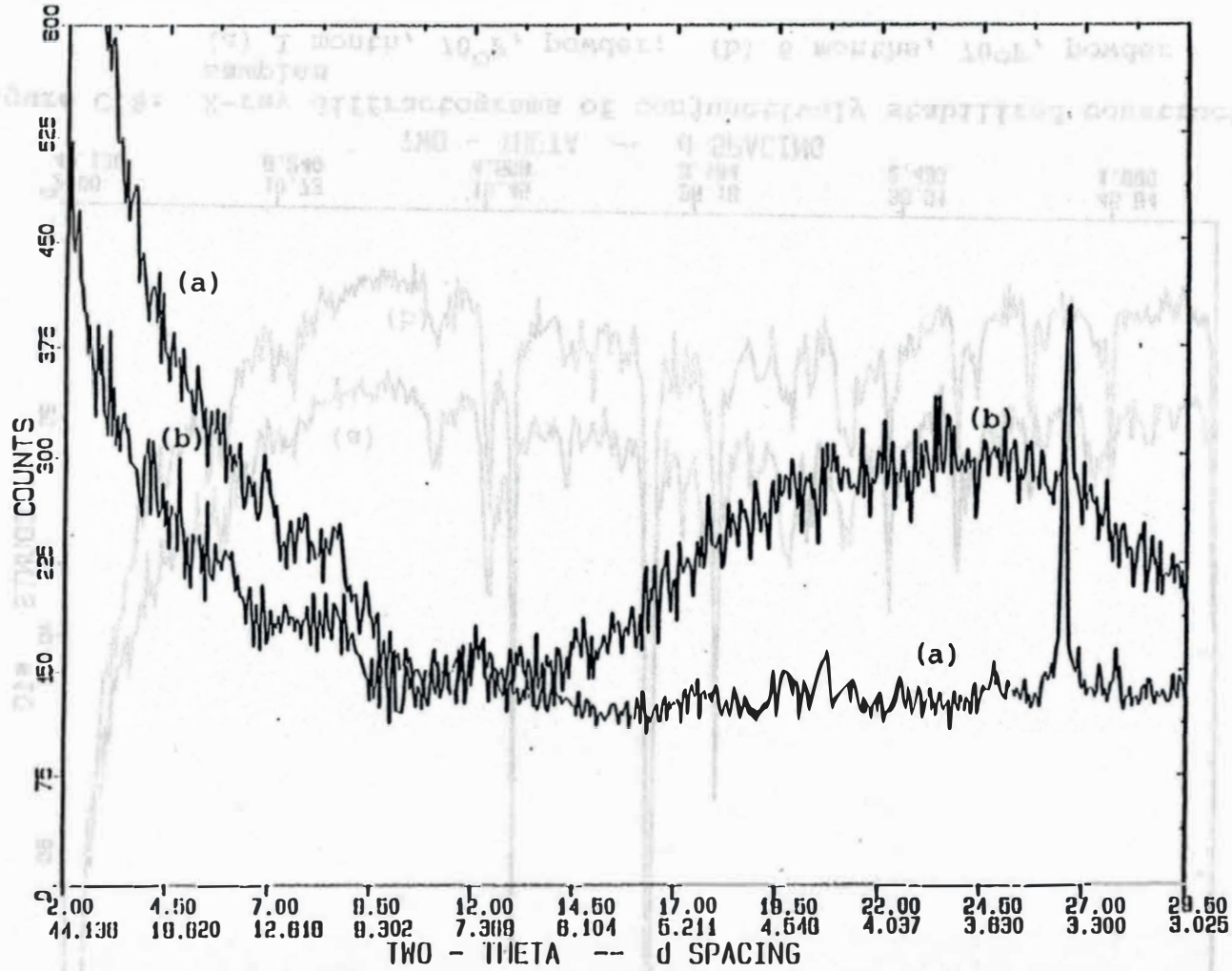

Figure C.7: X-ray diffractograms of fly ash stabilized construction samples (a) 1 month, 70°F, oriented; (b) 1 month 90°F, oriented

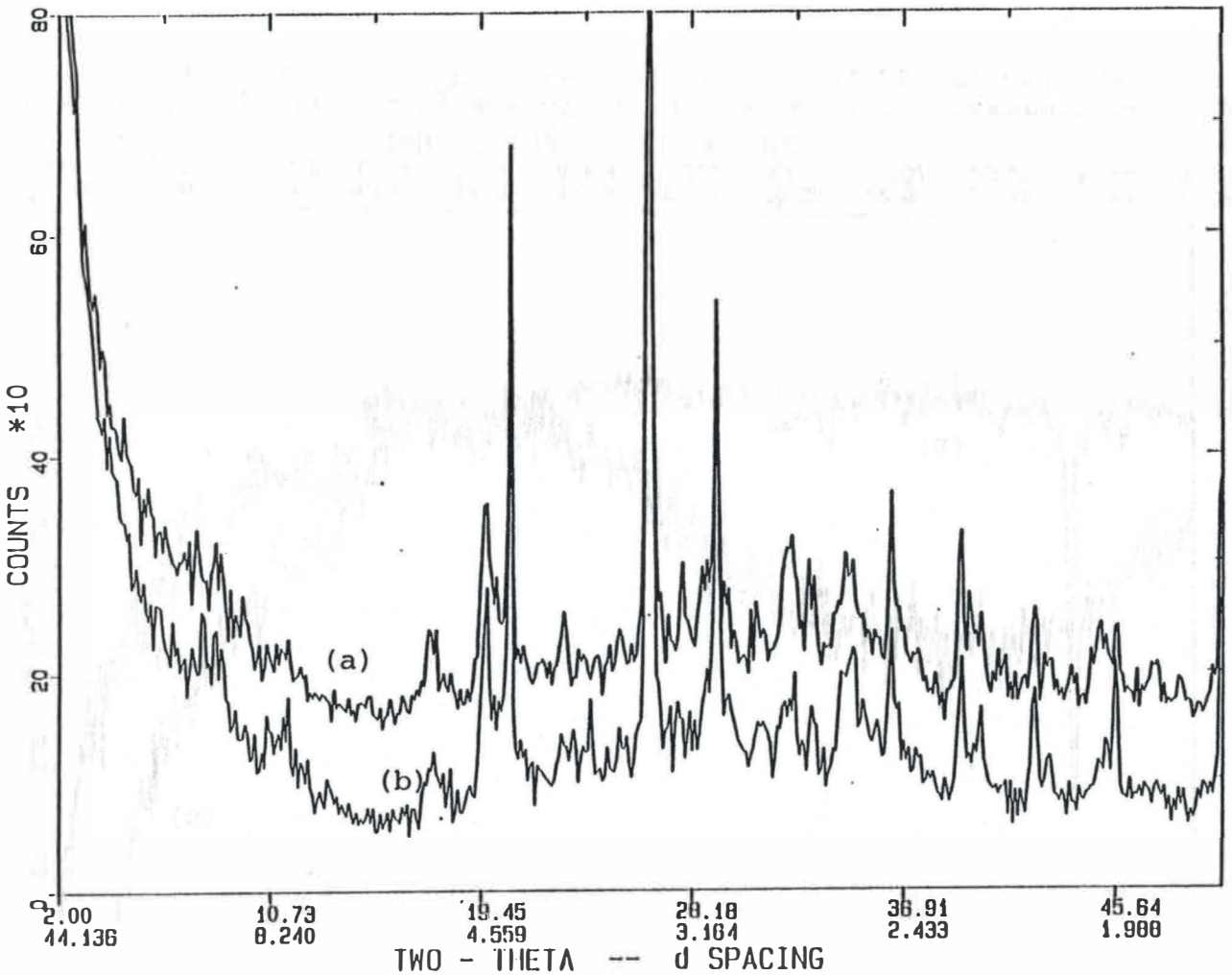

Figure C.8: X-ray diffractograms of conjunctively stabilized construction samples
(a) 1 month, 70°F, powder; (b) 6 months, 70°F, powder

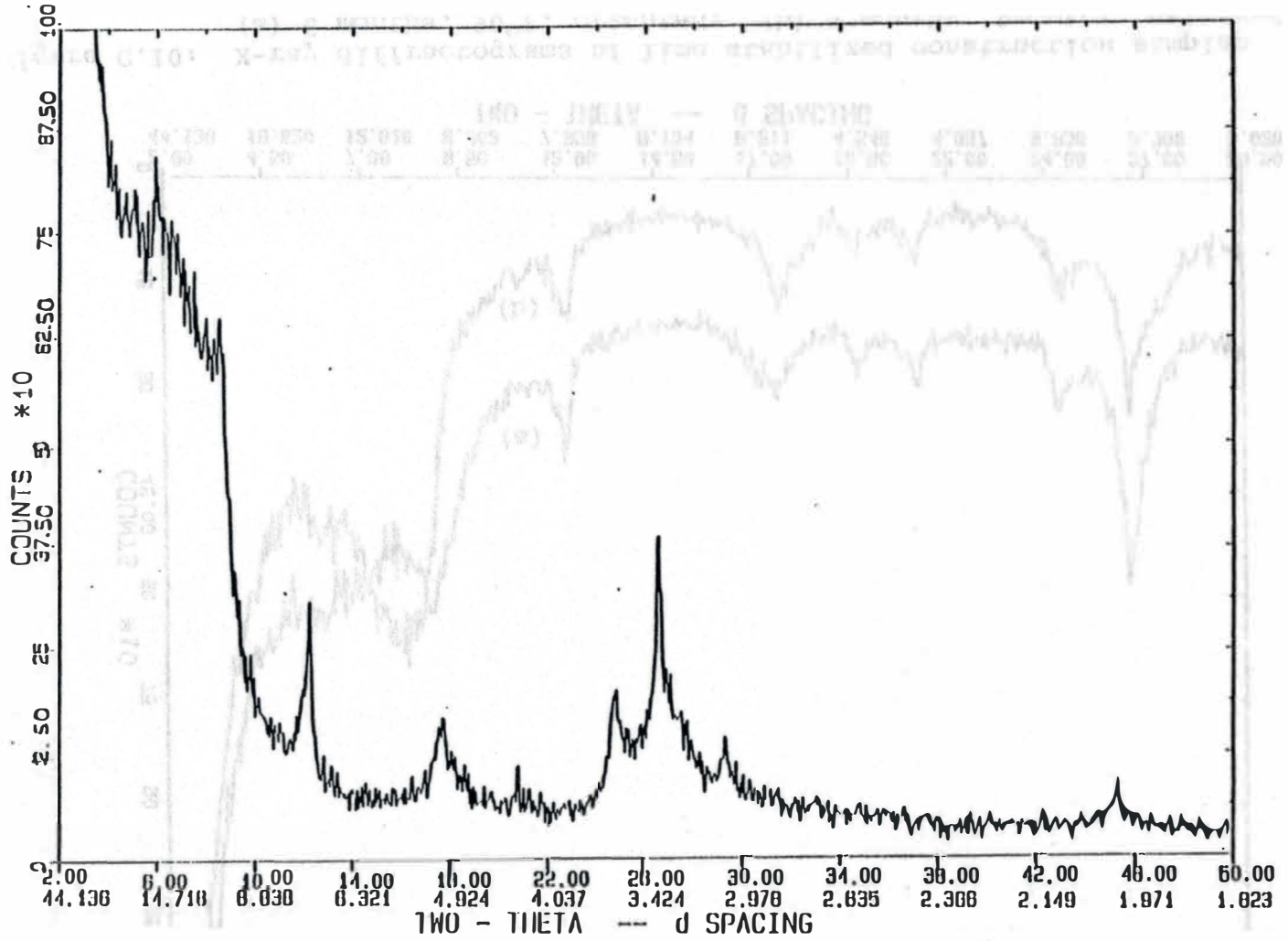

Figure C.9: X-ray diffractogram of cement stabilized construction samples (6 months, Proctor, oriented)

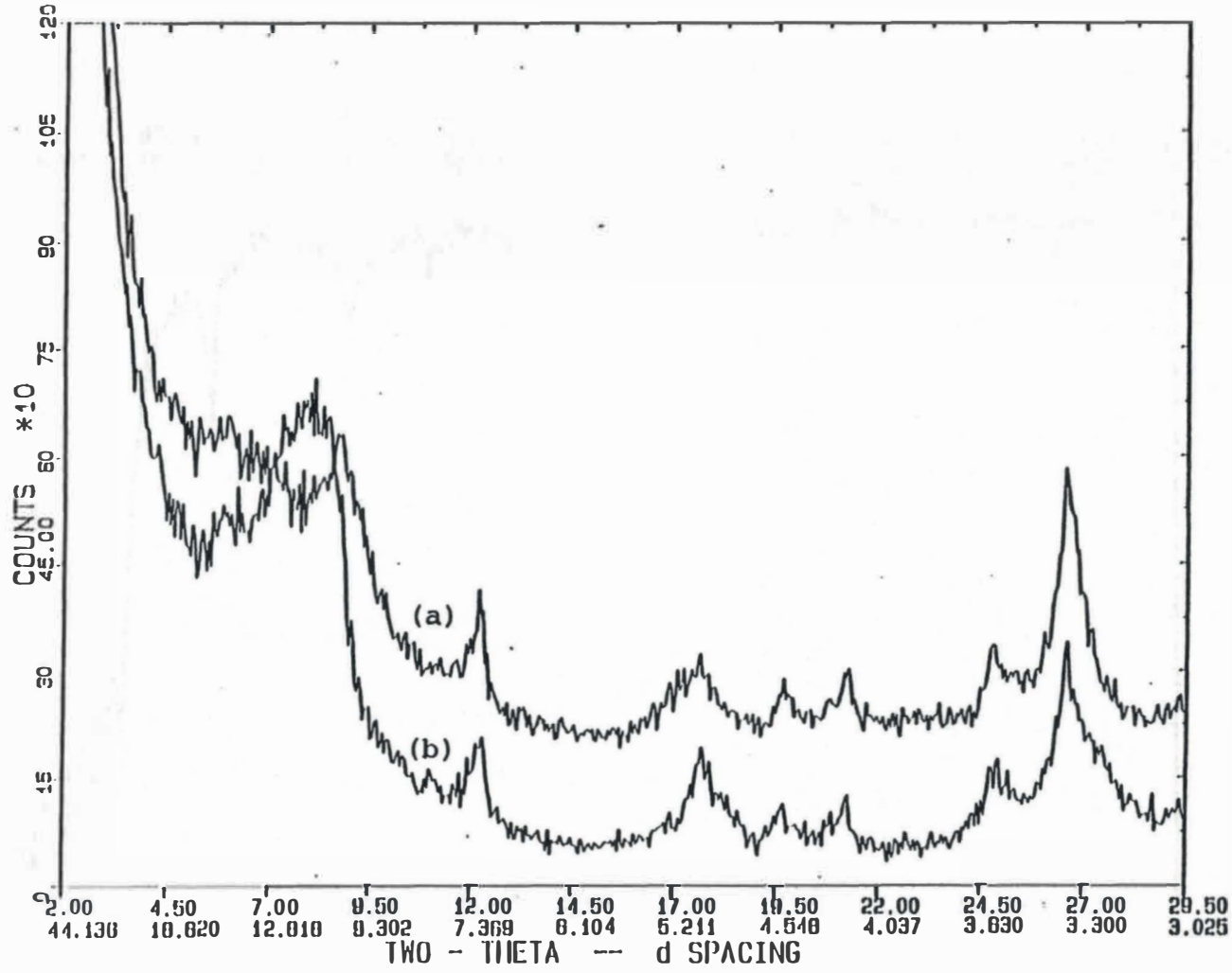

Figure C.10: X-ray diffractograms of lime stabilized construction samples (a) 6 months, 90°F, oriented; (b) 6 months, Proctor, oriented

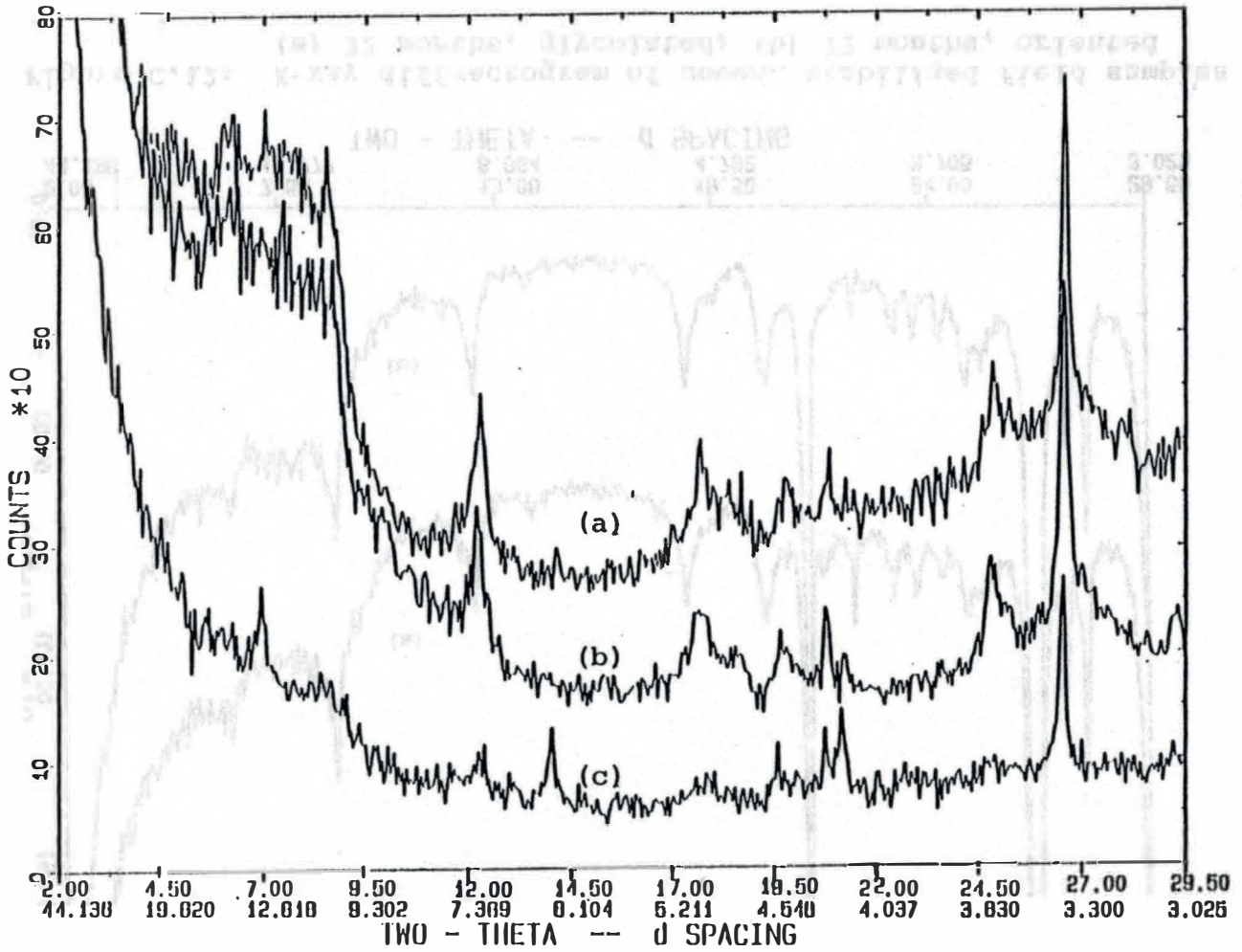

Figure C.11: X-ray diffractograms of fly ash stabilized construction samples (a) 6 months, Proctor, oriented; (b) 6 months, Proctor, oriented, glycolated; (c) 6 months, 90°F, oriented

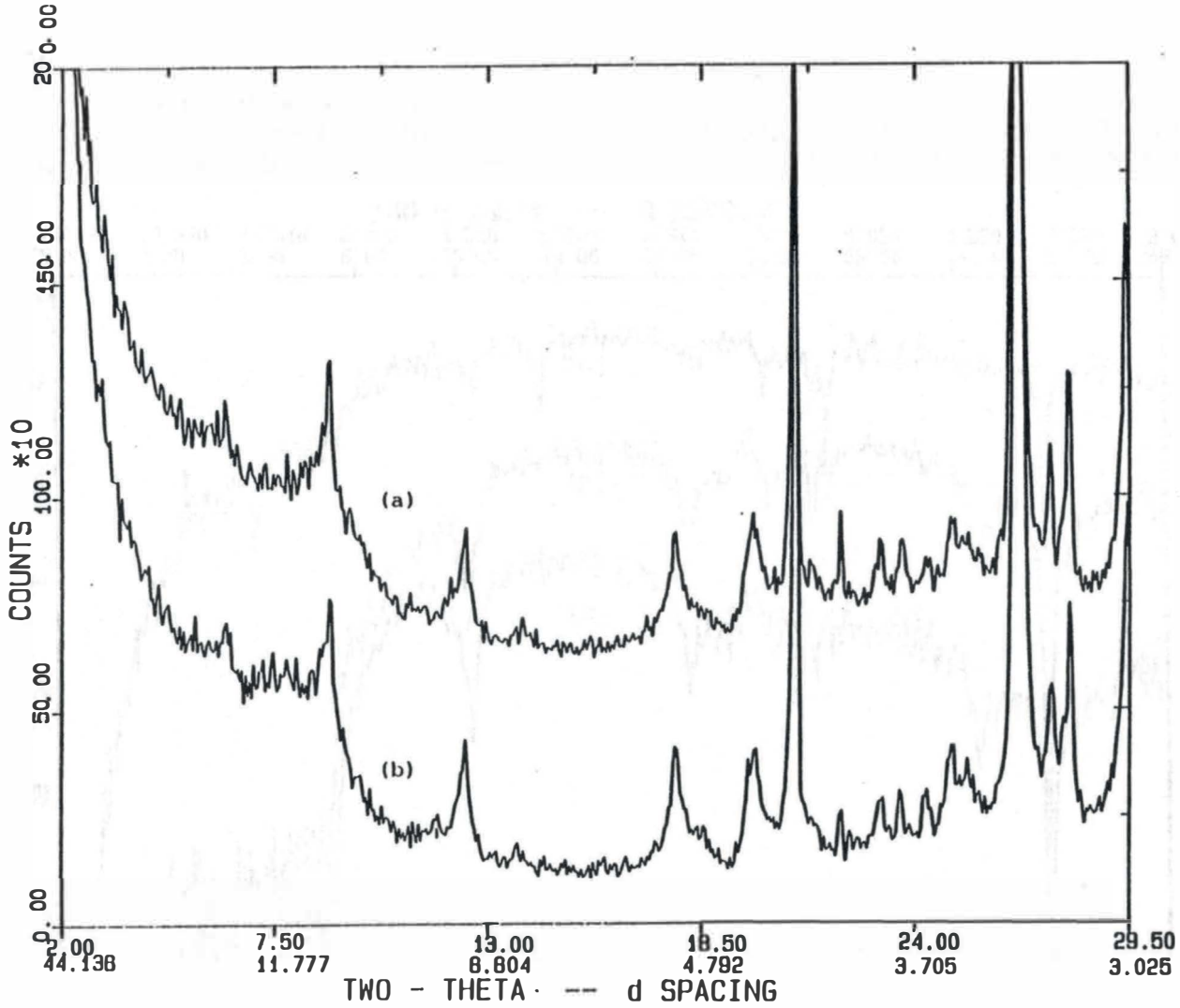

Figure C.12: X-ray diffractogram of cement stabilized field samples (a) 22 months, glycolated; (b) 22 months, oriented

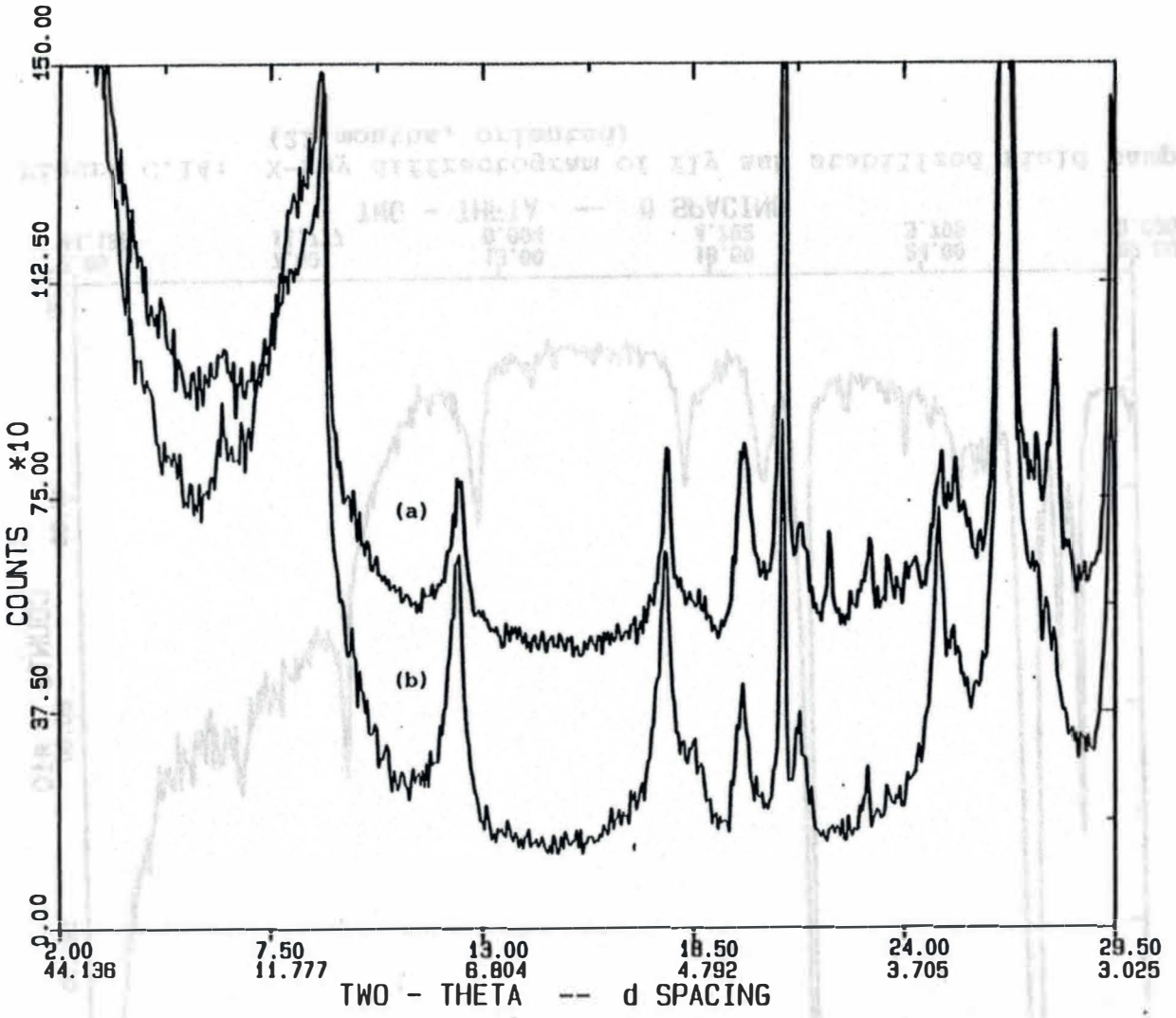

Figure C.13: X-ray diffractograms of lime stabilized field samples (a) 22 months, oriented, glycolated; (b) 22 months, oriented

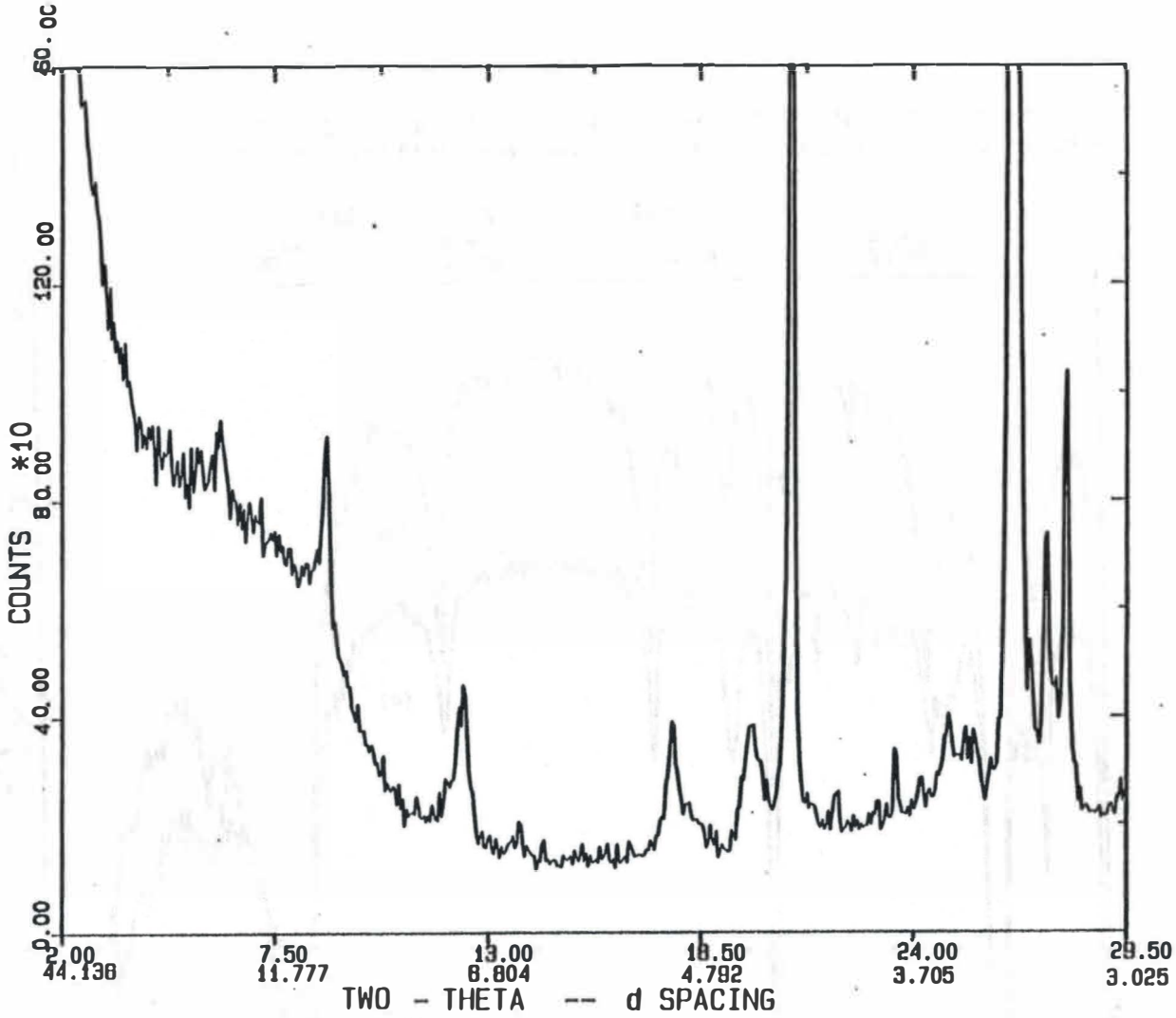

Figure C.14: X-ray diffractogram of fly ash stabilized field samples (22 months, oriented)

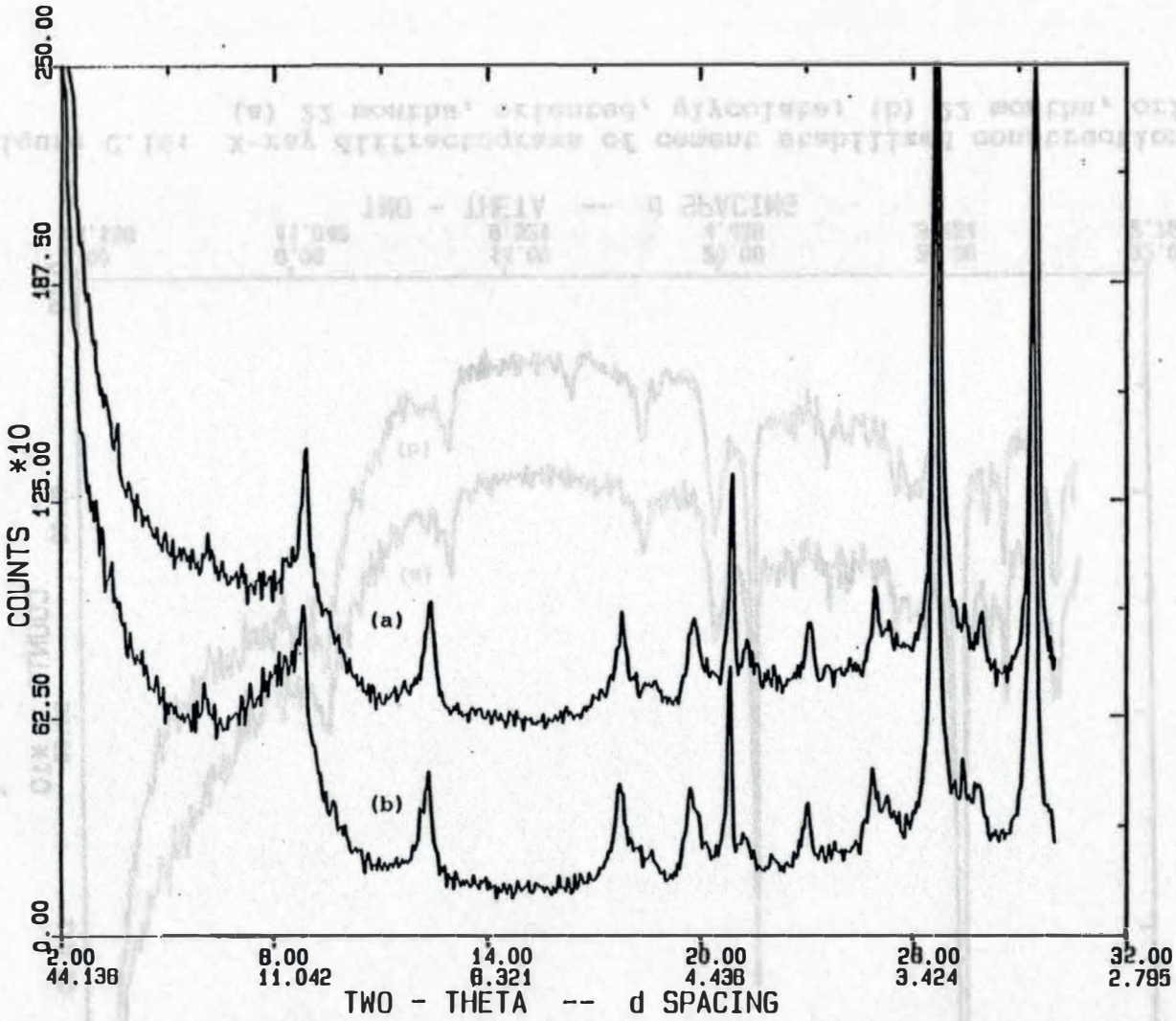

Figure C.15: X-ray diffractograms of conjunctively stabilized field samples (a) 22 months, oriented, glycolated; (b) 22 months, oriented

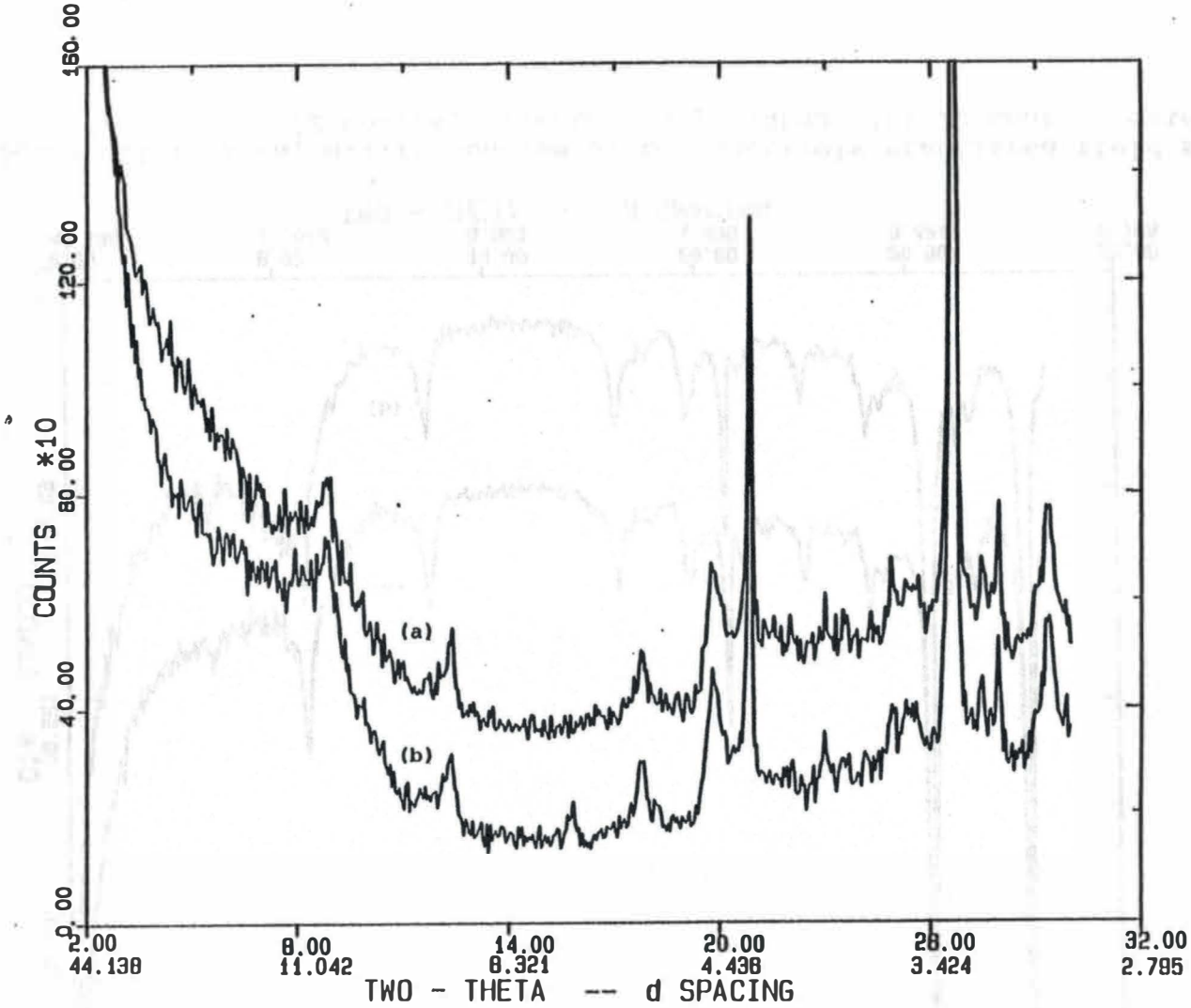

Figure C.16: X-ray diffractograms of cement stabilized construction samples (a) 22 months, oriented, glycolate; (b) 22 months, oriented

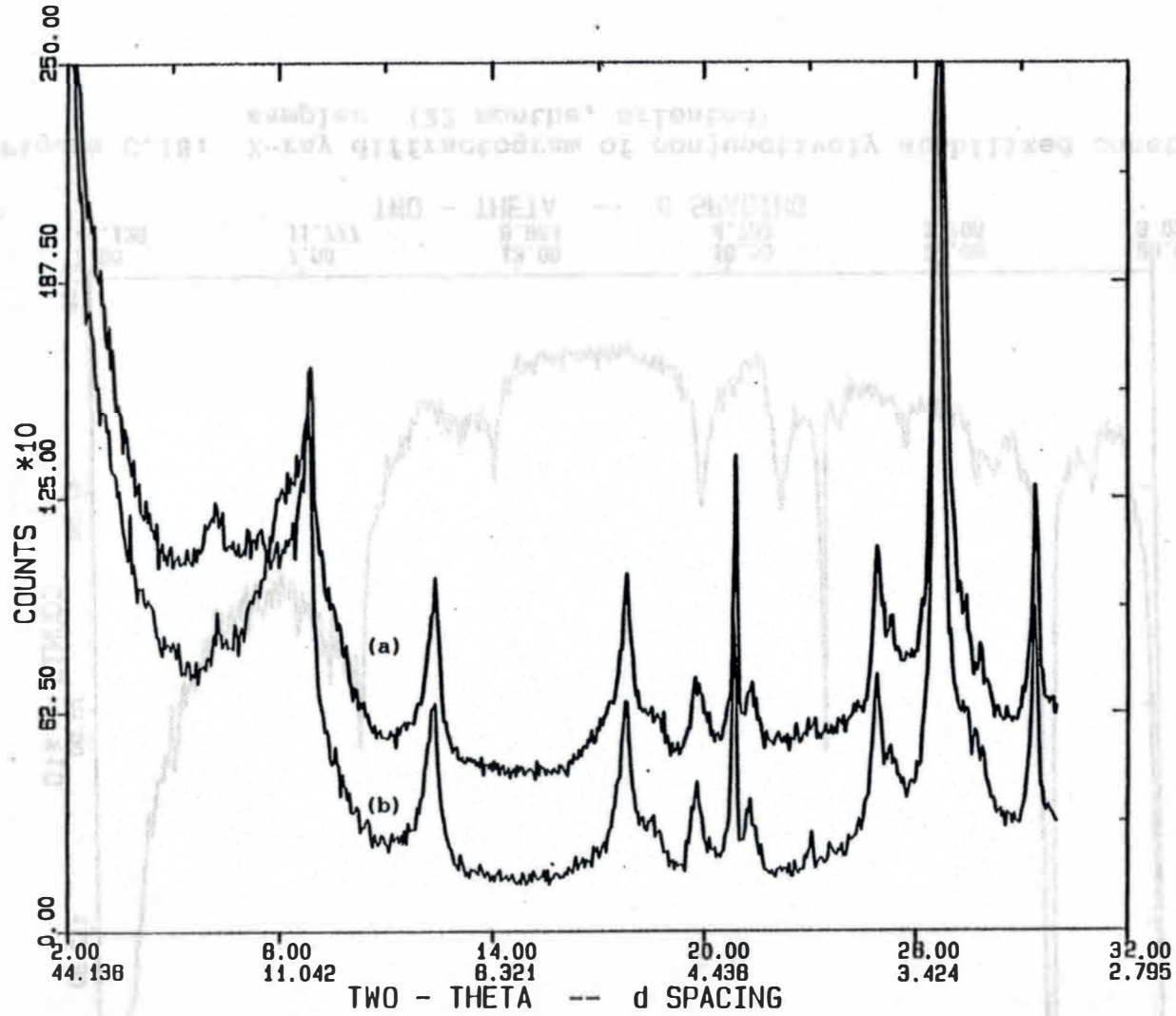

Figure C.17: X-ray diffractogram of lime stabilized construction samples (a) 22 months, oriented, glycolated; (b) 22 months, oriented

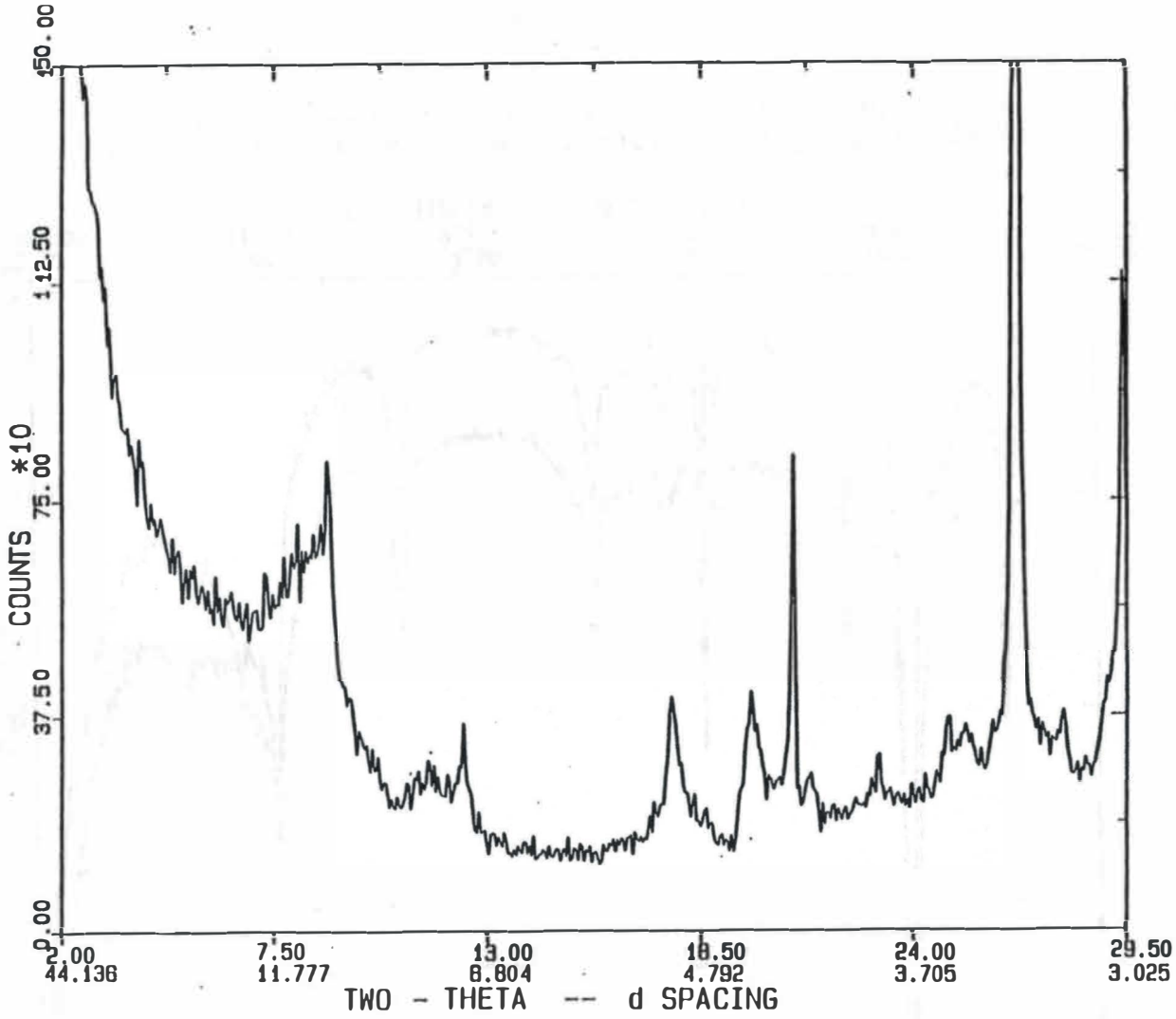

Figure C.18: X-ray diffractogram of conjunctively stabilized construction samples (22 months, oriented)

Table C.1. Crystalline Data of Raw Shale

2θ Degrees	d-Spacing Angstroms	* Integrated intensity
8.5973	10.2762	49575.7
12.4206	7.1202	3143.0
17.8042	4.9775	8459.2
24.9799	3.5616	5597.4
26.8169	3.3216	27118.7
35.9095	2.4987	653.9
45.4287	1.9948	4885.5

* Integrated intensity is an indicator of the size of the area under the peak of the diffractogram.

Table C.2. Crystalline Data of Cement Stabilized Field Sample Cured for One Month

2θ Degrees	d-Spacing Angstroms	Integrated intensity
5.943	16.0739	360.
6.277	14.0684	868.
8.754	10.0927	1319.
12.329	7.1730	555.
12.858	6.8788	109.
19.878	4.4649	540.
20.857	4.2553	492.
24.911	3.5713	314.
26.641	3.3432	2367.
34.958	2.5645	341.
36.573	2.4549	213.
39.497	2.2796	166.

Table C.3. Crystalline Data of Cement Stabilized Field Samples Cured for Six Months

2θ Degrees	d-Spacing Angstroms	Integrated intensity
12.310	7.1840	481.
17.768	4.9875	329.
19.813	4.4771	827.
20.819	4.2631	707.
24.906	3.5719	296.
26.617	3.3461	3695.
27.865	3.1991	411.
29.353	3.0401	550.
34.875	2.5704	553.
36.525	2.4850	511.
39.426	2.2835	229.

Table C.4. Crystalline Data of Lime Stabilized Field Samples Cured for One Month

2θ Degrees	d-Spacing Angstroms	Integrated intensity
6.063	14.5659	245.
8.732	10.1177	1695.
10.682	8.2745	97.
12.359	7.1553	469.
14.146	6.2555	103.
17.811	4.9756	483.
20.857	4.2554	408.
24.930	3.5686	462.
26.648	3.3423	2633.
29.462	3.0291	611.
36.547	2.4565	184.
39.504	2.2792	273.
45.448	1.9940	292.

Table C.5. Crystalline Data of Fly Ash Stabilized Field Samples Cured for Six Months

2θ Degrees	d-Spacing Angstroms	Integrated intensity
8.634	10.2321	175.
12.254	7.2165	359.
17.807	4.9768	206.
19.821	4.4754	576.
20.800	4.2669	278.
24.865	3.5778	149.
26.579	3.3508	1335.
29.213	3.0544	308.

Table C.6. Crystalline Data of Conjunctively Stabilized Field Samples Cured for One Month

2θ Degrees	d-Spacing Angstroms	Integrated intensity
8.817	10.0207	2179.
12.368	7.1501	417.
17.783	4.9835	716.
19.820	4.4757	836.
20.863	4.2542	577.
24.949	3.5659	235.
25.249	3.5242	91.
26.644	3.3428	3492.
27.884	3.1969	360.
29.411	3.0343	750.
34.651	2.5865	355.
34.902	2.5685	415.
36.555	2.4560	207.
39.507	2.2790	280.
42.425	2.1288	310.
45.393	1.9962	335.

Table C.7. Crystalline Data of Conjunctively Stabilized Field Samples Cured for Six Months

2θ Degrees	d-Spacing Angstroms	Integrated Intensity
6.2583	14.1109	456.6
8.7602	10.0854	15385.5
12.3330	7.1706	1344.5
14.1611	6.2488	392.6
17.8050	4.9773	3069.7
21.3225	4.1635	700.3
24.9259	3.5692	1328.5
26.6975	3.3362	5456.1
29.3525	3.0402	340.6
33.2522	2.6920	234.0
35.9422	2.4965	231.3

Table C.8. Crystalline Data of Cement Stabilized Construction Samples (Proctor Specimen)

2θ Degrees	d-Spacing Angstroms	Integrated intensity
6.0096	14.6939	479.0
8.5781	10.2991	3349.0
12.2518	7.2180	1107.9
17.7091	5.0040	435.3
20.7800	4.2710	172.6
24.8450	3.5806	520.6
26.5913	3.3493	1368.5
27.6922	3.2186	134.3
29.3300	3.0425	305.3
40.1598	2.2435	104.0
45.3107	1.9997	273.3

Table C.9. Crystalline Data of Lime Stabilized Construction Samples (Proctor Specimen)

2θ Degrees	d-Spacing Angstroms	Integrated intensity
8.346	10.5846	627.
8.663	10.1981	4583.
12.267	7.2091	877.
17.711	5.0036	853.
24.933	3.5681	283.
26.657	3.3411	2092.

Table C.10. Crystalline Data of Fly Ash Stabilized Construction Samples (Proctor Specimen)

2θ Degrees	d-Spacing Angstroms	Integrated intensity
4.001	22.0630	225.
8.647	10.2173	1267.
12.261	7.2123	723.
17.715	5.0024	652.
18.640	4.7563	179..
19.730	4.4958	449.
21.075	4.2118	113.
24.858	3.5788	736.
26.599	3.3483	1662.
34.560	2.5931	194.
36.456	2.4625	147.
45.318	1.9994	267.

Table C.11. Crystalline Data of Cement Stabilized Field Samples Cured for Twenty-Two Months

2θ Degrees	d-Spacing Angstroms	Integrated Intensity
6.246	14.1396	373.
8.886	9.9435	4180.
10.080	8.7678	155.
12.414	7.1243	1140.
13.776	6.4226	345.
17.889	4.9542	1135.
19.889	4.4604	1449.
20.923	4.2423	4820.
22.122	4.0150	208.
23.123	3.8434	415.
23.653	3.7584	308.
24.327	3.6558	322.
25.000	3.5589	1072.
25.359	3.5092	707.
26.707	3.3351	19871.
27.528	3.2375	564.
27.988	3.1853	904.
29.463	3.0291	3620.
30.486	2.9298	228.
31.291	2.8563	689.
33.231	2.6937	434.
35.032	2.5593	1980.
36.068	2.4882	510.
36.634	2.4510	1543.
37.689	2.3848	397.

Table C.12. Crystalline Data of Lime Stabilized Field Samples Cured for Twenty-Two Months

2θ Degrees	d-Spacing Angstroms	Integrated Intensity
8.861	9.9704	17919.
12.498	7.0763	2296.
17.847	4.9656	2540.
19.883	4.4616	2551.
20.916	4.2434	4943.
22.088	4.0208	376.
23.104	3.8463	575.
23.625	3.7627	267.
24.276	3.6632	387.
25.004	3.5582	967.
25.341	3.5116	1411.
26.705	3.3353	23196.
27.951	3.1894	2111.

C.13. Crystalline Data of Fly Ash Stabilized Field Samples Cured for Twenty-Two Months

2θ Degrees	d-Spacing Angstroms	Integrated Intensity
6.117	14.4358	634.
8.842	9.9926	10162.
12.372	7.1481	1701.
13.788	6.4175	333.
17.814	4.9751	1641.
19.843	4.4705	1331.
20.868	4.2533	6118.
23.638	3.7608	323.
24.938	3.5675	424.
25.366	3.5084	351.
26.676	3.3390	27938.
27.471	3.2441	874.
27.958	3.1887	2251.

Table C.14. Crystalline Data of Conjunctively Stabilized Field Samples Cured for Twenty-Two Months

2θ Degrees	d-Spacing Angstroms	Integrated Intensity
6.112	14.4489	375.
7.364	11.9944	243.
8.784	10.0590	7698.
12.357	7.1570	2098.
17.757	4.9909	1091.
18.591	4.7688	248.
19.780	4.4848	1382.
20.851	4.2568	1204.
21.295	4.1690	262
23.053	3.8548	724.
24.912	3.5713	1445.
25.207	3.5302	832.
26.629	3.3447	8309.
27.416	3.2505	117.
27.856	3.2001	799.

Table C.15. Crystalline Data of Cement Stabilized Construction Samples Curred for Twenty-Two Months

2θ Degrees	d-Spacing Angstroms	Integrated Intensity
8.852	9.9815	1167.
12.389	7.1384	673.
17.841	4.9676	959.
19.871	4.4644	2100.
20.873	4.2523	1819.
23.008	3.8623	355.
24.951	3.5658	304.
25.595	3.4775	396.
26.678	3.3387	8956.
27.943	3.1904	569.

Table C.16. Crystalline Data of Lime Stabilized Construction Samples Cured for Twenty-Two Months

2θ Degrees	d-Spacing Angstroms	Integrated Intensity
3.570	24.7272	2196.
6.292	14.0357	983.
8.793	10.0478	32203.
12.384	7.1411	3678.
16.425	5.3922	338.
16.577	5.3433	323.
17.799	4.9789	4460.
18.528	4.7847	1511.
19.826	4.4742	1987.
20.870	4.2527	2131.
21.317	4.1646	1327.
24.945	3.5665	2943.
25.218	3.5285	2129.
26.669	3.3397	19265.
27.450	3.2464	7742.
28.742	3.1034	588.

Table C.17. Crystalline Data of Fly Ash Stabilized Construction Samples Cured for Twenty-Two Months

2θ Degrees	d-Spacing Angstroms	Integrated Intensity
6.184	14.2804	776.
8.858	9.9747	1150.
12.425	7.1180	1064.
14.256	6.2076	197.
17.840	4.9679	801.
19.895	4.4589	1086.
20.876	4.2517	911.
21.396	4.1495	359.
24.165	3.6799	420.
25.099	3.5451	955.
26.668	3.3399	4545.
27.945	3.1901	475.
29.394	3.0361	367.

Table C.18. Crystalline Data of Conjunctively Stabilized Construction Samples Cured for Twenty-Two Months

2θ Degrees	d-Spacing Angstroms	Integrated Intensity
8.098	10.9089	257.
8.868	9.9629	8170.
12.408	7.1273	1199.
17.814	4.9747	1601.
19.859	4.4669	1782.
20.904	4.2459	1167.
21.361	4.1561	438.
23.095	3.8478	486.
24.957	3.5648	937.
25.384	3.5057	1060.
26.682	3.3381	10351.
27.886	3.1967	639.

APPENDIX D

TRAFFIC STATISTICS

TRAFFIC STATISTICS

The following average daily traffic volumes have been collected to date for the Ponca City project:

Dates	Daily Volume[1]	Weekday Volume[2]
November 1984 (7 days)	2,189	2,138
January 1985 (7 days)	3,164	3,368
Feb/Mar 1985 (14 days)	2,647	2,728
April 1985 (7 days)	---	---

[1] Average of all days in the study
[2] Average of Monday through Friday only

No volume trends are evident in this data. There may be over-counting in the January 1985 data set as the detector recorded implausibly high readings for certain hours. These were deleted but the overall counts are still higher than on the other count days. The April 1985 counting was unsuccessful because of a counter malfunction (extremely low counts).

The following vehicle classification counts by vehicle type and lane have been collected to date:

MAY 30-31 1985

TRAFFIC COUNTS

Vehicle Type	Inside Lane	Outside Lane	Total
Semi- and full trailer combinations	11	118	129 (3.2%)
All other vehicles	593	3,327	3,920 (96.8%)
Totals	604 (14.9%)	3,445 (85.1%)	4,049 (100.0%)

JAN 9-10 1985 (24 hrs.)

Vehicle Type	TRAFFIC COUNTS Inside Lane	Outside Lane	Total
Semi- and full trailer combinations	10	51	61 (2.8%)
All other vehicles	274	1,856	2,130 (97.2%)
Totals	284 (13.0%)	1,907 (87.0%)	2,191 (100.0%)

Heavy trucks (semi- and full trailer combinations) comprise about three percent of the total traffic volume. About 85 percent of the traffic uses the outside lane. The May 30-31, 1985, classification count seems to be high relative to the earlier count and the weekly counts, but the statistics are reasonable and consistent.

APPENDIX E

BENKELMAN BEAM DATA

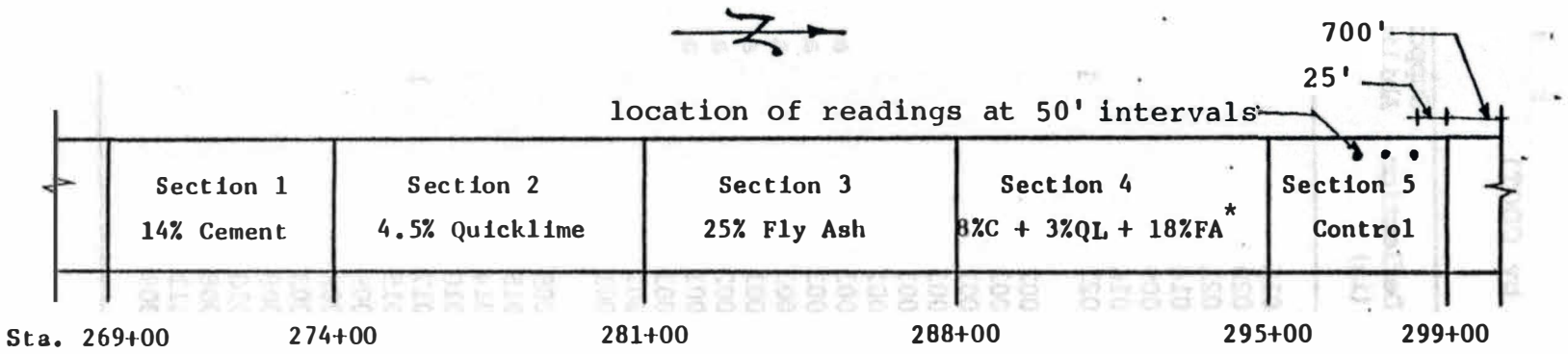

* C = Cement
QL = Quicklime
FA = Fly Ash

Figure E.1: Location of Benkelman beam readings

Table E.1. Performance Survey of the Test Section. Date 6-18-85 (provided by ODOT)

Test Section	*Mileage ft	Rut Depth in x 10^{-1}	Beam Deflection (in)	Supporting Ability (lb)
Control	725.00	0	0.015	** a
	775.00	1	0.020	16427.
	825.00	0	0.021	15504.
	875.00	1	0.014	a
	925.00	0	0.009	a
	975.00	0	0.016	a
	1025.00	1	0.021	15504.
Conjunctively Stab.	1075.00	1	0.002	a
	1125.00	1	0.003	a
	1175.00	1	0.001	a
	1225.00	0	0.001	a
	1275.00	0	0.001	a
	1325.00	0	0.001	a
	1375.00	1	0.001	a
	1425.00	0	0.003	a
	1475.00	2	0.003	a
	1525.00	1	0.001	a
	1575.00	1	0.002	a
	1625.00	1	0.001	a
	1675.00	1	0.001	a
	1725.00	0	0.002	a
	1775.00	0	0.001	a
Fly Ash Stab.	1825.00	0	0.009	a
	1875.00	1	0.015	a
	1925.00	1	0.014	a
	1975.00	0	0.010	a
	2025.00	0	0.017	19915.
	2075.00	0	0.015	a
	2125.00	1	0.009	a
	2175.00	1	0.008	a
	2225.00	1	0.003	a
	2275.00	2	0.008	a
	2325.00	1	0.010	a
	2375.00	1	0.008	a
	2425.00	1	0.011	a
	2475.00	1	0.009	a

(continued)

Table E.1. Performance Survey of the Test Section. Date 6-18-85 (provided by ODOT)

Test Section	*Mileage ft	Rut Depth in x 10^{-1}	Beam Deflection (in)	Supporting Ability (lb)
Lime Stab.	2525.00	1	0.006	a
	2575.00	0	0.004	a
	2625.00	0	0.009	a
	2675.00	0	0.006	a
	2725.00	1	0.008	a
	2775.00	1	0.006	a
	2825.00	0	0.008	a
	2875.00	1	0.009	a
	2925.00	2	0.012	a
	2975.00	1	0.009	a
	3025.00	1	0.012	a
Cement Stab.	3225.00	2	0.005	a
	3275.00	2	0.010	a
	3325.00	2	0.012	a
	3375.00	2	0.009	a
	3425.00	2	0.007	a
	3475.00	2	0.009	a
	3525.00	2	0.008	a
	3575.00	2	0.005	a
	3625.00	2	0.001	a

* Arbitrary Odometer Readings with first reading 25 ft from the end of the Control Section.

** a In excess of 20,000 lb.